SPATIAL DISTRIBUTION OF CUTICULAR WAX COMPOUNDS AND CUTICULAR WATER BARRIER PROPERTIES USING *COSMOS BIPINNATUS* AND *ARABIDOPSIS THALIANA* AS MODELS

by

Christopher Buschhaus

B.Sc., Trinity Western University, 2004

A THESIS SUBMITTED IN PARTIAL FULFILLMENT OF THE REQUIREMENTS FOR THE DEGREE OF

DOCTOR OF PHILOSOPHY

in

THE FACULTY OF GRADUATE STUDIES

(Botany)

THE UNIVERSITY OF BRITISH COLUMBIA

(Vancouver)

December 2010

ABSTRACT

Plant cuticles form an external barrier, primarily blocking water loss into the desiccating atmosphere but also inhibiting UV and pathogen penetration. Cuticles consist of hydrophobic wax – a complex mixture of very-long-chain aliphatics and alicyclics – on top of (epicuticular) and in between (intracuticular) the biopolymer cutin. Absolute and relative wax composition varies between species and organs. Considering the diversity of compounds and barrier functions, the question arises: How does each wax compound shape each function? This dissertation presents advancements using *Cosmos bipinnatus* and *Arabidopsis thaliana* in three research areas ranging from localization of compounds at the organ, cellular, and sub-cellular levels, to structural elucidation of novel compounds, and finally to functional characterization.

Waxes from *C. bipinnatus* petals, stems, and leaves were shown to be distinct. Petal wax comprised mainly primary alcohols as well as novel 1,2- and 1,3-diols and ketols. These classes were dominated by C_{22} and C_{24} chain lengths. The water resistances of the adaxial ($3.0\pm0.3 \times 10^4$ s/m) and abaxial ($1.5\pm0.2 \times 10^4$ s/m) surfaces of these petals were lower than average literature values for leaves but similar to fruit, suggesting that the wax composition on ephemeral organs creates a compromised water barrier.

Lateral wax heterogeneity was shown for trichomes, which tended to have longer compound chain lengths and a higher percentage of alkanes, as compared to pavement cells in both leaves and stems of *A. thaliana*. Moreover, a meta-analysis synthesizing the epicuticular and intracuticular wax compositions of all species investigated to date showed vertical wax heterogeneity. Noticeably, cyclic compounds preferentially accumulated in intracuticular wax. This finding was confirmed by over-expression of AtLUP4 in Arabidopsis, which caused β-amyrin accumulation in the intracuticular but not epicuticular wax layer. The presence of β-amyrin reduced the intracuticular wax-caused water resistance ($2.4\pm0.2 \times 10^3$ s/m) to three-quarters of the control ($3.4\pm0.5 \times 10^3$ s/m) while the epicuticular wax resistance for the over-expressor ($6.8\pm0.6 \times 10^3$ s/m) equaled that of the control ($6.6\pm0.9 \times 10^3$ s/m).

An understanding of how wax constituents affect cuticular functions will aid in breeding and designing plants capable of withstanding adverse biotic and abiotic conditions.

PREFACE

The work in Chapters 2 and 3 builds on preliminary research performed by D. Hager, who demonstrated the feasibility of analyzing the wax and water barrier effectiveness of *Cosmos bipinnatus* petals and first confirmed the identity of the 1,2- and 1,3-alkanediols. However, I performed and analyzed all of the research reported in these chapters.

The experiments in Chapter 4 were performed with the help of an undergraduate, M. Wu, whom I directly instructed and supervised.

Chapter 5 was written in collaboration with my supervisor, Dr. R. Jetter, who originally drafted the introduction and review of method development sections of this chapter and provided significant editing on the remaining sections. I performed all of the data collection and analysis, composed the original text for all remaining sections, and extensively edited the fore-mentioned section drafts produced by Dr. R. Jetter.

The experiments, analyses, and writing in all of the remaining chapters were completely my contributions.

TABLE OF CONTENTS

LIST OF TABLES

LIST OF FIGURES

LIST OF ABBREVIATIONS

BSTFA: bis-N,O-(trimethylsilyl)trifluoroacetamide

CER: Eceriferum

CoA: Coenzyme A

EGTA: Ethylene glycol tetraacetic acid

FAR: Fatty acyl reductase

FID: Flame ionization detection

GC: Gas liquid chromatography

KCS: β-keto-acyl coenzyme A synthase

KCR: β-keto-acyl coenzyme A reductase

LAH: Lithium aluminium hydride

LUP: Lupeol

MAH1: Mid-chain alkane hydroxylase 1

MS: Mass spectrometry

MWC: Minimal water conductance

P: Permeance

PAS2: Pasticcino 2

PEN: Pentacyclic

R: Resistance

TLC: Thin layer chromatography

TTPS: Triterpenoid synthase

VLC: Very-long-chain

WSD1: Wax ester synthase/acyl-coenzyme A:diacylglycerol acyltransferase 1

ACKNOWLEDGMENTS

The research and learning culminating in my PhD would not have been possible without the support of many people. I wish to express my gratitude to my supervisor, Dr. R. Jetter who offered invaluable assistance, support, training, guidance, and hours of intellectually stimulating conversation. Deepest gratitude is also due to the members of the supervisory committee, Dr. A. Glass, Dr. L. Kunst, and Dr. L. Samuels, whose knowledge and assistance helped make this study successful.

Special thanks to all my lab mates, including post-docs and graduate students: Y. Cao, Dr. S. Greer, Dr. O. Guhling, X. Ji, Dr. F. Li, C. van Maarseveen, Dr. M. Wen, R. Yao, T. Yeats, and Dr. Z. Wang, for sharing lab duties and literature as well as providing extremely valuable assistance. Great appreciation is due to the undergraduate students I have supervised who have contributed many hours to the ongoing research: E. Alikpala, V. Boyeva, I. Dragan, K. Liu, and M. Wu.

I acknowledge the financial support provided by the Natural Sciences and Engineering Research Council of Canada (NSERC) and the University of British Columbia.

I thank my extended family for their comments and questions, support and encouragement.

And lastly, I wish to express my love and gratitude to my beloved family; for their understanding and endless love, through the duration of my studies.

Soli Deo Gloria

Chapter 1
Introduction and background to plant cuticle structure, composition, and function

1.1 Introduction

The outermost surface of land plants, the cuticle, has a collective surface area two times greater than the Earth's area (Riederer *et al.* 1995). This forms a vast border for interaction between plants and their environment. The ubiquitous nature and potential ecological importance of this layer raises three fundamental questions: (1) Why do cuticles exist? What are their functions? (2) How do they perform these functions? What are their compositions? And (3) how effectively do they perform these functions? It is generally assumed that the main function of plant cuticles is to reduce non-stomatal water loss (Riederer *et al.* 1995). This dehydration barrier permits plant survival within the earth's atmosphere. However, secondary functions have also been suggested such as blocking pathogens, xenobiotics, and UV light (Kerstiens 1996b). In order to optimize these, plants might have to compromise the effectiveness of the cuticle as a water barrier. Physiological studies are needed to provide a greater understanding of the mechanism of cuticular resistance to water movement and the cuticle's effectiveness as a water barrier despite other, potentially competing functions. These studies must be guided by the structure and composition of cuticles which is controlled by cuticle biosynthesis.

1.2 Cuticle structure

Cuticles are multi-layered, composite structures (Figure 1.1; Jeffree 1996). The outermost layer of the cuticle is composed of a thin, continuous wax film (epicuticular wax). In many species, wax crystals project from the film into the surrounding environment. The next layer underneath the epicuticular wax is composed of intracuticular wax within a cutin/cutan biopolymer matrix. Cellulose fibrils likely extend from the cell wall into the cutin and intracuticular wax. It remains unclear how far the fibrils extend into the cuticle and whether their presence is universal. In some species, a pectinaceous layer is thought to separate the cuticular layer from the cell wall, although the composition and species distribution of pectin remains uncertain.

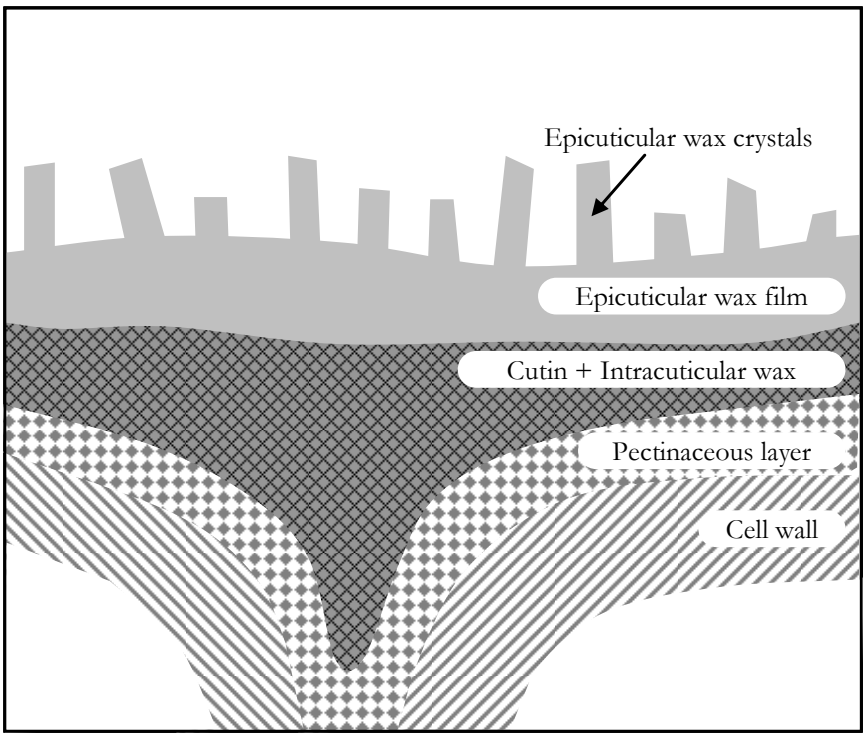

Figure 1.1 A schematic cross-section of a plant cuticle showing spatially distinct layers. The epicuticular wax (film and in some species crystals) is situated external to the intracuticular wax, which is interspersed within the cutin matrix. The pectinaceous layer separates the cuticle from the cell wall. Figure adapted from Jeffree (1996).

1.3 Cuticle composition

The structural biopolymer matrix of the cuticle consists of cutin and cutan, which make up 40% to 80% of the cuticle's weight (Heredia 2003). Cutin contains hydroxylated, epoxy hydroxylated, and di-acids 16 to 18 carbons in length ester-linked into a polymer, at least in part via glycerol units. This is believed to result in a three-dimensional lattice. Cutan is thought to be similar in composition to cutin except that cutan forms cross-linking ether bonds and consequently does not depolymerize upon ester hydrolysis. Thus, cutan is defined as the matrix residue that is present after cutin monomers have been removed by cleaving the ester bonds. Its exact composition and structure must still be elucidated. Plants may contain cutin, cutan, or any ratio of the two depending on development stages and species. Correlations between the cutin: cutan ratio and cuticle characteristics have not yet been found.

Plant wax is a complex mixture of open-chain aliphatics and alicyclics. The aliphatics are comprised of very-long-chain fatty acids and their derivatives, such as aldehydes, alkanes, primary and secondary alcohols, esters, and ketones (Jetter *et al.* 2007). These occur in homologous series ranging in length from 20 to 70 carbons, although compounds with 26-31 carbons dominate. Waxes also include cyclic compounds such as triterpenoids and phenolics. Triterpenoids are 30 carbon molecules which are usually pentacyclic. Phenolics, such as flavonoids and phenylpropanoids, contain one or more aromatic ring. Both of these groups contain various attached functional groups. The presence of specific wax constituents and their relative percentages differ between plant species and between different organs of the same species (Jetter *et al.* 2007). Distinct compositions have also been observed between the intracuticular and epicuticular wax (Jetter *et al.* 2000). Based on this finding, it was originally speculated that the wax may form a gradient with more hydrophilic compounds near the cell wall and more lipophilic compounds at the exterior edge. However, the literature on possible gradients between both wax layers has not been reviewed to date, and therefore the general patterns for distribution of wax compounds between the intra- and epicuticular compartments cannot be assessed. Furthermore, the presence of a gradient within either the epi- or intracuticular wax has not yet been shown. Finally, many constituents within the wax mixtures of the plant species investigated to date could not be identified, and the structures of those novel compounds are still being elucidated.

1.4 Wax biosynthesis – very-long-chain aliphatics

The specific wax composition on any given plant surface depends on the present wax biosynthetic machinery. For the ubiquitous very-long-chain aliphatic compounds, this machinery includes enzymes responsible for first elongating acyl-Coenzyme A (CoA) intermediates and second modifying the elongated products into the respective compound classes (Reviewed in Kunst *et al.* 2007; Samuels *et al.* 2008). As the majority of research characterizing these enzymes has been performed on *Arabidopsis thaliana*, this organism will be used to briefly exemplify the current understanding of wax precursor elongation and modification.

Elongation proceeds in cycles that extend the starter chain by two carbons. Each cycle is known to require four enzymes (Samuels *et al.* 2008). A β-ketoacyl-CoA synthase (KCS) first

condenses an acyl-CoA with malonyl-CoA to form β-ketoacyl-CoA. This is subsequently reduced to β-hydroxyacyl-CoA, dehydrated to enoyl-CoA and then again reduced to a final saturated acyl-CoA. Arabidopsis contains 21 KCSs, of which only five have been characterized (Joubes *et al.* 2008). Of these five, only KCS6/CER6 has been shown capable of elongating compounds to typical (i.e.: C_{30}) wax chain lengths. The KCS enzymes likely control substrate/product chain-length specificity (Millar *et al.* 1997). In contrast, the final three reactions in all elongation cycles are catalyzed by single gene products, namely KCR1, PAS2, and CER10, regardless of the chain length (Zheng *et al.* 2005; Bach *et al.* 2008; Beaudoin, Wu *et al.* 2009).

After the chain length distribution is set by the elongase complex, further modifying enzymes generate compound classes in varying ratios (Samuels *et al.* 2008). The alcohol (reduction) pathway involves a fatty acyl reductase (FAR; specifically CER4 in Arabidopsis; Rowland *et al.* 2006) to reduce acyl-CoAs to primary alcohols, which are then either exported to the cuticle or esterified to (typically C_{16} or C_{18}) fatty acids by WSD1 (Li *et al.* 2008). Alternatively, the alkane (decarbonylation) pathway yields aldehydes and alkanes with the aid of (at least) CER3 and CER1. Alkanes may be oxidized to mid-chain secondary alcohols and ketones by the cytochrome P450-dependent enzyme MAH1 (Greer *et al.* 2007). Although many wax biosynthetic genes have been characterized, details of the pathways still require confirmation.

1.5 Wax biosynthesis – triterpenoids

The formation of pentacyclic triterpenoids relies on the presence of triterpenoid synthases (TTPS). All plant cells form the compound 2,3-oxidosqualene, an intermediate in the production of membrane steroids. Single enzymes convert this linear substrate into numerous pentacyclic products.

The *Arabidopsis thaliana* genome contains thirteen potential TTPSs. Of the twelve that have been expressed in yeast, eleven have been shown to be multifunctional (i.e.: synthesizing more than one product; see Table 1.1 and references there-in). Only AtLUP4 was found to produce a single product (β-amyrin; Shibuya *et al.* 2009). Only four (AtLUP1, 2, and 4 and AtPEN6) produced triterpenoids that have also been found in cuticular wax in appreciable quantity (Table 1.1).

The cuticular wax of Arabidopsis has been shown to contain pentacyclic triterpenoids (Jenks *et al.* 1995; Husselstein-Muller *et al.* 2001; Shan *et al.* 2008). The three triterpenoids β-amyrin, lupeol, and its derivative trinorlupeol account for the majority of the cuticular triterpenoids, although minor quantities of β-amyrinone, lupenone, trinorlupenone and α-amyrin have also been detected (Shan *et al.* 2008). Within the Columbia ecotype, triterpenoids have been found in all aerial organs except rosette and cauline leaves (Shan *et al.* 2008). However, it is not clear which one(s) of the 13 TTPSs are responsible for synthesizing specific triterpenoids in each organ. The pentacyclic triterpenoids in Arabidopsis accumulate in cuticular wax to nearly double the concentration found in the underlying tissue (Shan *et al.* 2008), suggesting that pentacyclic triterpenoids are preferentially destined for the cuticle. Similar epidermis-increased synthesis of pentacyclic triterpenoids has been shown for *Ricinus communis* (Guhling *et al.* 2006), *Kalanchoe daigremontiana* (Wang *et al.* 2010a), and *Solanum lycopersicum* (Wang *et al. 2010b*). This also implies that triterpenoids can be exported from the epidermis to the cuticle.

Table 1.1 Annotated triterpenoid synthases in *Arabidopsis thaliana*, along with their aliases, *in vitro* yeast products, and respective references.

Name	Gene	Products formed in yeast	Reference
AtLUP1	At1g78970	lupeol, β-amyrin, unidentified	(Herrera *et al.* 1998)
		lupeol (39%), 3,20-dihydroxylupane (39%), β-amyrin (8%), germanicol (7%), taraxasterol (4%), ψ-taraxasterol (3%),	(Segura *et al.* 2000)
		Lupeol	(Husselstein-Muller *et al.* 2001)
AtLUP2	At1g78960 (YUP8H12R.43)	lupeol, taraxasterol, β-amyrin, ψ-taraxasterol, bauerenol, α-amyrin, multiflorenol, butyrospermol, tirucalla-7, 21-dien-3β-ol	(Kushiro *et al.* 2000)
		β-amyrin, α-amyrin, lupeol	(Husselstein-Muller *et al.* 2001)
LUP3 / CAMS1	At1g78955	camelliol C (98%), archilleol A, β-amyrin	(Kolesnikova *et al.* 2007)
LUP4	At1g78950	β-amyrin	(Shibuya *et al.* 2009)
LUP5	At1g66960 (F1019.4)	tirucalla-7,21-diene-3β-ol, 2 unidentified	(Ebizuka *et al.* 2003)
PEN1	At4g15340	no products	(Husselstein-Muller *et al.* 2001)
		arabidiol (major), arabidiol-20,21-epoxide (minor)	(Xiang *et al.* 2006)
PEN2 / BARS1	At4g15370	baruol (90%) + 22 very minor products	(Lodeiro *et al.* 2007)
PEN3	At5g36150	tirucalla-7,21-diene-3β-ol + minor products	(Morlacchi *et al.* 2009)
PEN4 / THA1	At5g48010	thalianol	(Fazio *et al.* 2004)
PEN5 / MRN1	At5g42600	marneral (major), marnerol (major), camelliol C (tr), achilleol A (tr), 1 unidentified	(Xiong *et al.* 2006)
PEN6	At1g78500 (T30F21.16)	lupeol, bauerenol, α-amyrin, 6 unidentified	(Ebizuka *et al.* 2003)
		lupeol, bauerenol, α-amyrin, α-seco-amyrin, β-seco-amyrin	(Shibuya *et al.* 2007)
PEN7 / LAS1 / LSS1	At3g45130	lanosterol, 1 unidentified	(Suzuki *et al.* 2006)
		lanosterol	(Kolesnikova *et al.* 2006)

1.6 Wax structure model

At the molecular level, a model has been proposed for the physical structure of plant wax based on its chemical nature, which can explain most of the observed functional properties. This structure can be categorized into four zones (Figure 1.2; Riederer *et al.* 1995; Reynhardt 1997). Zone A represents crystalline regions. In this zone, the hydrocarbon tails of the aliphatics maintain all trans conformations between the carbons and produce a molecule that is linear overall. As a result, the tails can densely align and order, since they are held together by van der Waals interactions (Merk *et al.* 1998). Ordered wax molecules aligned in parallel form crystalline, aliphatic sheets, whose presence is supported by nuclear magnetic resonance (Schreiber *et al.* 1997), Fourier transform infrared spectroscopy (Merk *et al.* 1998), and X-ray diffraction (Riederer *et al.* 1995) studies. These sheets have a flat surface that is thought, based on polarized light studies, to be aligned parallel to the cuticle surface (Riederer *et al.* 1995). However, the mean and range of areas for crystalline sheets are completely unknown.

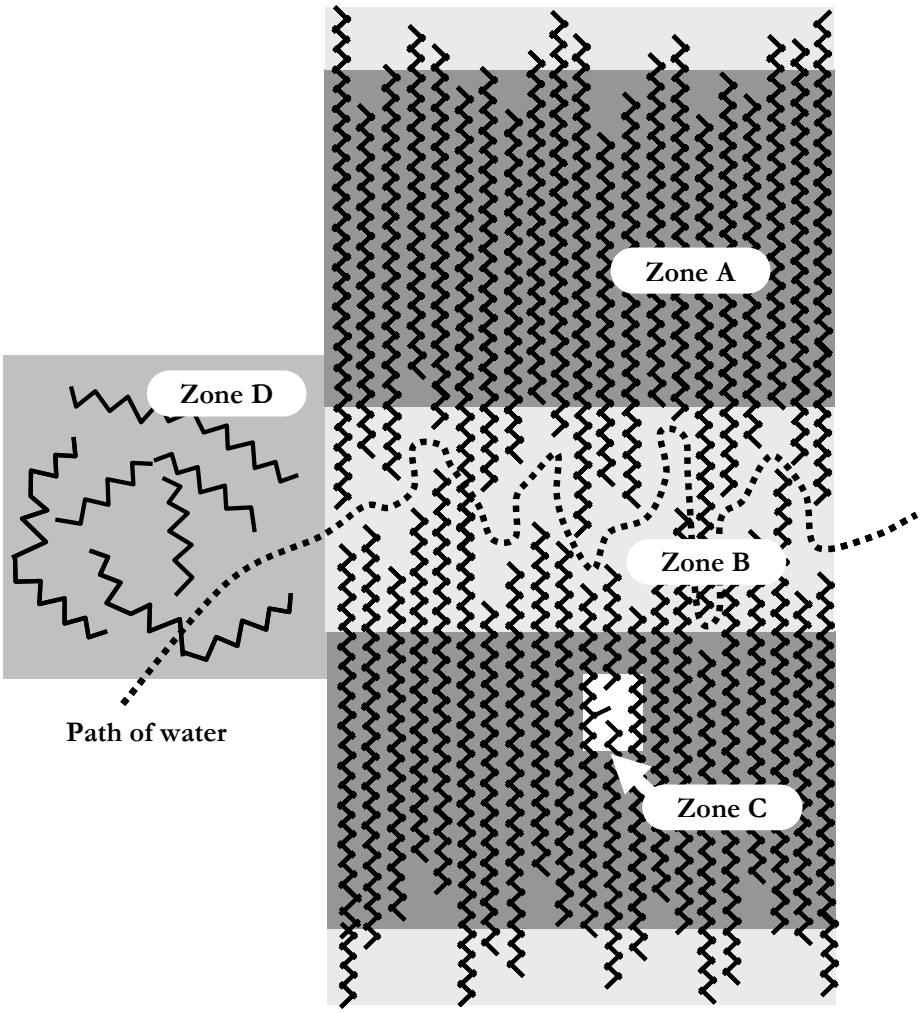

Figure 1.2 Model of the molecular structure of wax. Solid black lines represent individual, aliphatic wax molecules while the dashed line delineates a probable pathway for water molecules. Zone A (dark gray) shows linear molecules forming a crystalline region. Zones B (light gray), C (white), and D (medium gray) represent disordered, amorphous wax between, within, and separate from Zones A, respectively. The amorphous regions result from molecule geometries that do not permit ordered packing. Figure adapted from Reynhardt (1997).

Zone B encompasses the areas between neighboring crystalline sheets (Figure 1.2; Riederer *et al.* 1995). Because the tail lengths of wax molecules range from 20 to 35 carbons (excluding the 32 to 64 carbon wax esters that span two Zone A's), hydrocarbon tails probably protrude unequally from the crystalline regions. These longer ends prevent a continuous series of crystalline sheets by creating a gap between adjacent sheets. The longer chain ends may also twist and interweave which causes disorder in conjunction with the bulky, functional head

groups. Also, it is possible that some alicyclics intercalate here between the crystalline regions. The total result is a zone of disordered, solid, amorphous wax. The volume and thickness of this zone have neither been measured nor estimated.

Very similar to Zone B, Riederer *et al.* (1995) suggest a third zone, Zone D, which is also comprised of disordered, amorphous wax (Figure 1.2). In contrast to Zone B, Zone D is created from wax molecules that are excluded from crystalline sheets. Since the longer chains should crystallize first, the shorter chains would less likely be included in the crystalline regions and thus should dominate this amorphous zone. Additionally, since unsaturated and branched chains might disrupt the ordered packing and thus also the van der Waals forces if combined with the straight chains, they too should be present at higher amounts in this zone. Alicyclic compounds are probably preferentially located in this zone as well. The ratio of solid: liquid amorphous wax within this zone would depend on temperature. Such a zone has not been shown experimentally to exist in cuticular wax.

In very small proportions or in clusters, aliphatics with secondary functional groups or branches may either be incorporated into crystals (Zone C) or form their own crystals (Figure 1.2; Riederer *et al.* 1995). Again, the presence of such a zone has not been shown for plant wax. Overall, this model suggests that wax composition defines the physical, molecular structure.

This structural model leaves two major questions: In which zone(s) are individual compounds found? Do compound classes, groups of compounds with similar chain lengths, and combinations thereof increase or decrease crystallinity? For example, do homologous compounds co-crystallize to form crystalline regions? Do compounds from mixed compound classes but similar chain lengths co-crystallize or are crystalline regions pure in composition? It remains unknown whether one or all of these possibilities occur in plants.

1.7 Water pathway model

In consideration of the proposed model for the molecular arrangement of wax, how exactly does water move through the cuticle? In the lipophilic pathway, water is thought to diffuse through the amorphous regions (zones B and D) where the wax molecules are less densely packed, as water cannot enter the wax crystalline regions (zone A; Figure 1.2; Riederer *et al.*

1995; Riederer *et al.* 2001). The cuticular water barrier is thus formed by crystalline regions of hydrophobic, aliphatic wax molecules. These regions drastically lengthen the pathway through the wax. The length ratio between a direct path across the cuticle and the longer route around the crystalline domains is termed the 'tortuosity factor' (Baur *et al.* 1999). Since an increase in tortuosity increases water resistance, wax compounds that increase crystallinity should correspondingly increase water resistance. However, just as the contribution of wax compound classes and chain lengths to crystallinity has not been established, the contribution of specific wax compounds to the water barrier also remains unknown.

This model has not been tested, largely because the crystalline and amorphous zones cannot be directly visualized. Accordingly, their geometries and dimensions, which are crucial in forming the water barrier, also cannot be determined. Moreover, the distribution of compounds within and between these postulated zones has not been analyzed and remains unknown. To begin to address this issue, one first possible task is to intentionally manipulate the proportions of crystalline and amorphous domains such as by increasing the quantity of alicyclic wax molecules, as these would form or accumulate in amorphous domains (Zones B and/or D; Figure 3).

1.8 Water barrier effectiveness

Similar to the wide range of compositions observed in waxes of diverse species, the effectiveness of the cuticle at blocking water movement, its primary function, also varies considerably. The transpiration barrier effectiveness of cuticles may be measured by the amount of water that moves across them since cuticles are pervious barriers. The flux of water across a cuticle (J; kg m^{-2} s^{-1}) is proportional to the magnitude of the force driving the movement, namely, the difference in water concentration between either sides of the cuticle (Δc; kg m^{-3}; Riederer *et al.* 1995):

Equation 1.1 $$\mathbf{J = P\Delta c}$$

The proportionality constant P (m s^{-1}), or permeance, accounts for how easily water (or any specific permeant) passes through a cuticle and is therefore species and organ specific.

Opposite to permeance, resistance (R; s m^{-1}) is the inhibition of water movement through a cuticle. Resistance and permeance may be interconverted according to the equation:

Equation 1.2 $\mathbf{R = P^{-1}}$

Both resistance and permeance may be considered measures of effectiveness and ineffectiveness of a cuticle's primary function, respectively. Moreover, because they remain independent of water concentration, these values provide a way to compare the effectiveness of cuticles as barriers between any plant species under standard conditions.

Most studies to date have determined P for easily isolated and manipulated cuticles from astomatous surfaces. Similar measurements may also be made for cuticle-covered tissues that contain stomata. For surfaces with (presumably) closed stomata, the value obtained is referred to as the minimum conductance (g_{min}) instead of P since some residual stomatal conductance may remain. It remains unclear how much water escapes through apparently closed stomata. However, it has been estimated to be in the same order of magnitude as that escaping through the cuticle (Kerstiens 1996a) and has been calculated to contribute 35% of g_{min} for *Hedera helix* (Šantrůček *et al.* 2004).

Water permeance values and the corresponding cuticle effectiveness vary widely. In addition to differences between species, general trends have been observed for organs. Permeances of leaf cuticles averaged 1.42 x 10^{-5} m s^{-1} as compared to that of fruit cuticles that averaged 9.93 x 10^{-5} m s^{-1} (Kerstiens 1996a). On average then, leaf cuticles provide a better barrier against water movement than fruit cuticles. No published water permeance values are known for flower petals or stems.

Published water permeance values for land plants range from 0.36 x 10^{-6} to 200 x 10^{-6} m s^{-1} (Kerstiens 1996a). This difference of three orders of magnitude suggests that some plants have compositions, and thus structures, that are relatively unfavorable to blocking water. For these plants to maintain such compositions, some of the compounds present might also contribute to an alternative function(s).

1.9 Secondary functions

Several secondary functions have been shown or hypothesized for the cuticle (Kerstiens 1996b). For abiotic interactions, the cuticle functions as the last barrier for escaping internal compounds, including metabolites and ions, and as the first barrier encountered by all foreign chemicals, including herbicides, pesticides, and pollutants. It also forms the first protection from rain and wind. The cuticle keeps the plant clean as described by the 'lotus effect' (a self-cleaning mechanism whereby a super-hydrophobic surface causes surface water to bead, role, and wash off surface particulates; Neinhuis *et al.* 1997) and in some species may act as a sunscreen by absorbing ultraviolet light (Kerstiens 1996b). For biotic interactions, the cuticle also functions as the initial barrier. It physically resists penetration by fungi and insects while its chemical anti-feedants deter herbivores. Alternatively, the cuticle chemicals may act as signaling molecules for host recognition. Finally, the cuticle is the foundation for the phyllosphere (microorganisms residing on a plant surface). It is uncertain for most of these interactions whether or not the role the cuticle plays is a real function or simply a characteristic that allows for the interaction. living

In light of the ecological and physiological functions, the current understanding of cuticular structure, composition and function reveals three key ideas. (1) Cuticles have multiple functions. (2) Cuticle composition varies between species, organs, and cuticle layers. (3) The composition differentially determines the effectiveness of various functions. From these three points the question arises: **How does each cuticular compound affect each function?** To begin to address this question, contributions are required from many aspects of cuticle research, including structure elucidation of novel compounds, localization of compounds in layers (subcellular) as well as on cell types and organs, and functional characterization. Each aspect also requires a suitable model system. To help answer the fundamental question, the research presented in this thesis addresses three specific aspects: What compounds are present (mainly chapter 3 but also chapters 2, 4, and 6)? Where are the compounds located and how uniform is cuticular wax composition at the cellular (chapters 2 and 4) and subcellular levels (chapters 5 and 6)? How does wax composition affect water permeability (chapters 2 and 6)? In the following, the specific research questions and approaches taken in the various chapters will be introduced.

1.10 Petal cuticles

The ecological functions of petal cuticles involved in attracting pollinators might reduce the primary function of limiting water loss to a functional minimum. In other words, if a petal's wax composition were fully optimized for limiting water loss, then ecological functions such as scent release might be hampered (see "water barrier effectiveness" and "secondary functions"). Correspondingly, if the composition were optimized for ecological functions, the plant might suffer from severe water loss. A compromise in composition is therefore necessary to ensure the best balance of functions. Petals should therefore provide an interesting model for studying the balance between both functions, and should more clearly show which compounds truly increase the water barrier as opposed to compounds that decrease the barrier (see "wax structure model" and "water pathway model") because they are necessary for another function.

Petals also offer physical advantages as a model system for studying the function-composition question. They are frequently devoid of stomata and often have large surface areas, which facilitate their manipulation for extracting wax and setting up permeance studies. Despite these advantages, no known reports to date detail the permeability of flower petal cuticles (see "water barrier effectiveness". Obtaining such data would broaden the range of systems available for probing structure-function relationships. The Asteraceae species *Cosmos bipinnatus* makes an ideal candidate for studying petal permeances and cuticle composition. This resilient plant grows rapidly and produces many flowers over a several week period. It exhibits the positive attributes of flowers in general, such as no stomata and large petal area. For these reasons, the ray flowers of *C. bipinnatus* were examined in Chapter 2 to determine the following:

1) What is the wax composition on the adaxial and abaxial petal surfaces of *C. bipinnatus* and how does it compare to the stem and leaf wax compositions?

2) How permeable to water are these petal cuticles and how do these values compare to values known for leaf and fruit cuticles?

A more detailed analysis of *C. bipinnatus* petal wax composition (beyond the wax compound classes identified in "cuticle composition") revealed five unidentified homologous series of

very-long-chain compounds. Thus, in chapter 3, GC-MS was used to analyze various derivatives of the compounds in these series in order to discover:

1) What are the structures of the unidentified compounds in the five homologous series found in *C. bipinnatus* petal wax?

Analysis of petal composition and water resistance provides new data on how plant organs balance diverse cuticle functions. However, it cannot determine the function(s) of specific compounds such as the novel compounds described in Chapter 3. Further comparisons such as would be obtained by analyzing additional species would be limited due to confounding potential differences in cell shape, cutin, and/or wax compounds present. Until significant advances are made in molecular genetic techniques for species with large flowers that permit intentional manipulation of petal wax composition, analyses attempting to link composition to function will remain strictly descriptive.

1.11 Arabidopsis as a model system

A system is needed where wax composition can be easily modified within the same species. For this reason, *Arabidopsis thaliana* was considered. Several gene mutations have been identified that each alter the aliphatic wax composition in *A. thaliana* (Reviewed in Kunst *et al.* 2007), including several that result in distinguishable wax chemotypes in leaves.

Although the molecular genetic tools have been developed for *A. thaliana*, the leaves of this species contain protruding hairs – trichomes – that confound permeance analyses, similar to the paraboloid adaxial epidermal cells in *C. bipinnatus*. This occurs through both increasing the true surface area over a complex trident shape as well as through modifying the external water concentration in the vicinity of trichomes. Thus, a mutant without trichomes would facilitate further wax composition/function studies. As well, no studies to date have quantitatively addressed potential cell-type specific wax compositions; it is not known whether trichome wax is identical in composition to pavement cell wax. For these reasons, the leaf and stem waxes from the trichomeless mutant *gl1* were analyzed to establish a baseline control. This was then compared to leaf and stem waxes as well as pure leaf trichome wax from both WT and *cpc tcl1 etc1 etc3*, a mutant with an abundance of trichomes. Thus, in Chapter 4, the following questions were addressed:

1) What are the wax compositions on *Arabidopsis thaliana* trichomes and non-trichome epidermal cells?

2) How do these differ with respect to chain length distribution (wax elongation) and compound class ratios (wax modification)?

After demonstrating cell-specific wax composition (that depends on the specific VLC aliphatic biosynthetic machinery outlined in "Wax biosynthesis – very-long-chain aliphatics") and firmly establishing the composition of the trichomeless mutant *gl1*, further composition and water resistance studies could begin. Prior to performing a more detailed analysis of *A. thaliana* leaf wax by examining the epicuticular and intracuticular wax layer compositions (see "cuticle structure"), literature was surveyed in Chapter 5 to evaluate the following:

1) What methods are now available for selective sampling of epi- and intracuticular waxes?

2) Do trends in compound partitioning exist between the epicuticular and intracuticular wax layers?

3) What are the possible mechanisms causing compositional differences between the epicuticular and intracuticular wax layers?

4) What are the implications of wax compounds partitioning into distinct layers on cuticle function?

This meta-analysis revealed that cyclic compounds such as pentacyclic triterpenoids partitioned almost exclusively into the intracuticular wax layer. Moreover, according to the current theory on the molecular nature of the water barrier, bulky cyclic compounds should greatly increase the volume of the amorphous domain and consequently cause a significant reduction in the water barrier effectiveness (see "wax structure model" and "water pathway model"). For these reasons, β-amyrin was produced in *A. thaliana* leaves by over-expressing AtLUP4 (the only monofunctional triterpenoid cyclase in *A. thaliana* where the product has been found in cuticular wax; see "wax biosynthesis - triterpenoids") and extensive leaf wax analyses were performed. Specifically, Chapter 6 addresses the following questions:

1) As compared to the total leaf wax, how distinct is the wax composition on the adaxial and abaxial surfaces of the leaf?

2) Within the adaxial leaf wax, what are the absolute and relative contributions of the epicuticular and intracuticular wax layers?

3) Where do non-naturally occurring triterpenoids (specifically β-amyrin) partition if they are produced in a clean leaf background?

4) How much does each wax layer block water movement?

5) How does the presence of cyclic triterpenoids affect cuticular water barrier properties?

In conclusion, the research presented here first explored and refined cuticular wax compositions at the organ, cellular and sub-cellular levels. Waxes from *Cosmos bipinnatus* petals, stems, and leaves were shown to be distinct. Lateral wax heterogeneity was detected between waxes covering pavement cells and trichomes in *Arabidopsis thaliana*. The cyclic compound β-amyrin accumulated solely in the intracuticular wax layer when produced in leaves that lack pentacyclic triterpenoids. This non-uniformity of cuticular composition suggests that the wax must mediate specific secondary functions in the different locations. Second, this research examined the effectiveness of the water barrier in two systems. Petal cuticles from *C. bipinnatus* were overall less effective at blocking water than leaves and fruit of species reported in the literature. Pentacyclic triterpenoids decrease the effectiveness of the water barrier in *A. thaliana*.

Chapter 2
Petal wax from *Cosmos bipinnatus* 'Pinkie' cuticles contains shorter constituents than stem and leaf waxes and creates a comparatively poor water barrier

2.1 Introduction

Plant flowers are specially adapted to ensure reproductive success. In many species, petals with papillose cells project from prominently displayed flowers while showing their pigmentation and emitting scents in order to attract and assist pollinators. However, petals must also resist unfavourable environmental conditions such as a desiccating atmosphere. The characteristics that increase reproductive success also make petals more vulnerable to drying out: high surface areas in exposed locations, restriction to transparent water barrier compounds, and water barriers permeable to small molecules (Goodwin *et al.* 2002; Baudino *et al.* 2007). Thus, despite their short life span, petals must protect themselves with a water barrier that still permits these ecological functions or, at a minimum, attains a compromise between competing functions. In other words, petals must be simultaneously optimized for successful pollination and water retention. This raises several questions: 1) How effective are petal cuticles at blocking water and what is the minimum necessary effectiveness? 2) What chemical composition is necessary for a water barrier and/or for pollinator interactions and are these compounds compatible?

The (in)effectiveness of a water barrier may be characterized by quantifying the permeance (P; m s^{-1}) or, inversely, resistance (R; s m^{-1}; Riederer *et al.* 1995). These proportionality constants equal the water flux (*J*; kg m^{-2} s^{-1}) across a barrier as a proportion of the force driving the water movement (effectively the change in water concentration, Δc; kg m^{-3}) according to the equation:

Equation 2.1 $$P = J/\Delta c$$

Because P and R are independent of water concentration, these values provide a way to compare the effectiveness of water barriers between any plant species or organ under standard conditions.

Water permeance values and the corresponding barrier effectiveness vary widely, with a range of 0.36-200 x 10^{-6} m s^{-1} for plant surfaces tested to date (Kerstiens 1996a). Since the average leaf permeance (1.42 x 10-5 m s-1) was less than the average fruit permeance (9.93 x 10-5 m s-1.), then in general leaves produce a better barrier against water movement than fruit (Kerstiens 1996a). To date, no water permeance values have been published for petals and thus cannot be compared to these organs.

The water barrier coating the primary parts of shoots consists of a lipophilic layer called the cuticle. Although this layer seamlessly coats the entire surface, including that of petals, its composition differs between species, organs and even within organs. The cuticle consists of a polymer cutin interspersed and covered with waxes (Walton 1990; Nawrath 2006; Jetter *et al.* 2007; Pollard *et al.* 2008). Waxes ubiquitously include very-long-chain compounds, including alkanes, aldehydes, primary and secondary alcohols, fatty acids, esters, and ketones ranging in chain length from 20 to 70 carbons (Jetter *et al.* 2007). The ratio between these derivatives varies spatially and temporally (e.g. (Jenks *et al.* 1995; Jetter *et al.* 2001). As well, wax may contain cyclic compounds such as pentacyclic triterpenoids (Jetter *et al.* 2007). Although any combination of these compounds may be used in petal cuticles to ensure the best balance of functions, petal wax from species examined to date show that their compositions predominantly fall within the range of compounds observed on other organs (Kolattukudy *et al.* 1974; Akihisa *et al.* 1997; Griffiths *et al.* 2000).

Petals provide an excellent model for studying cuticular wax composition and water permeability. Broad, flat petals facilitate experimental set-up while the lack of stomata on the petals of many species reduces confounding factors. Moreover, if petals indeed have a relatively high permeability, they broaden the range of systems available for probing structure-function relationships. For these reasons along with its rapid maturation and prolific flower production, *Cosmos bipinnatus* 'Pinkie' was selected for further analysis. The ray flowers were examined to determine 1) what is the wax composition on the adaxial and abaxial petal surfaces and how does this compare to the stem and leaf wax? And 2) how permeable to water are these petal cuticles and how do these values compare to values known for leaf and fruit cuticles?

2.2 Methods

2.2.1 Plant material

Seeds of *Cosmos bipinnatus* 'Pinkie' (Stokes Seeds Ltd., St. Catherines, Canada) were placed on an agar medium (5 mM KNO_3, 2.5 mM KH_2PO_4, 2 mM $MgSO_4$, 2 mM $Ca(NO_3)_2$, 50 μM NaFe(EDTA), 70 μM H_3BO_3, 14 μM $MnCl_2$, 10 μM NaCl, 1 μM $ZnSO_4$, 0.2 μM $NaMoO_4$, 0.05 μM $CuSO_4$, 0.01 μM $CoCl_2$, and 7% agar; Somerville *et al.* 1982), stratified for 2-3 days at 4°C, and then germinated under continuous light (~150 μmol $m^{-2}s^{-1}$ photosynthetically active radiation) for a week at 20°C. Seedlings were transplanted into soil (Sunshine mix 4) and grown under 12 hour days / 12 hour nights at a constant 20°C temperature. In addition to frequent watering to keep the soil moist, the plants were watered weekly with MiracleGro. Petals from flowers were harvested 3-7 days post anthesis for wax and permeance analyses (Figure 2.1 A, B). Stems from internodes 5-6 and the distal 3-5 cm of leaves originating from nodes 4-5 were harvested approximately two months after germination and used for wax analyses (Figure 2.1 C, D).

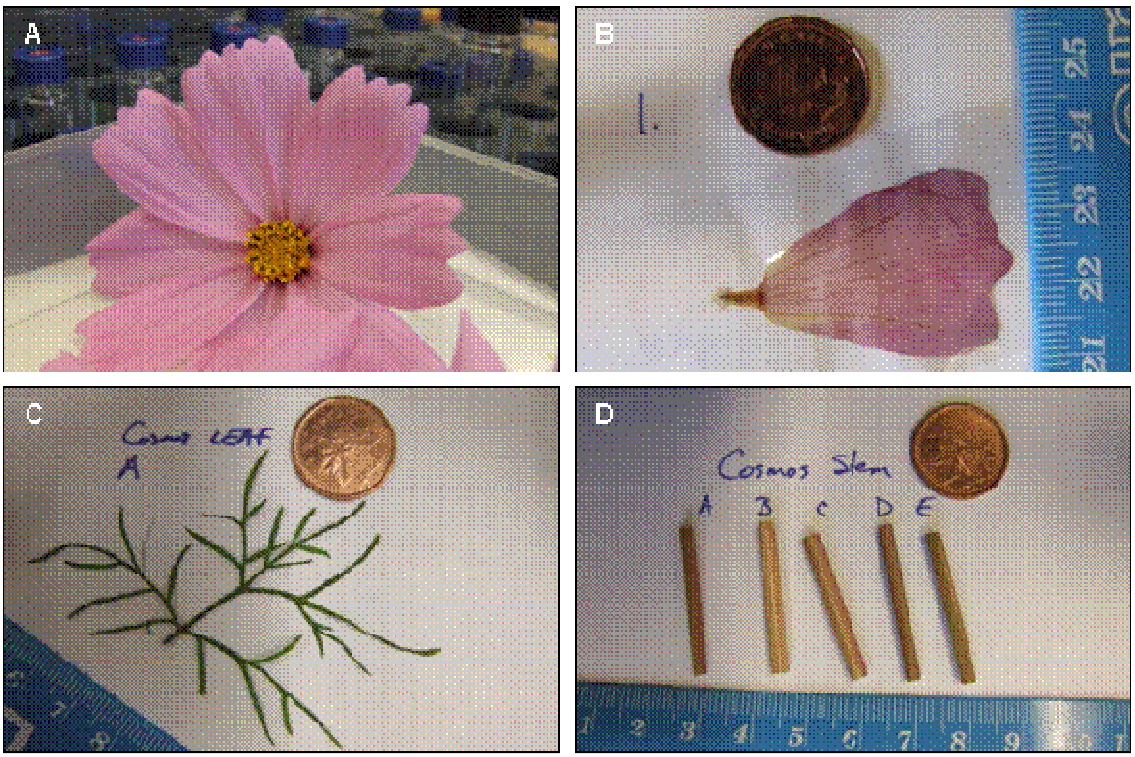

Figure 2.1 The wax composition and water permeability was analyzed for ray flower petals (A, B), while the wax composition was also investigated for leaves (C), and stems (D) of *Cosmos bipinnatus*

2.2.2 Microscopy

Petals were examined by cryo-scanning electron microscopy (SEM). Specimens were first infused with osmium vapour, attached to the specimen holder using Tissue Tek and then plunge-frozen in liquid nitrogen. From then on, samples were maintained under vacuum and/or at approximately -150°C. After transfer into the preparatory chamber (Leica EM CPC), surface ice crystals were sublimed at –50°C for 30 minutes and a probe was used to break the frozen petal to view epidermal cells in cross-section. The petal was then coated with ~8 nm of gold before viewing with a Hitachi S4700 scanning electron microscope equipped with a temperature-controlled stage (Emitech K1250 Cryo-System). ImageJ (Abramoff *et al.* 2004) was used to measure epidermal cell radii (r) and heights (h) from digital images of the samples. From these, the increase in surface area (SA) was calculated by dividing the paraboloid surface area ($SA = (\pi r/6h^2)((r^2+4h^2)^{2/3}-r^3)$) by the apparent surface area of a circle ($SA = \pi r^2$).

2.2.3 Wax extraction and derivatization

To extract the waxes from entire petals, leaves, or stems, the organs were submerged for 30 sec in $CHCl_3$ containing a defined quantity of *n*-tetracosane as an internal standard. Samples were re-submerged for 30 sec in fresh $CHCl_3$ and the two solutions were pooled. Adaxial or abaxial-specific wax was extracted by pressing a glass cylinder on to the petal surface (Jetter *et al.* 2000). $CHCl_3$ with a defined quantity of *n*-tetracosane was added for 30 sec with gentle agitation and then removed. A second wash with $CHCl_3$ for 30 sec was added and the two solutions pooled. The solvent from the pooled samples was evaporated under a gentle stream of N_2 gas while heating at 50°C. Samples were derivatized with excess of bis-N,O-(trimethylsilyl)trifluoroacetamide (BSTFA) in pyridine for 30 min at 70°C. The solvents were then evaporated before $CHCl_3$ was again added to the wax.

2.2.4 Wax identification and quantification

Wax constituents were separated by capillary GC (6890N, Agilent, Avondale, PA, USA; column 30 m HP-1, 0.32 mm i.d., df=0.1 μm) using the following temperature program: on-column injection at 50°C, oven held for 2 min at 50°C, raised by 40°C min^{-1} to 200°C, held for 2 min at 200°C, raised by 3°C min^{-1} to 320°C, and held for 30 min at 320°C. For compound identification, the GC was linked to a mass spectrometric detector (5973N, Agilent) and the

inlet pressure programmed for a constant 1.4 ml min^{-1} flow of He carrier gas. For compound quantification, the GC with inlet pressure programmed for constant flow of 2.0 ml min^{-1} of H_2 carrier gas was connected to a flame ionization detector (FID).

The quantity (μg) was established by comparing peak areas to that of n-tetracosane, the internal standard added at a specific quantity to the total wax extracts. To determine the extracted surface area, apparent surface areas were calculated with ImageJ software from digital photographs of the samples and multiplied by 2 for total apparent petal or leaf surfaces areas or multiplied by π for total stem surface area. Wax loads (μg cm^{-2}) were determined by dividing the compound quantity by the corresponding extracted surface area.

2.2.5 Water permeability analyses

Water loss was measured following Knoche *et al.* (2001). Briefly, petals were sealed across the opening of a cylindrical water-filled chamber with silicon grease applied along the ring of petal-chamber contact (Figure 2.2). The surfaces facing the water were scratched to ensure continuous access of water into the petals and thus maintain (as close as possible) 100% internal water concentrations. Chambers were inverted over silica desiccant in order to reduce the external water concentration to essentially 0%. Overall, this produced a gradient from 100% to 0% across the cuticle. Samples were allowed to equilibrate overnight at 25°C before gravimetrically measuring water loss. If the water flux accounted for less than 0.995 of the variation, the flux value was removed from further calculations. Dividing the water flux by the change in concentration (equal to the density of water at 25°C) yielded the permeance. Permeances are reported as geometric means in accordance with Baur (1997). Controls were created by puncturing sub-millimetre holes through the cuticle using a fine needle attached to a micromanipulator.

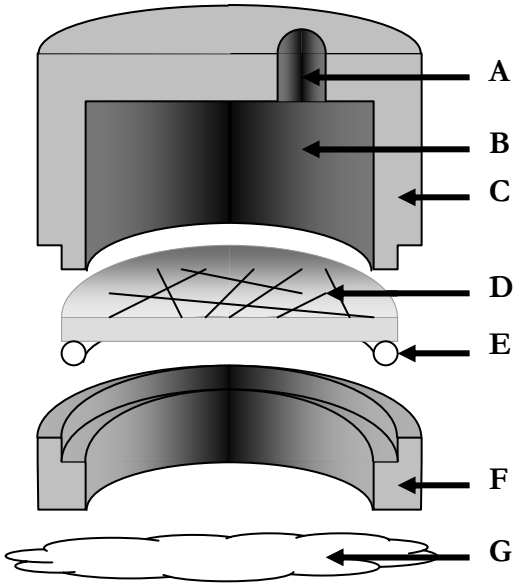

Figure 2.2 Experimental set-up for quantifying cuticle permeability. A plant surface scratched on the physiologically inner surface (D) is sealed between the base (C) of a stainless steel chamber and the lid (F) with a bead of silicon (E). The lid is then secured to the base with tape. Next, the reservoir (B) within the base is filled with water through the hole (A), which is subsequently sealed with tape. The chamber is finally placed over dessicant (G) in order to create a water concentration gradient from 100% (in B and D) to essentially 0% at G.

2.3 Results

2.3.1 Epidermal cell shapes

The outer surfaces of cosmos ray petals as viewed by scanning electron microscopy did not contain stomata or trichomes. However, the epidermal pavement cells showed distinct topologies between the abaxial and adaxial surfaces (Figure 2.3). The abaxial surface showed minor undulations in cross-section and the apparent surface area effectively equaled the true surface area. In contrast, the adaxial surface contained papillose cells that averaged 33±5 μm in diameter by 45±8 μm in protruding height (height difference between cell tip and the contact points with neighbouring cells; n=53 for both measurements). Assuming a paraboloid shape, this equates to a 3.8±0.5-fold increase in true surface area over the apparent surface area. All further analyses accounted for this greater surface area. No epicuticular wax crystals were visible on either surface.

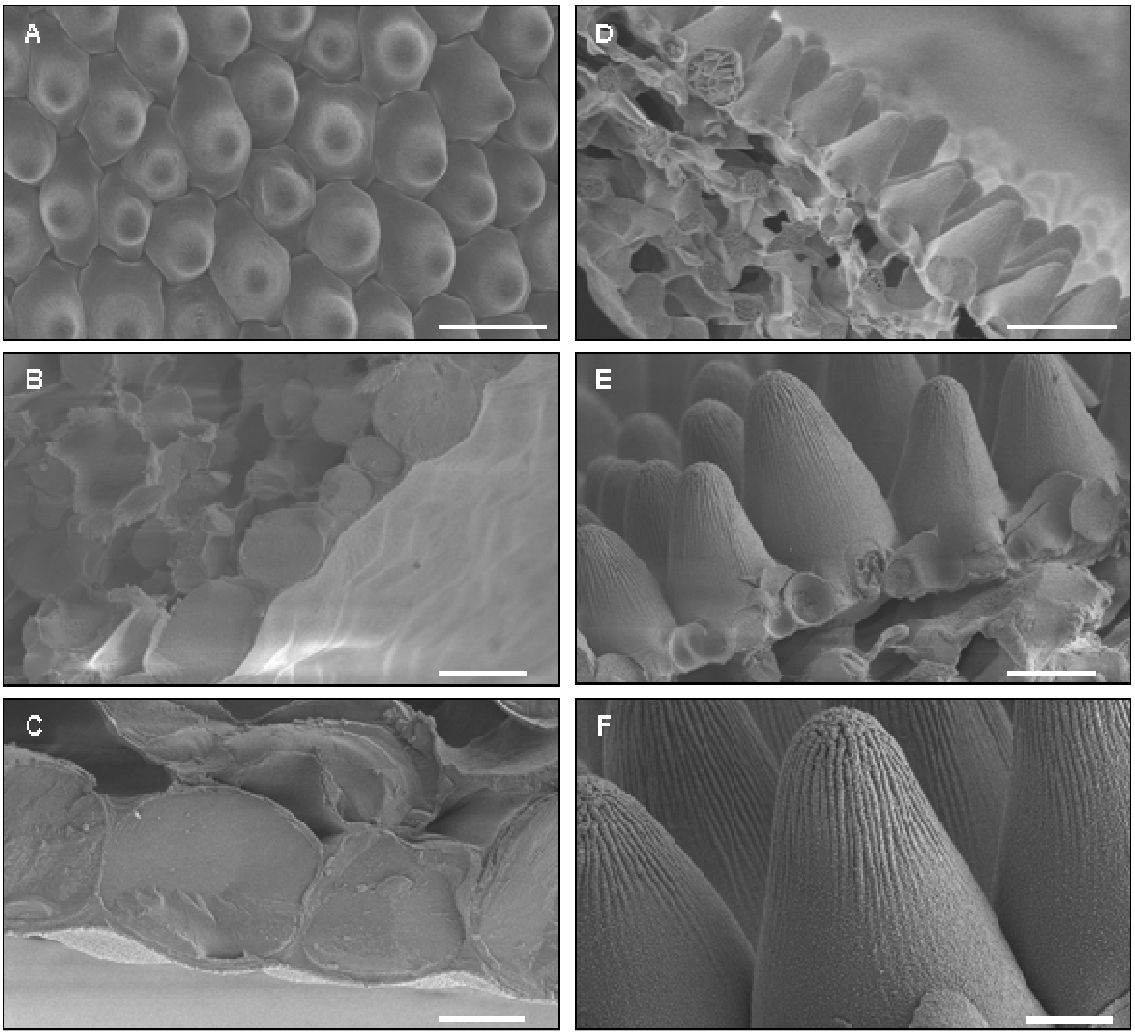

Figure 2.3 Scanning electron micrographs of *Cosmos bipinnatus* petals. Face-on (A) and cross sections (B-F) of the adaxial (A,D,E,F) and abaxial (B,C) petal epidermal cells. Bars = A,D – 50 μm B,E – 20 μm; C,F – 10 μm

2.3.2 Petal wax composition

Cosmos petals were coated in 2.7±0.4 μg/cm^2 of wax. By compound class, half of the wax was primary alcohols (1.5±0.1 μg/cm^2) while the rest consisted of alkanes (0.43±0.03 μg/cm^2), acids (0.26±0.02 μg/cm^2), triterpenoids (0.11±0.01 μg/cm^2), triterpenoid esters (0.08±0.01 μg/cm^2) and trace quantities of alkyl esters (<0.01 μg/cm^2; Figure 2.). The remaining 0.36±0.08 μg/cm^2 of the detected wax could not be identified.

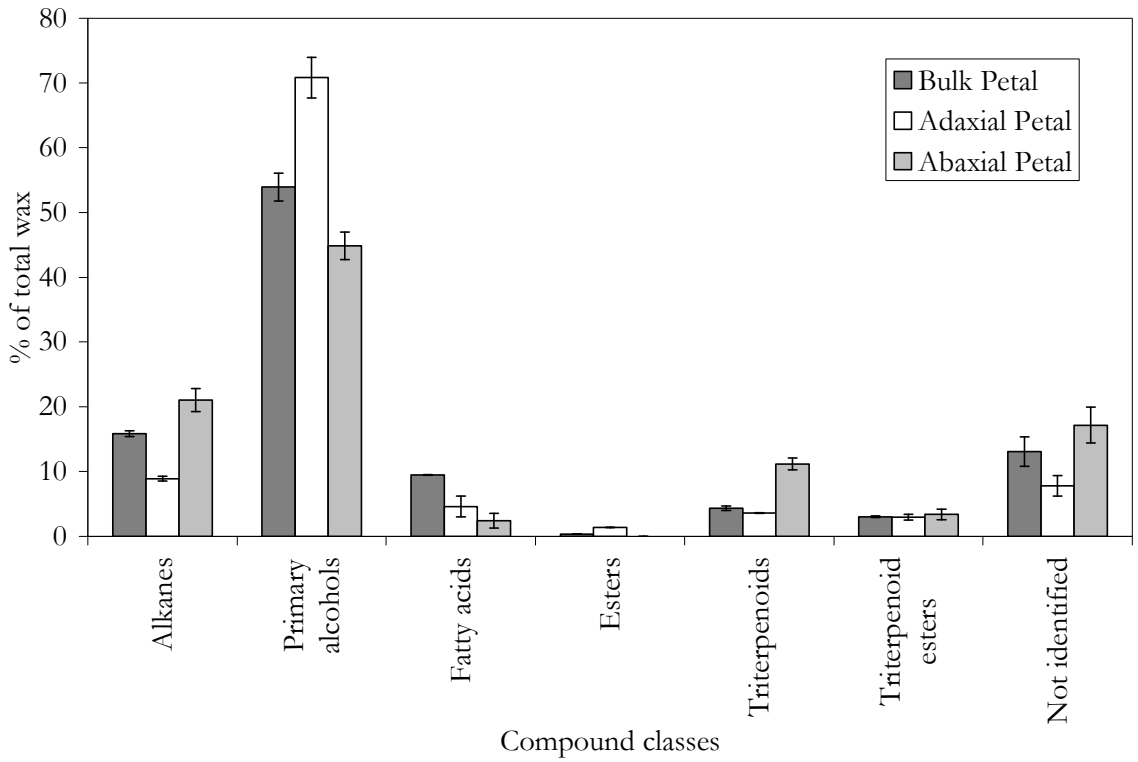

Figure 2.4 Wax compound classes (% of total wax ±SD) extracted from the entire (total), adaxial, and abaxial surfaces of *Cosmos bipinnatus* petals

The distribution and predominant compound chain lengths varied within each class (Figure 2.). Primary alcohols ranged from 20 to 30 carbons in length with mainly even numbers of carbons. C22 and C24 alcohols dominated this class and were also esterified to hexadecanoic acid in the only two esters detected. Alkane chain lengths ranged from 23 to 31 carbons, with C27 and C29 alkane present in greatest amounts. Because C25 alkane could not be separated from other compounds by only gas chromatography (GC), the alkanes were first isolated by thin layer chromatography before analysis by GC. From this, the quantity of pentacosane was calculated to be 0.05 $\mu g/cm^2$. Although the compound classes primarily contained homologous series of compounds with either even or odd numbers of carbons, minor quantities of tricosanol and pentacosanol (<2% and <1% of the compound class), and octacosane (<3% of the compound class) were also detected.

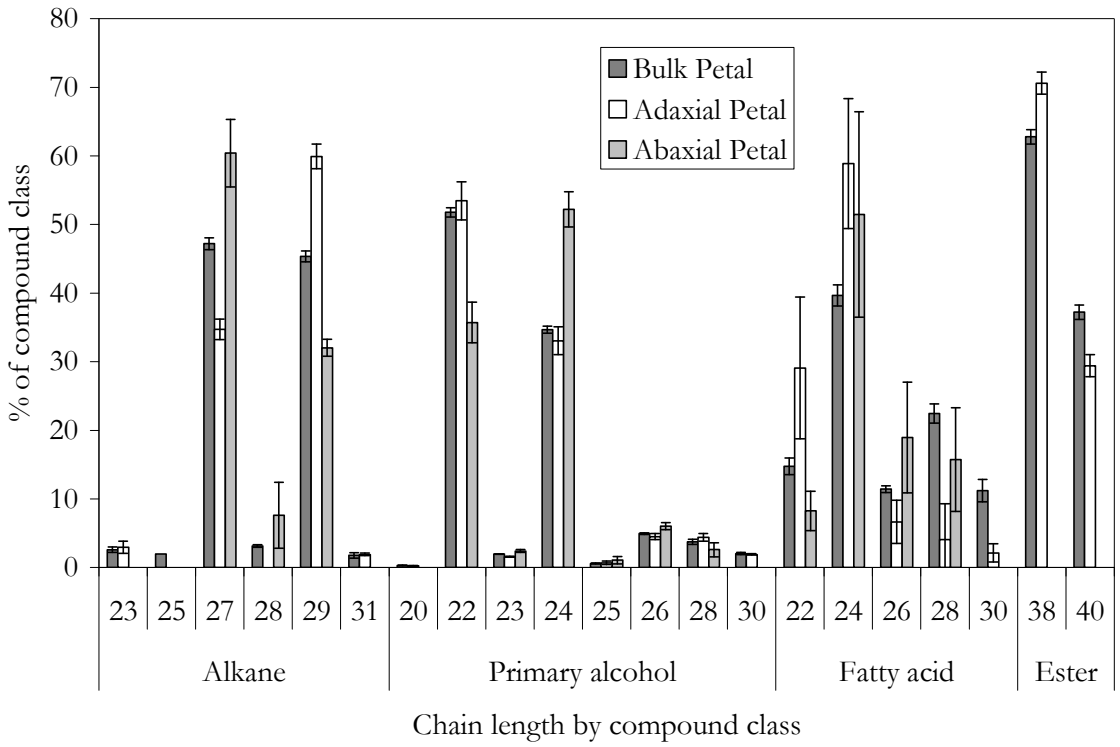

Figure 2.5 Chain length distribution (% of compound class ±SD) of wax compound classes extracted from the entire (total), adaxial, and abaxial surfaces of *Cosmos bipinnatus* petals.

To further probe the uniqueness of the petal wax composition, the adaxial and abaxial surfaces were analyzed independently (Figure 2.). The adaxial cuticle contained 2.2±0.4 μg/cm^2, 25% less than the 2.8±0.6 μg/cm^2 of wax found on the abaxial surface. Primary alcohols constituted 70% of the adaxial wax but only 45% of the abaxial wax. Conversely, the relative abundances of abaxial alkanes (20%) and triterpenoids (10%) were twice as high as those in adaxial wax (10% and 5%). Alkyl esters were only detected in the adaxial cuticle.

The specific compounds present in the adaxial and abaxial wax closely matched the bulk composition, but, similar to the differences in the relative quantities of compound classes, chain length distribution with each class also differed between both surfaces (Figure 2.). Within the primary alcohols, docosanol (55%) and tetracosanol (35%) were most abundant on the adaxial surface. On the abaxial surface, these compounds were also dominant but in reverse proportions (30% versus 50% respectively). An opposite effect was found in the

alkanes where the heptacosane and nonacosane comprised 35% and 60% of the adaxial alkanes but inversely 60% and 30% on the abaxial surface.

2.3.3 Leaf and stem waxes composition

To determine whether petal wax composition is organ distinct, leaf and stem waxes were also investigated (Figure 2.). Leaves were coated with 12.4±0.8 μg/cm^2 of wax, four times the quantity found on petals. Two compound classes comprised half of the wax, with alkanes (4.0±0.6 μg/cm^2) contributing more than primary alcohols (2.4±0.4 μg/cm^2). Acids (0.5±0.1 μg/cm^2), esters (0.2±0.1 μg/cm^2), triterpenoids (1.6±0.3 μg/cm^2), and triterpenoid esters (1.8±0.2 μg/cm^2) each added less than 15% to the overall wax load. The remainder of the wax (1.6±0.4 μg/cm^2) could not be identified.

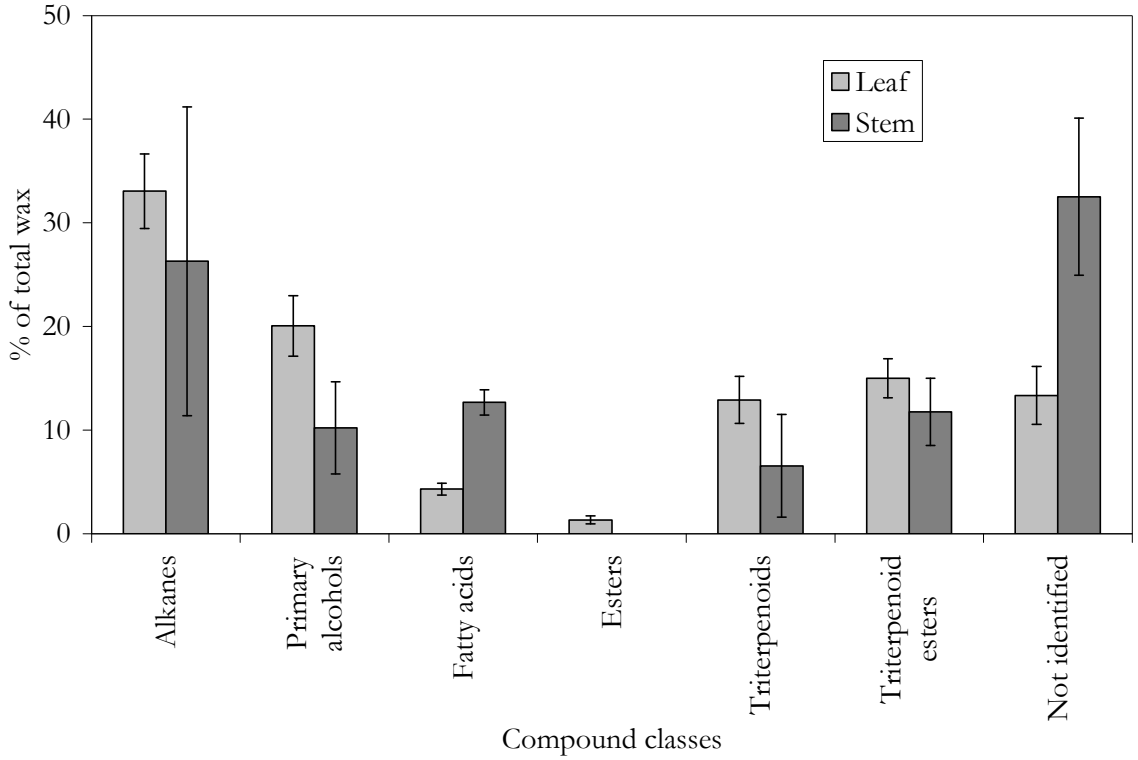

Figure 2.6 Wax compound classes (% of total wax ±SD) extracted from the leaves and stems of *Cosmos bipinnatus*

The chain length distribution was similar between the compound classes, unlike in petals (Figure 2.). The longest chain length in the alkanes, alcohols, and free acids was 32 carbons

while the shortest chain lengths were 27, 22, 20 carbons respectively. The majority of the alkanes were nonacosane and hentriacontane (40% each), reflecting a dominance of odd-chain-length compounds. The alcohols and free fatty acids were dominated by 28 (50% and 35% respectively) and 30 (20% for both) carbon compounds within a mainly even-chain-length homologous series. The esters were 46 and 48 carbons in length, with hexacosanol and octacosanol esterified in combination with hexadecanoic, octadecanoic, or cosanoic acids.

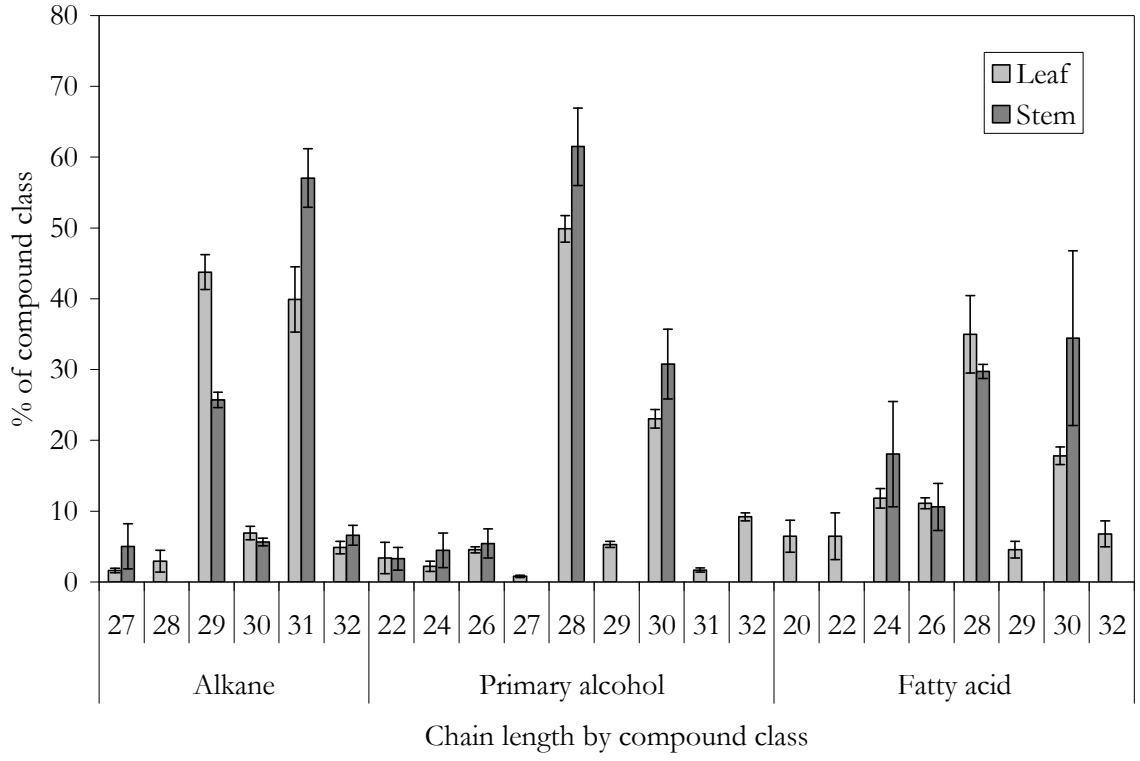

Figure 2.7 Chain length distribution (% of compound class ±SD) of wax compound classes extracted from leaves and stems of *Cosmos bipinnatus* petals.

The stem wax load (9±2 μg/cm^2) was three times that of petal wax but only three-quarters of the stem load. Similar to leaves, alkanes formed the most abundant class (3±2 μg/cm^2; Figure 2.). Free fatty acids (1.1±0.3 μg/cm^2) and alcohols (0.8±0.3 μg/cm^2) made up the rest of the identified straight-chain compounds. Triterpenoids (0.5±0.3 μg/cm^2) and triterpenoid esters (1.0±0.2 μg/cm^2) were also present. One-third (2.8±0.7 μg/cm^2) of the wax remained unidentified.

The relative chain length distributions within stem compound classes closely mirrored the distributions found in leaf wax (Figure 2.). Alkanes ranged from 27 to 32 carbons long, and were dominated by nonacosane (25%) and hentriacontane (60%). The longest alcohols (20-30 carbons) and acids (24-30 carbons) only reached 30 carbons, an decrease in 2 carbons from the respective classes in leaves. Compounds one carbon shorter than the dominant alkanes also dominated the alcohols and acids.

2.3.4 Water permeability through petal cuticles

The pinnate structure of *Cosmos bipinnatus* leaves and the cylindrical stem shape prevented cuticular water permeability analyses on these organs. However, the macroscopically flat, astomatous surface of the petals allowed water loss across the cuticle to be measured. Water loss across the cuticle was linear with respect to time (Figure 2.); Samples for which the r^2 value of the best-fit linear regression line was less than 0.995 were discarded. After factoring in the driving force, the calculated cuticular water permeance on the abaxial petal surface was $6.7 \pm 0.5 \times 10^{-5}$ m/s (n=29). For the adaxial surface, without taking into account the extra surface area caused by the papillose cell shape, the permeance was $1.3 \pm 0.1 \times 10^{-4}$ m/s (n=26). Using the true surface areas, the resistances for the abaxial and adaxial surfaces were $1.5 \pm 0.2 \times 10^{4}$ and $3.0 \pm 0.3 \times 10^{4}$ s/m (Figure 2.).

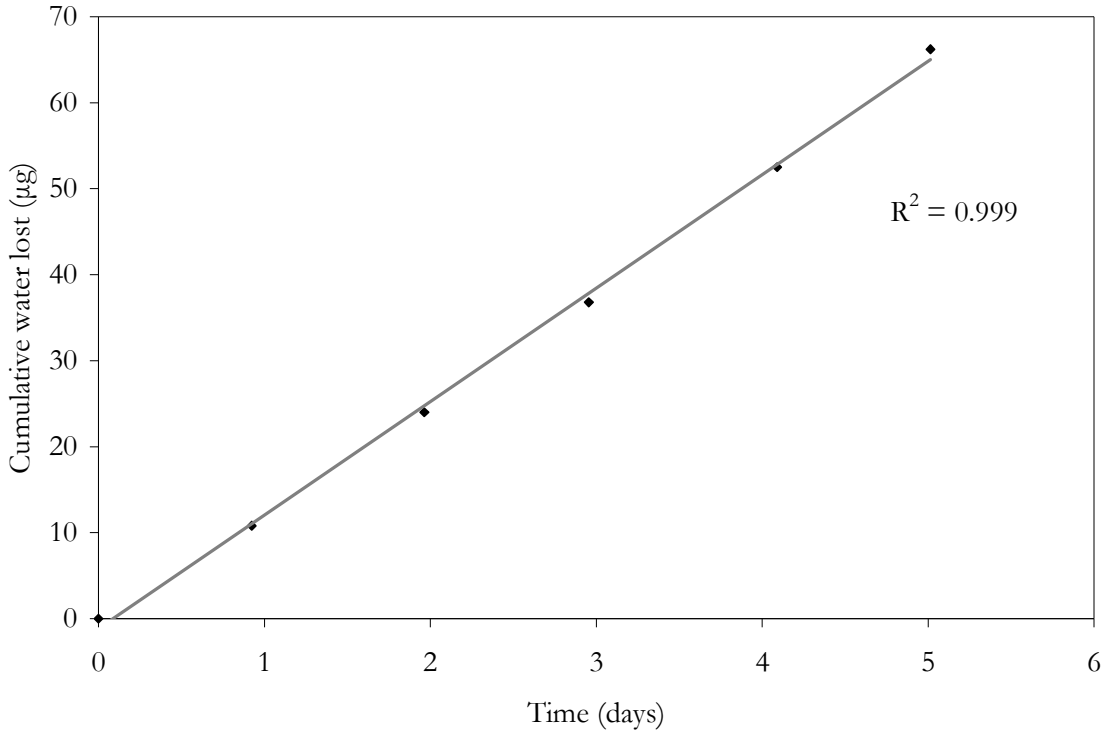

Figure 2.8 An example of water flux determination by measuring water loss per time. Slopes with correlation coefficients greater than 0.995 were used for further calculations.

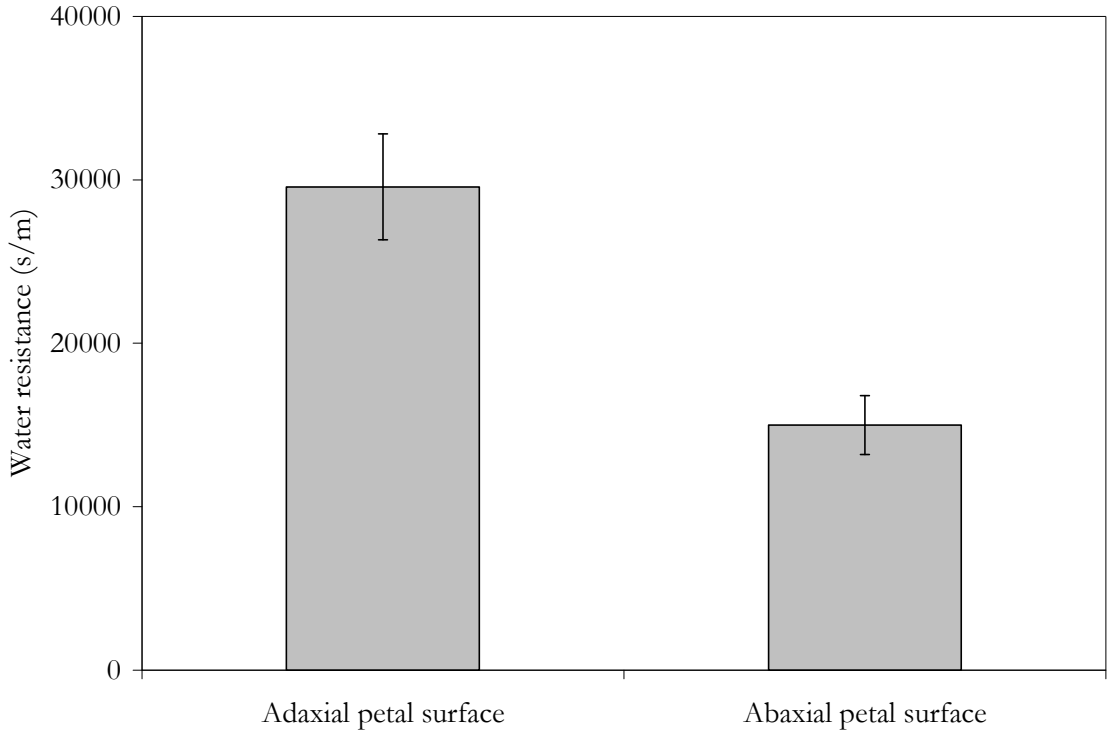

Figure 2.9 Water resistances (s/m; geometric mean ±SE) of the adaxial (n=24) and abaxial (n=29) surfaces of *Cosmos bipinnatus* petals.

To analyze the potential contribution of microscopic holes, the permeabilities of petal cuticles were measured after puncturing the petal with one or two micro-holes (<0.3mm diameter; Figure 2.). Based on apparent surface areas, the permeabilities after one and two holes for the abaxial surface were 1.3±0.3 and 2.1±0.4 x 10^{-4} m/s while for the adaxial surface they were 2.3±0.7 and 3.8±0.8 x 10^{-4} m/s.

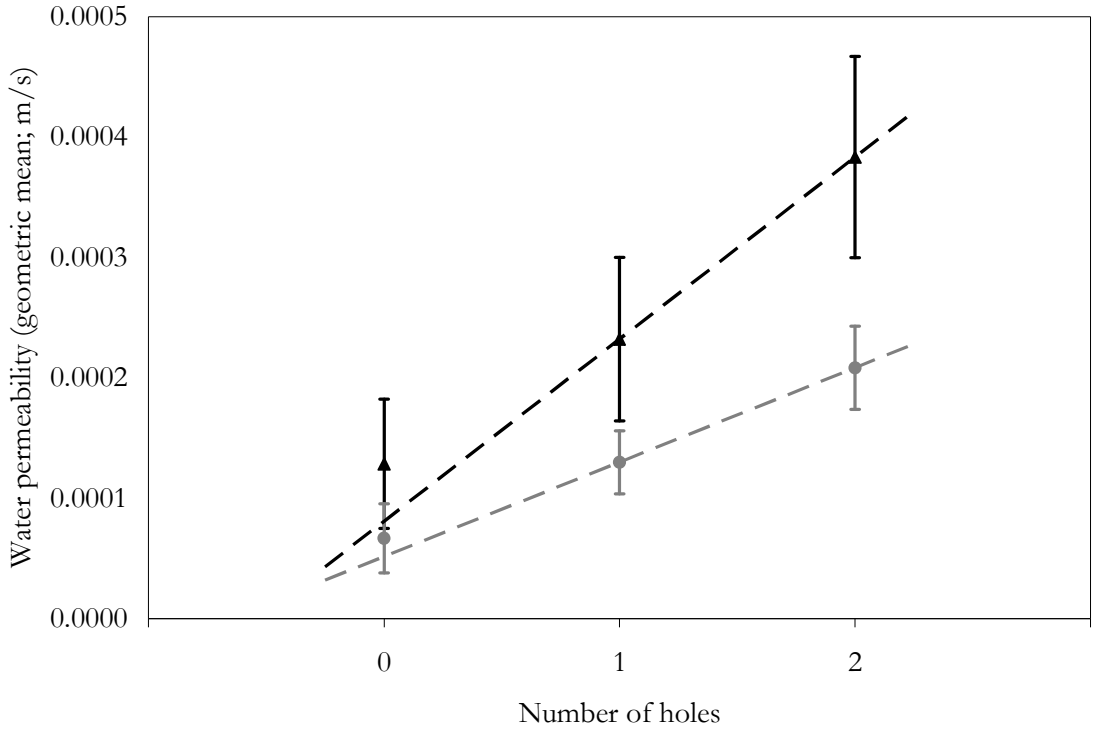

Figure 2.10 Adaxial (black) and abaxial (grey) cuticle water permeabilities (m/s; averages ±SD) with 0, 1, and 2 holes. The linear regression extrapolated from pierced cuticles shows the expected permeability values for a non-punctured cuticle. (N > 24 for 0 holes; N = 2-3 per 1 or 2 holes)

2.4 Discussion

Petals are specialized organs that can enhance reproductive success through aiding pollination by animals. Because petals come in contact with small invertebrates (e.g. pollinators) and may thus contain semiochemicals (compounds that convey information between a plant and another organism) , the petal wax composition of *Cosmos bipinnatus* was analyzed and compared to that of the leaves and stems. Differences between petal wax versus leaf and stem wax exist at all three levels: total wax load, relative quantities of compound classes, and chain length distributions within classes.

First, petals contain only one-quarter to one-third the quantity of wax found on leaves and stems. While the petal wax load is significantly lower, it falls within the range of reported wax loads (eg. 1 and 10 $\mu g/cm^2$ for Arabidopsis leaves and stems (Jenks *et al.* 1995). Second,

subdividing the petal wax into compound classes revealed that most of the wax (45-70% for the abaxial and adaxial surfaces) was primary alcohols. In contrast, leaves and stems contained mainly alkanes while alcohols contributed less than 20%. It seems likely that primary alcohols play a role in achieving petal-specific functions. This is further supported by, third, examining the chain length distributions within classes. Docosanol and tetracosanol dominate the petal wax. These chain lengths are shorter than typical plant waxes, which usually are longer than 26 carbons, and specifically shorter than the alcohols found in cosmos leaf and stem wax. Although the alkanes are also slightly shorter in petal wax, this was a difference of only two carbons as opposed to 4-6 carbons for the alcohols, suggesting that petal epidermal cells are capable of synthesizing longer-chained compounds but preferentially do not do this for alcohols. Cloning and characterization of the respective KCS(s) and FAR(s) will reveal whether substrate specificity or substrate availability controls the chain lengths. Thus, in summary, cosmos petals have atypically large quantities of shorter (22-24 carbon) primary alcohols as compared to leaves and stems.

Wax controls the cuticular functions, of which the foremost function is blocking undesirable water loss (Riederer *et al.* 1995). It has been proposed that wax molecules align in parallel in an all-trans conformation to form crystalline domains (Riederer *et al.* 1995; Reynhardt 1997). Shorter compounds would result in small crystalline domains while compounds with additional functional groups would interrupt the packing geometry and thus disturb crystalline domain formation. These apolar domains prevent water penetration, forcing individual molecules to weave a tortuous path through the amorphous regions along the edges of crystalline domains.

The high relative quantity of shorter primary alcohols in petals likely reduces crystalline domain dimensions as compared to leaves and stems that have more, longer-chain alkanes and therefore petal wax should permit increased water loss through the cuticle. Water permeance data from studies using the same methods as employed here showed average water resistances (inverse of permeances) across species for leaves and fruit of 7×10^4 s/m and 1×10^4 s/m (Kerstiens 1996a). In comparison, the effectiveness of a petal cuticle at blocking water, analyzed for the first time in this study, is similar to fruit but less than half of that of leaves, thus indicating that for this species petal cuticles form relatively poor water barriers.

Additional studies surveying water loss from petals of diverse species would clarify whether petals typically have higher permeabilities than other organs or whether *C. bipinnatus* is unique.

Not only was cuticular resistance to water loss different between petals and literature values for leaves, the resistance also differed between the upper and lower surfaces of the petal. The water barrier coating the adaxial surface was twice as resistant as the water barrier on the lower surface. However, the adaxial surface as compared to the lower surface contained a higher percentage of the shorter-chain alcohols and, based solely on this aspect, would be expected to have a more permeable cuticle. However, two other factors may significantly influence the permeability. At the composition level, the abaxial wax contains a higher percentage of triterpenoids. As these pentacyclic compounds likely hamper the formation of crystalline domains, they may consequently increase the permeability of the abaxial surface (Riederer *et al.* 1995). In addition, on a structural level, the topography of the adaxial surface varies dramatically. This in turn influences the effective distance of the unstirred boundary layer. In other words, the concentration of water immediately exterior to the cuticle probably is greater in the valleys between cells. This in turn would decrease the driving force (decrease the change in concentration) which subsequently would cause an apparent increase in water resistance.

The permeabilities reported here for petal cuticles likely reflect the true water barrier properties. On both the adaxial and abaxial surfaces, the permeabilities closely matched the values predicted from extrapolating back after one or two micro-punctures. Because the difference in the effect of 0, 1 and 2 punctures is less than the determined permeance values, it cannot be conclusively ruled out that small holes may exist. The sum total of all such possible holes would be less than the cross-section of the piercing needle. However, the same methods were employed for both the top and bottom petal surfaces and, because the top surface with the papillose cells should be more difficult to seal and more fragile, it is probable that this surface would be damaged more easily than the lower surface and thus have a lower apparent water resistance. Since this was not found, support is lent to the measured permeabilities truly reflecting the barrier properties.

This research details the effectiveness of petal water barriers and the chemical composition behind this barrier. Building on this, the question arises: why are cuticles compromised? Why are barrier-disrupting compounds present? The most plausible answer is that cuticles

participate in secondary functions and that the plant has reached a compromise in composition to permit both functions. For example, in some species cuticles might need to remain permeable to scents. If the wax were entirely crystalline, even the movement of these lipophilic compounds should be severely limited. Thus, the molecular structure, which is based on the composition, must balance scent emission with water retention. Alternatively, the compounds may provide chemical signals to pollinators or conversely deter undesired organisms. On a more basic level, the plant may balance the energy costs of producing much longer compounds with the ephemeral existence of the petal. As such, perhaps the cuticular water block is sufficient considering the resources necessary for forming longer compounds as compared to the short term additional loss of water. Further studies examining the potential structural and biological functions of docosanol and tetracosanol may allow answers to these questions.

Chapter 3
Very-long-chain α- and β-alkanediols and ketols from *Cosmos bipinnatus* cuticles

3.1 Introduction

The cuticles coating petals form a site of rich ecological interactions between the plant and its environment. This external layer maintains the same basic barrier functions as cuticles covering other aerial, primary plant organs, including most importantly blocking water loss as well as reducing UV damage, particulate accumulation, and xenobiotic penetration (Riederer *et al.* 1995; Kerstiens 1996b; Barthlott *et al.* 1997; Krauss *et al.* 1997). For the petals of many species, this external surface also physically contacts pollinators and opportunistic insects seeking pollen. It seems likely that this interaction is mediated by semiochemicals occuring at this surface. Moreover, the ephemeral nature of petals permits such compounds within the cuticle, even at the expense of reducing the barrier properties, as this added cost is short-lived.

With the potential for ecophysiologically active compounds within the cuticles of petals, their composition must be determined. Cuticles consist of two major components. The first, cutin, is a lipophilic polymer of glyerol and long-chain hydroxy- and diacids cross linked by ester and likely ether bonds (Walton 1990; Nawrath 2006; Pollard *et al.* 2008). Waxes, the second component, comprise very-long-chain compounds ranging from C_{20} to C_{52} with various functional groups (Walton 1990; Jetter *et al.* 2007). Alkanes, primary alcohols, aldehydes, and fatty acids are ubiquitous. Some species also contain wax with in-chain functional groups including secondary alcohols and ketones, β-diols, α- and β-ketols, and hydroxy-aldehydes. Cyclic compounds such as pentacyclic triterpenoids or alkylresorcinols may also be present (Jetter *et al.* 2007).

As part of on-going research attempting to correlate wax composition to cuticle function, the wax of *Cosmos bipinnatus* petals was analyzed (See Chapter 2). Homologous series of novel compounds were found with MS characteristics similar to very-long-chain compounds, indicating not-yet-described compound classes. Before further investigations into compound functions can proceed, the compound structure must be determined. Thus, the objective of

this research was to identify the unknown compounds. Wax constituents were separated by TLC, transformed into various derivatives, and analyzed by GC-MS for structure assignment.

3.2 Methods

3.2.1 Plant material

Seeds of *Cosmos bipinnatus* 'Pinkie' were placed on an Arabidopsis growth medium (Somerville *et al.* 1982), stratified for 2-3 days at 4°C, and then germinated under continuous light (~150 μmol $m^{-2}s^{-1}$ photosynthetically active radiation) for a week at 20°C. Seedlings were transplanted into soil (Sunshine mix 4) and grown under 12 hour days/12 hour nights at a 20°C constant temperature. Soil was kept moist with frequent watering and amended occasionally with fertilizer (MiracleGro). Petals from flowers 3-7 days post anthesis were used for wax analyses.

3.2.2 Wax extraction and derivatization

To extract the total wax from both sides of the petals, ray petals were submerged for 30 sec in $CHCl_3$ containing a defined quantity of *n*-tetracosane as an internal standard. Samples were re-submerged for 30 sec in fresh $CHCl_3$ and the two solutions were pooled. For side-specific wax extraction, a glass cylinder was pressed onto the petal surface (Jetter *et al.* 2000). $CHCl_3$ with a defined quantity of *n*-tetracosane was added for 30 sec with gentle agitation and then removed. A second wash with $CHCl_3$ for 30 sec was added and the two solutions pooled.

Some of the extracted wax was derivatized directly. The solvent from the pooled samples was evaporated under a gentle stream of N_2 gas while heating at 50°C. Samples were derivatized with excess of bis-N,O-(trimethylsilyl)trifluoroacetamide (BSTFA) in pyridine for 30 min at 70°C, the excess solvents evaporated, and $CHCl_3$ again added to the wax. Other portions of the extracted wax were first separated into compound classes by TLC (sandwich technique [Tantisewie *et al.* 1969]; silica gel, mobile phase $CHCl_3$) and visualized by staining with primuline (a dye that when bound to methylene units fluoresces under UV light) before viewing under UV light. Bands were removed from the plates, eluted with $CHCl_3$, filtered, and concentrated in a stream of N_2 before derivatizing as described above. Select bands were further reduced by excess $LiAlH_4$ in refluxing tetrahydrofuran overnight, hydrolysed with H_2O,

and extracted with $CHCl_3$. The reaction products were then further derivatized by BSTFA as described above.

3.2.3 Wax identification and quantification

Wax constituents were separated by capillary GC (6890N, Agilent, Avondale, PA, USA; column 30 m HP-1, 0.32 mm i.d., df=0.1 μm) using the following temperature program: on-column injection at 50°C, oven held for 2 min at 50°C, raised by 40°C min^{-1} to 200°C, held for 2 min at 200°C, raised by 3°C min^{-1} to 320°C, and held for 30 min at 320°C. For compound identification, the GC was linked to a mass spectrometric detector (5973N, Agilent) and the inlet pressure programmed for a constant 1.4 ml min^{-1} flow of He carrier gas. For compound quantification, the GC with inlet pressure programmed for constant flow of 2.0 ml min^{-1} of H_2 carrier gas was connected to a flame ionization detector (FID). The quantity (μg) was established by comparing peak areas to that of n-tetracosane, the internal standard added at a specific quantity to the total wax extracts. For co-eluting compounds, peak areas of characteristic ions (M^+ for primary alcohols, m/z 205 for 1,2-diols, and m/z 219 for 1,3-diols) were quantified by MS. These were converted to relative percentages by multiplying with the ratios of the quantity of standards (measured by GC-FID) to the quantities of respective ions (measured by GC-MS). Absolute quantities were determined by multiplying the relative percent with the absolute quantity of the impure peak. Extracted surface areas were determined from digital photographs of the samples using ImageJ software (Abramoff *et al.* 2004) and corrected for the undulating topography as described in Chapter 2.

3.2.4 Synthesis of standards

2-Hydroxy hexadecanoic acid, 3-hydroxy hexadecanoic acid, 2-hydroxy eicosanoic acid, and 2-hydroxy docosanoic acid were subjected to reduction by excess $LiAlH_4$ in refluxing tetrahydrofuran overnight, hydrolysis with H_2O, and extraction of the newly-formed diols with $CHCl_3$. Standards were derivatized and analyzed as described above.

3.3 Results and Discussion

Chloroform-soluble surface lipids extracted from *Cosmos bipinnatus* petals were separated by TLC into ten fractions. Although previously identified compound classes accounted for most bands, two bands contained novel compounds. The first band A (R_f = 0.03) migrated between

the origin and fatty acids suggesting either primary/secondary diols or compounds with three or more functional groups. GC-MS chromatograms of this fraction displayed the presence of two homologous series, A1 and A2, each with seven compounds. TMSi derivatives from both series showed characteristic fragments m/z 73 $[OTMSI]^+$, m/z 103 $[CH_2OTMSi]^+$ and m/z 147 $[(CH_3)_2SiOSi(CH_2)]^+$, indicative of alcohols and specifically primary alcohols and diols, respectively (Figure 3.1 and Figure 3.2). Unique to A1 was the presence of fragment m/z 205 $[CH(OTMSi)CH_2OTMSi]^+$ caused by α-fragmentation of 1,2-diols (Figure 3.1). The most prominent compound in A1 also contained a second α-fragment m/z 383 $[C_{21}H_{42}OTMSi]^+$ and its daughter ion m/z 293 $[C_{21}H_{42}]^+$, ion m/z 471 $[M\text{-}CH_3]^+$ and molecular ion m/z 486. These chain-length specific fragments together with fragments characteristic of 1,2-diols indicated that this compound was 1,2-docosanediol. The remaining compounds in the series were likewise 1,2-diols ranging from C_{20} to C_{26} with higher abundances of even-numbered chain lengths. Mass spectra of synthesized standards matched those from the samples.

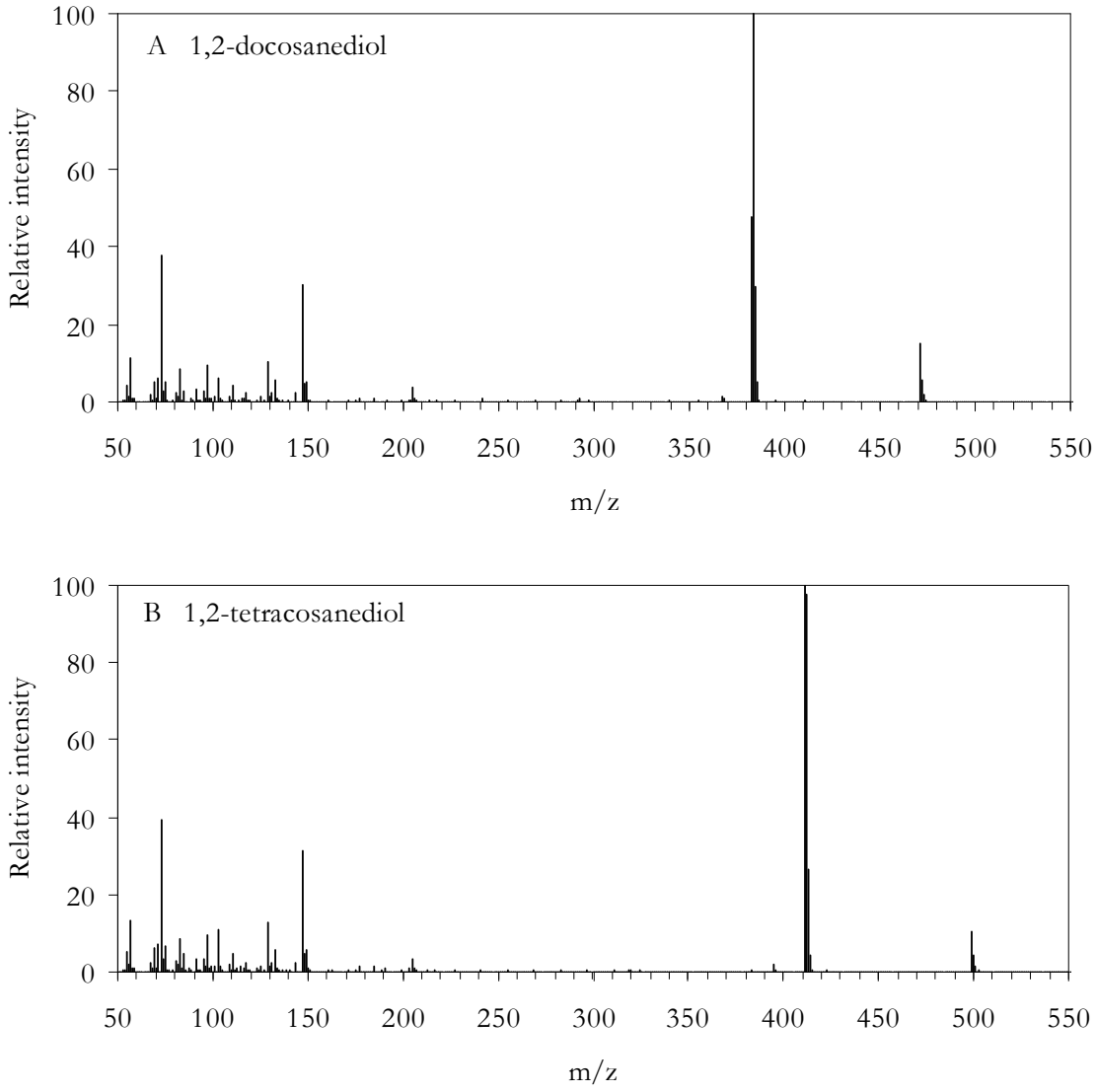

Figure 3.1 Mass spectra of the bis-TMSi derivatives of the prominent very-long-chain 1,2-diols 1,2-docosanediol (A) and 1,2-tetracosanediol (B) from the petal wax of *Cosmos bipinnatus*

TMSi derivatives of compounds in the second series A2 all contained the fragment *m/z* 219 $[CH(OTMSi)CH_2CH_2OTMSi]^+$ found in 1,3-diols. The most abundant compound in this series was characterized by an α-fragment *m/z* 369 $[C_{19}H_{38}OTMSi]^+$ one methylene unit shorter than the dominant compound in A1 but identical ions *m/z* 471 $[M\text{-}CH_3]^+$ and molecular ion *m/z* 486 (Figure 3.2). Based on this information, this compound was identified as 1,3-docosanediol. Molecular ions and α-fragments of the remaining compounds indicated that this series of 1,3-diols contained predominantly even numbered homologs with carbons ranging from C_{20} to C_{26}.

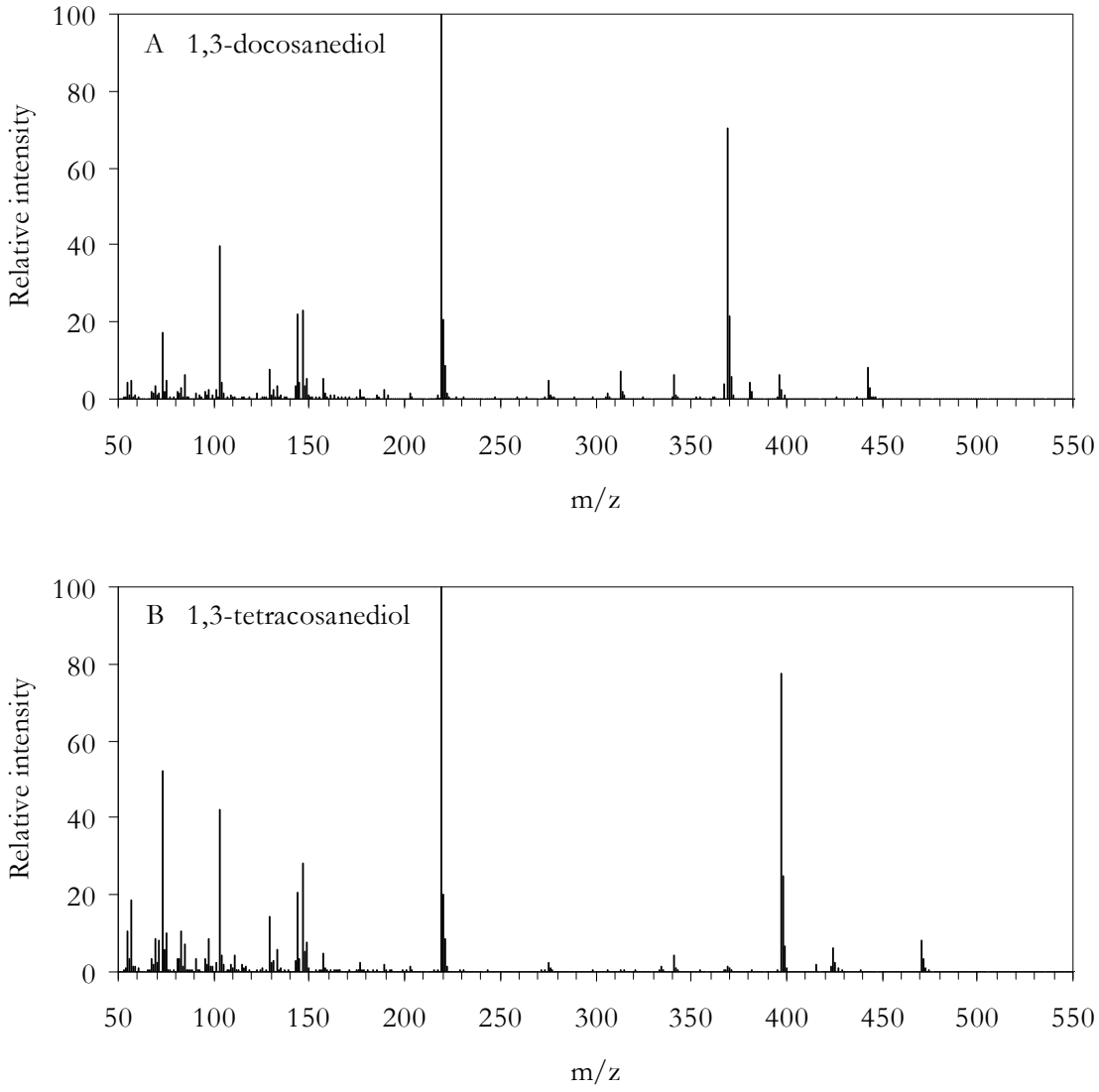

Figure 3.2 Mass spectra of the bis-TMSi derivatives of the prominent very-long-chain 1,3-diols 1,3-docosanediol (A) and 1,3-tetracosanediol (B) from the petal wax of *Cosmos bipinnatus*

Under the various GC conditions attempted, both 1,2-diols and 1,3-diols co-eluted with primary alcohols two methylene units shorter that were also present in the petal wax extract. After correlating the quantity of standards as determined by GC-FID to the quantity of the ions m/z 205, 219, and M^+ produced by GC-MS for 1,2-diols, 1,3-diols, and primary alcohols, the percentage of individual compounds were determined for each mixed-compound peak in the petal wax samples. The upper petal surface contained 0.11±0.02 μg/cm^2 of 1,2-diols while the lower surface had a comparable quantity of 0.09±0.01 μg/cm^2 (Figure 3.3) The homolog

distribution for both surfaces was 10% C_{20}, 60% C_{22} and 30% C_{24}. 1,3-diols were present at quantities one order of magnitude less than the 1,2-diols, with 0.013±0.002 μg/cm^2 in the wax from the upper petal surface and 0.015±0.003 μg/cm^2 in the lower surface wax (Figure 3.3). The total 1,3-diols had a chain length distribution of 5% C_{20}, 75% C_{22}, and 20% C_{24} for both surfaces. In contrast, corrected quantities of primary alcohols were over ten times greater than the two diol classes taken together, with 1.7±0.2 μg/cm^2 in the wax on the upper surface and 1.2±0.1 μg/cm^2 on the lower surface. The chain length distribution of the primary alcohols matched that found in Chapter 2.

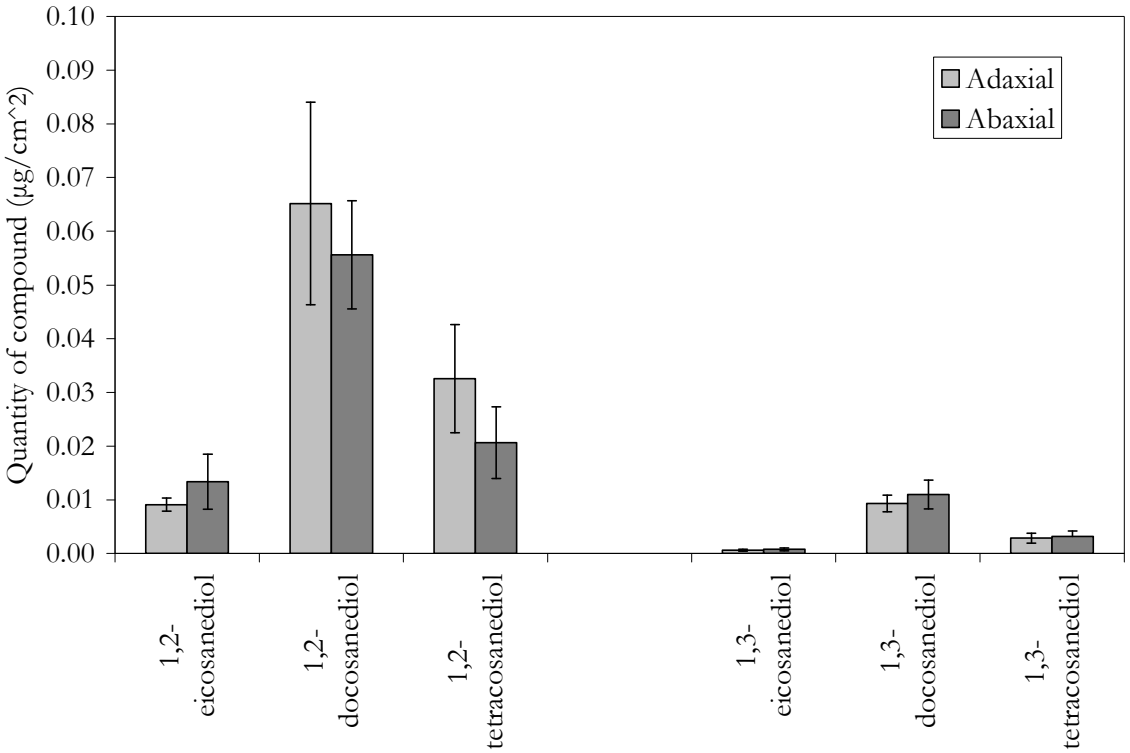

Figure 3.3 Quantities (μg cm^{-2} ±SD) of 1,2-diols and 1,3-diols found in the adaxial and abaxial petal waxes of *Cosmos bipinnatus*

It is interesting to predict the biosynthetic route leading to the two classes of diols found in *C. bipinnatus* petal waxes. Diol formation may proceed by forming the primary alcohol or the secondary alcohol first. No biosynthetic examples of α- or β-oxidation of primary alcohols are known. However, there is precedence for the latter case, as *Zonotrichia leucophrys* (white

crowned sparrow) was found to contain an enzyme activity reducing long-chain 2-hydroxy-fatty acids (likely esterified to CoA) to corresponding 1,2-diols (Kolattukudy 1972). *C. bipinnatus* may contain a similar fatty acyl reductase (FAR) that has specificity for α-hydroxylated CoA esters. Also, the FAR may instead primarily synthesize the large quantities of primary alcohols of corresponding chain lengths found in *C. bipinnatus* petal wax but have secondary, non-specific reducing activity for α-hydroxylated acyl-CoA substrates.

Most of the petal waxes examined to date for species in the Asteraceae have been shown to contain VLC, poly-hydroxylated compounds (Akihisa *et al.* 1997; Akihisa *et al.* 1998). Although mid-chain β-diols may be formed through polyketide biosynthesis, the hydroxyl groups were found on both even and odd-numbered carbons. Thus, they are likely formed after elongation through oxidation of specific methylene units. Similar oxidation reactions may be involved in forming the diols observed in *C. bipinnatus*.

The enzyme in *C. bipinnatus* responsible for oxidizing the α-carbon of C_{22} substrates displayed chain length specificity. The C_{22} and C_{24} diols were expected in equal quantities since the possible substrates (C_{22} and C_{24} primary alcohols or C_{22} and C_{24} acyl-CoAs) were present in equivalent amounts. However, the C_{22} diol was the most abundant homologue, which suggests a preference for C_{22} over C_{24} substrates. A possible chain length specificity for C_{20} substrates cannot be inferred from the present chemical data alone, since the low quantity of C_{20} diol may be a consequence of substrate availability (low quantities C_{20} alcohol) or chain length specificity (discrimination against C_{20} acyl-CoA or C_{20} alcohol).

TLC separation of the *C. bipinnatus* waxes yielded a second band with novel compounds, migrating between the free fatty acids and primary alcohols (R_f = 0.14) and suggesting the presence of either two secondary functional groups or a primary and a secondary functional group of which a maximum of one could be an alcohol. The GC-MS chromatogram and spectra revealed three homologous series, B1, B2, and B3. Their spectra lacked the ion *m/z* 147 $[(CH_3)_2SiOSi(CH_2)]^+$ characteristic of diols suggesting less than 2 hydroxyl groups and thus the presence of (at least) one carbonyl group. Derivatization of the carbonyl(s) to hydroxyl groups by LAH resulted in the formation only two homologous series of 1,2-diols and 1,3-diols, indicating that functional groups were on C-1 and C-2 or on C-1 and C-3 exclusively. Since the underivatized compounds were less polar than an acid, the possible compound

identities include 2-hydroxy aldehydes, 2-keto alcohols, or 1,2-ketals or the β-oxidized equivalents.

The series B1 and B2 each contained seven compounds. After BSTFA derivatization, the two homologous series both contained the ion *m/z* 73 $[TMSi]^+$ indicating the presence of a hydroxyl functional group after treatment with BSTFA. This finding pointed to the presence of ketols and/or hydroxy-aldehydes in both series. However, it should be noted that identical ions greater than the M^+ for a ketol were found for compounds in both series. To explain this result, it may be hypothesized that the ketols (or hydroxy aldehydes) were derivatized to enediols, with desaturation occurring between C-1 and C-2 or between C-2 and C-3. Such tautomerization has been shown to occur for 2,3-dihydoxy fatty acid esters when derivatized to TMSi ethers in the presence of pyridine (Schmitz *et al.* 1975).

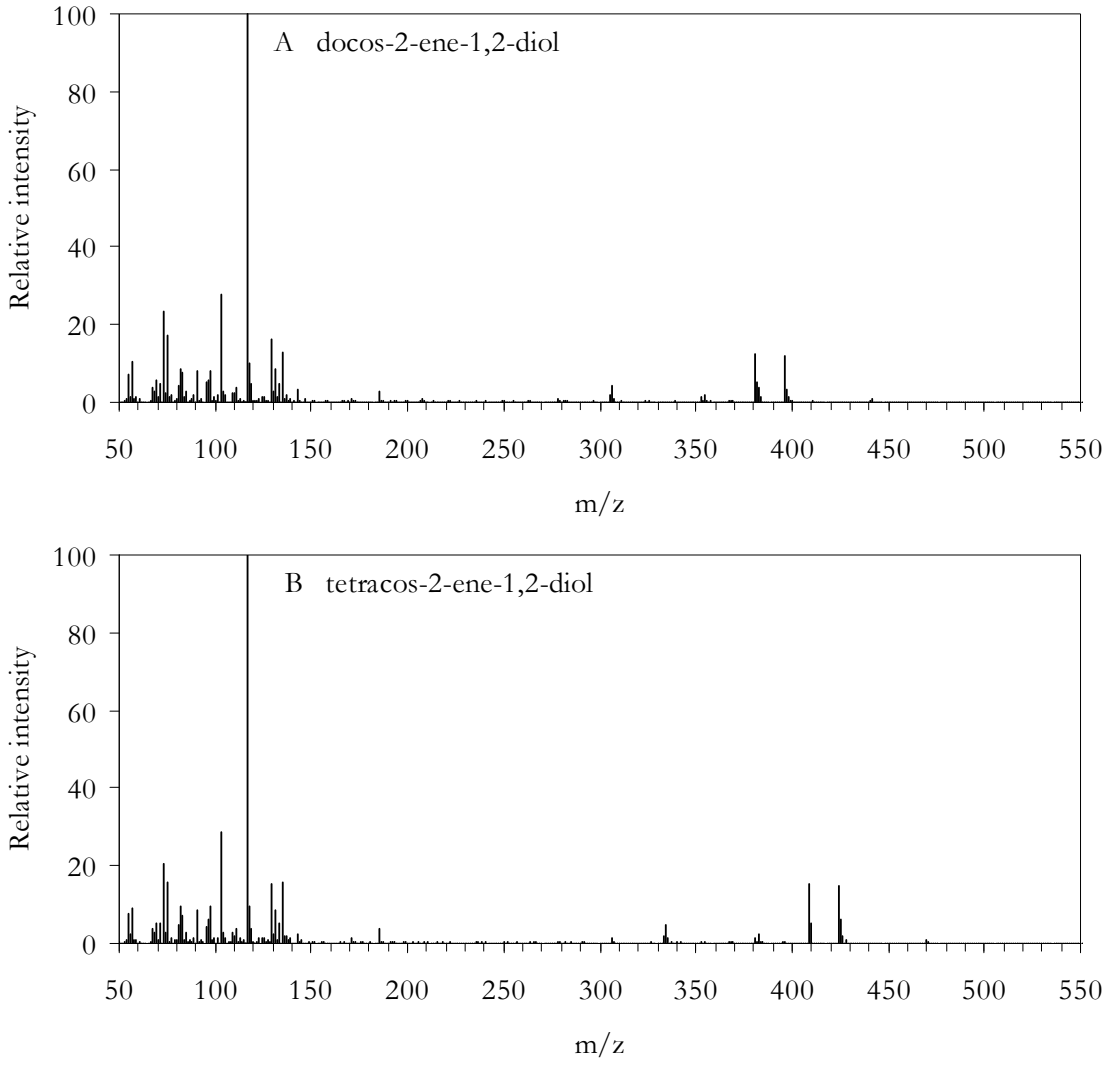

Figure 3.4 Mass spectra of the bis-TMSi derivatives of the prominent very-long-chain 2-ketols (after tautomerization to enediols) docos-2-ene-1,2-diol (A) and tetracos-2-ene-1,2-diol (B)

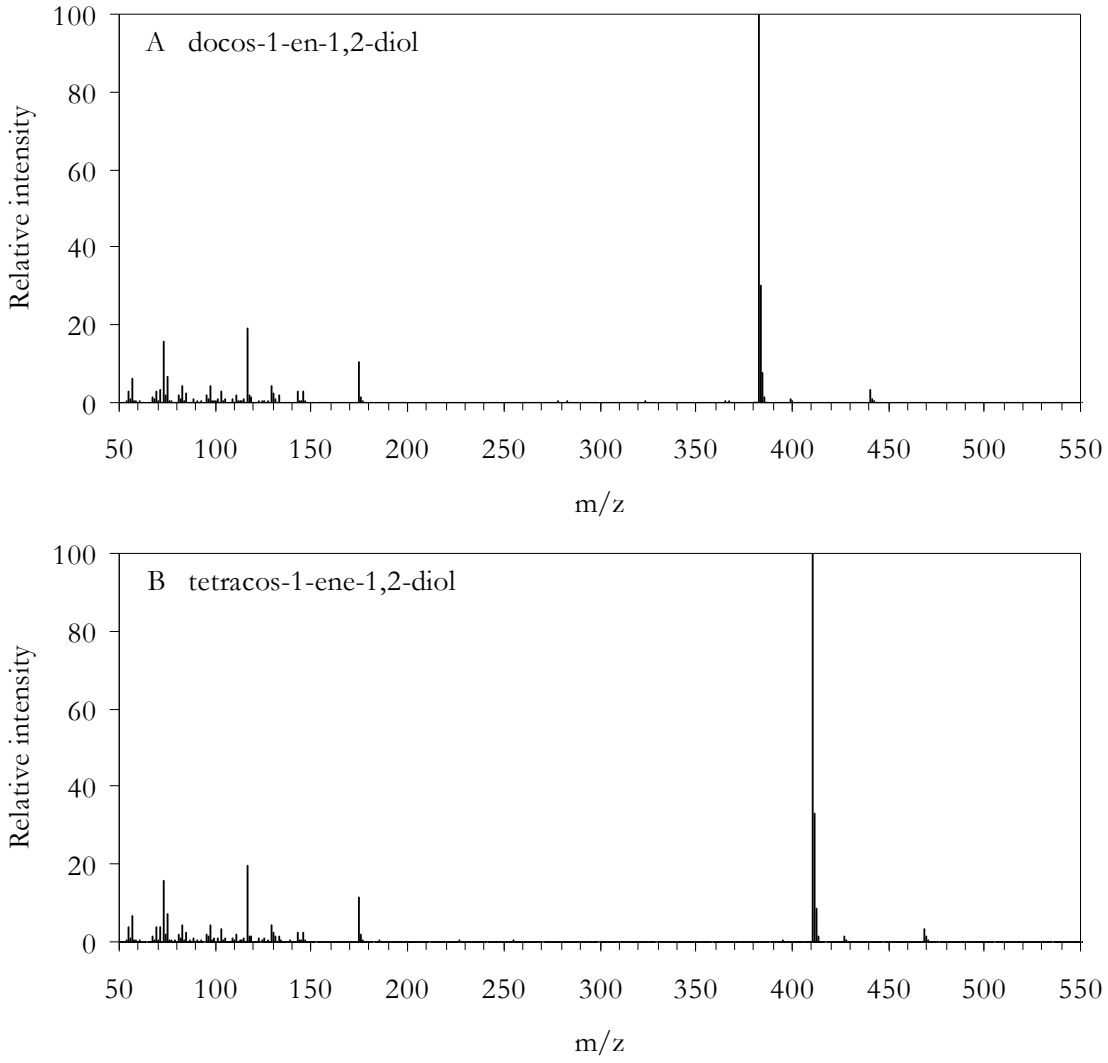

Figure 3.5 Mass spectra of the bis-TMSi derivatives of the prominent very-long-chain 2-ketols (after tautomerization to enediols) docos-1-ene-1,2-diol (A) and tetracos-1-ene-1,2-diol (D) from the petal wax of *Cosmos bipinnatus*

Based on these findings, potential fragments were assigned to the observed ions. The most prominent peak in B1, as an example, contained the ion *m/z* 103 $[CH_2OTMSi]^+$ indicating the presence of a primary alcohol and the corresponding α-fragment *m/z* 381 $[C_{21}H_{40}OTMSi]^+$, suggesting that the double C=C resides between C-2 and C-3 (Figure 3.4). The ion *m/z* 396 and its daughter ion *m/z* 306 result from the loss a first TMSi followed by a hydrogen extraction and then loss of the second TMSi group. The identity of the intense peak at *m/z* 117 remains unclear, but may be $[CHOCH_2OSi(CH_3)_2]^+$. Based on these assignments, the

compound was identified as docos-2-ene-1,2-diol. The remaining compounds in the series were similarly identified as C_{20} to C_{26} enediols with even-numbered carbon chains predominating. The original structures were inferred to be a corresponding series of 2-ketols.

The most prominent peak in B2 contained the same M^+ as the prominent peak in B1, suggesting a structure differing only in the location of the double bond (Figure 3.5). A strong α-fragment at *m/z* 383 $[C_{21}H_{42}OTMSi]^+$ requires the double to be located between C-1 and C-2. The ion *m/z* 175 may be the product of a McLafferty rearrangement with a hydrogen extraction $[CH_2CH_2CH_2COHCH_2OTMSi]^+$. This peak was tentatively identified as docos-1-ene-1,2-diol. Based on the chain-length specific fragments, the remaining peaks were identified as the C_{20} and C_{24} homologs of this compound. The enediols likely formed during BSTFA treatment, either from hydroxyl aldehydes or ketols. However, the former are unstable under ambient conditions, spontaneously converting to the latter, and thus only ketols can be the natural product present. Therefore, both derivatives B1 and B2 were likely formed in parallel from one and the same starting material.

Petal wax contained 0.070±0.08 μg/cm^2 of 2-ketols, corresponding to 2.6±0.2% of the total wax. This class comprised 15% 1-hydroxy-eicosan-2-one, 40% 1-hydroxy-docosan-2-one, and 45% 1-hydroxy-tetracosan-2-one (Figure 3.6). Because these chain lengths parallel those found for the 1,2-diols in chain-length range and relative distribution, it is possible that the ketols are formed from 1,2-diols. It is possible that this occurs by further oxidation of the C-2 hydroxyl group to a geminal diol followed by dehydration to a carbonyl group. This would permit the same oxidizing enzyme that forms 1,2-diols to also form the ketols. Precedence for such a double oxidation exists. In *Arabidopsis thaliana*, the mid-chain hydroxylase 1 (MAH1) converts nonacosane first to nonacosan-15-ol and second to nonacosan-15-one in the stem wax (Greer *et al.* 2007).

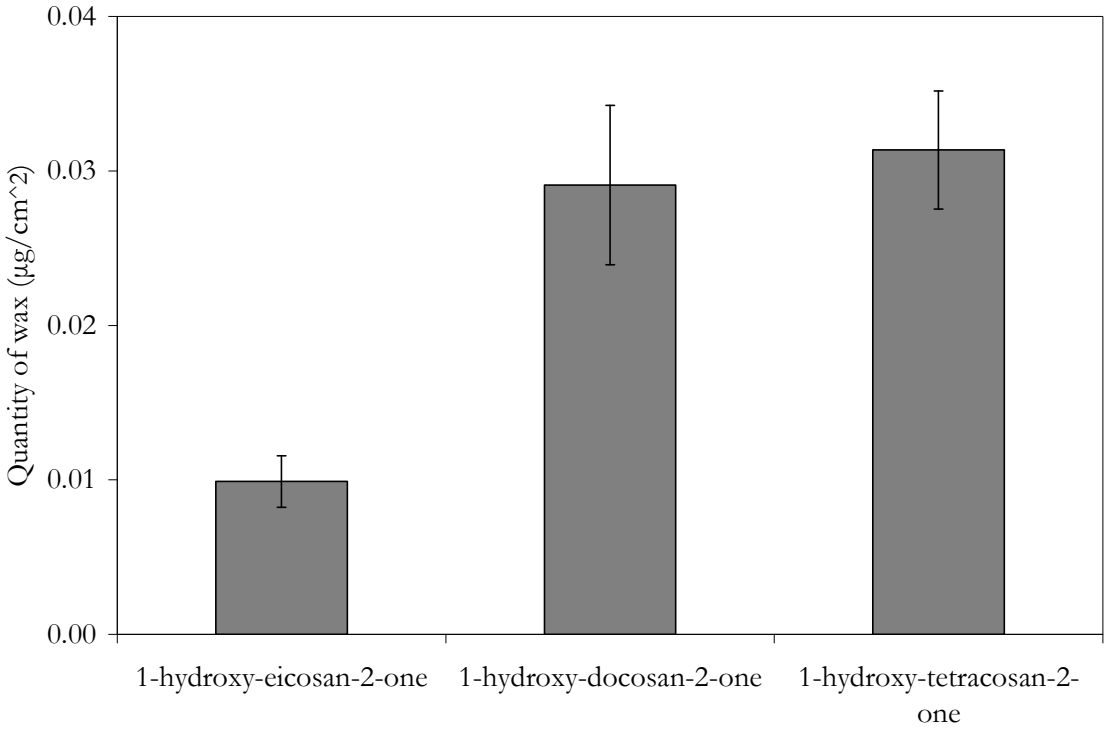

Figure 3.6 Chain length distribution of 2-ketols in the petal wax of *Cosmos bipinnatus* (µg cm^{-2} ±SD)

The third series B3 contained three compounds characterized by the fragment *m/z* 145. Using the most prominent compound, fragment *m/z* 412 and the dominant fragment *m/z* 397 were interpreted as the M^+ and $[M\text{-}CH_3]^+$ (Figure 3.7). The presence of an α-fragment *m/z* 103 ($[CH_2OTMSi]^+$) indicative of a primary alcohol but the lack of a diol signal *m/z* 147 suggests that only a single hydroxyl group existed and that it was positioned on C-1. The characteristic ion *m/z* 145 ($[COCH_2CH_2OTMSi]^+$) represented the α-bond fragment of the carbonyl group. Based on this evidence, the compound was identified as 1-hydroxy-dodecan-3-one. Using the chain length specific fragments, the series was identified as 3-ketols ranging in length from C_{20} to C_{24}. This identification is further supported by the LAH derivative products. In addition to the 1,2-diols (generated from the 2-ketols above), only 1,3-diols were found, which would be generated by 3-ketols.

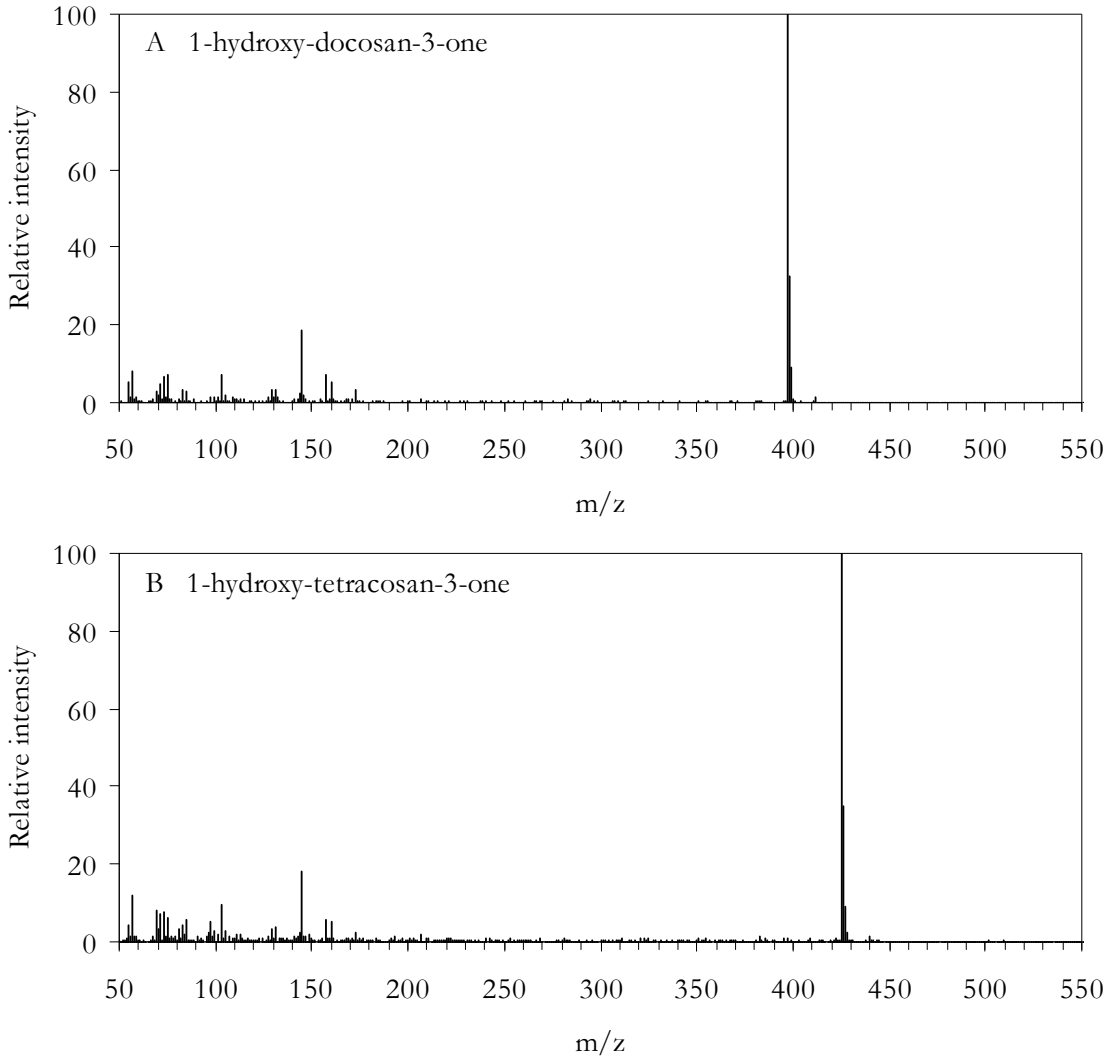

Figure 3.7 Mass spectra of the bis-TMSi derivatives of the prominent very-long-chain 3-ketols 1-hdyroxy-docosan-3-one (A) and 1-hydroxy-tetracosan-3-one (B) from the petal wax of *Cosmos bipinnatus*

The *C. bipinnatus* petal wax contained only trace quantities of 3-ketols. Since the chain length distribution and relative quantities of 3-ketols matches that of 1,3-diols, it is possible that these compounds are derived from the corresponding diol via a second oxidation on C-3 of 1,3-diols. This would parallel the production of 2-ketols from 1,2-diols.

In conclusion, four homologous series of novel wax constituents were found in the petal wax of *Cosmos bipinnatus*. Based on their identical chain length distributions and relative

abundances, the series likely are biosynthetically related. The enzyme first oxidizing the C-2 methylene unit to form 1,2-diols likely can perform a second, consecutive oxidation to 2-ketols. Alternatively, lack of product specificity might lead the same enzyme to also form small amounts of 1,3-diols and 3-ketols.

Chapter 4
Cell type-specific analysis of surface lipids in *Arabidopsis thaliana*: trichomes have cuticular waxes containing longer hydrocarbons than other epidermal cells

4.1 Summary

The cuticle provides plants a first defence against adverse, above-ground biotic and abiotic conditions. For maximal effectiveness, the cuticle must coat not only pavement cells but also entirely cover specialized epidermal cells like trichome and guard cells. It remains unknown whether the composition of cuticular waxes differs over these cell types. To address whether cell-type specific compositions exist between trichomes and other epidermal cells in *Arabidopsis thaliana*, the total waxes of stems and leaves from a mutant with an absence of trichomes (*gl1*) was compared first to waxes from wild type and a trichome-abundant mutant (*cpc tcl1 etc1 etc3*) and second to wax from isolated trichomes. In the stem wax, compounds longer than 31 carbons in length increased in relative abundance in *cpc tcl1 etc1 etc3* over *gl1*. Similarly, the leaf wax from the excess-trichome mutant contained a higher relative abundance of compound longer than 32 carbons as compared to *gl1*. This is further supported by the wax composition from isolated trichomes that contained alkanes and primary alcohols. Clearly, lateral cuticle wax variation occurs between different epidermal cell types. The cell-type specific compositions indicate that all epidermal cells contain the necessary enzymatic machinery for wax biosynthesis, and that elongation processes differ between cell types.

4.2 Introduction

Plants reduce the risk of dehydration by covering their non-woody shoot surfaces with a hydrophobic skin termed the cuticle. While primarily serving as a transpiration block (Riederer *et al.* 1995), this outer plant surface also interfaces with the environment. The cuticle promotes the removal of dust, spores, and other particulates (i.e.: the lotus effect; Barthlott *et al.* 1997) and obstructs pathogen and ultra-violet light penetration (Krauss *et al.* 1997). This coating may also chemically interact with other organisms, as signalling or defense compounds (Eigenbrode *et al.* 1995; Müller 2006).

These functions are controlled by the composition. Cuticles consist of two components, the polymer cutin and waxes that are synthesized in the underlying epidermal cells. Cutin contains

cross-linked long chain hydroxy- and di-acids and glycerol (Walton 1990; Nawrath 2006; Pollard *et al.* 2008). Waxes comprise very-long-chain (26-52 carbon) compound classes (Walton 1990; Jetter *et al.* 2007). The compounds occur as homologous series since each elongation round adds two carbons: a β-ketoacyl-CoA synthase (KCS) condenses an acyl-coenzyme A (CoA) with malonyl-CoA to form β-ketoacyl-CoA (Samuels *et al.* 2008). This is subsequently reduced to β-hydroxyacyl-CoA, dehydrated to enoyl-CoA and then again reduced to a final saturated acyl-CoA by KCR1, PAS2, and CER10, respectively (Zheng *et al.* 2005; Bach *et al.* 2008; Beaudoin, Wu *et al.* 2009). The KCS, of which Arabidopsis has 21 (Joubes *et al.* 2008), likely controls substrate/product chain-length specificity while each of the final three reactions is catalyzed by a single enzyme regardless of the chain length (Millar *et al.* 1997).

After the chain length distribution is set by the elongation enzymes complex, further modifying enzymes generate compound classes in varying ratios. The alcohol (reduction) pathway produces alcohols by CER4 and esters by WSD1 while the alkane (decarbonylation) pathway yields aldehydes, alkanes, secondary alcohols and ketones (Samuels *et al.* 2008). Many of the wax biosynthetic genes have been characterized but details of the pathways still require confirmation. Waxes may also include cyclic compounds like pentacyclic triterpenoids and flavonoids (Jetter *et al.* 2007). The presence and relative abundance of specific wax compounds have been shown to vary between different species, different organs within a species, and even different parts of the same organ (i.e.: abaxial versus adaxial leaf surfaces).

The functional effectiveness of the cuticle depends on its continuity; it has therefore been assumed that all epidermal cell types are covered with cuticular waxes. Arabidopsis leaves and stems contain level pavement and guard cells, which will be considered collectively for this chapter, and protruding trichomes. Although some trichomes in some species are modified for the production and secretion of specific, usually herbivore-deterring metabolites (i.e.: glandular trichomes), Arabidopsis contains only simple, non-secreting trichomes that likely inhibit insect movement, reduce mechanical abrasion, and increase the boundary layer (Wagner *et al.* 2004).

Does the specific cuticular wax composition vary between different epidermal cell types? Because trichomes protrude, they likely experience greater levels of abrasion and wind-induced drying as compared to pavement cells and thus may require a unique wax composition.

Several lines of experimental evidence suggest distinct wax compositions on differing epidermal cell types. Cell-specific expression has been experimentally determined for some wax biosynthesis genes. The wax mid-chain alkane hydroxylase *MAH1* was expressed in stem pavement cells but not in trichomes or guard cells (Greer *et al.* 2007). CER4 was also localized to stem pavement cells but was restricted to trichomes for leaves (Rowland *et al.* 2006). Localization studies of other known wax biosynthesis proteins did not report either their presence or absence in trichomes. However, microarray experiments comparing trichomes to pavement cells and guard cells to pavement cells show differential expression of some lipid-related genes, implying that the wax composition also varies between cell-type (Marks *et al.* 2009). In addition to differences in expression levels and location, ion flux across the cuticle differed between epidermal cell types, which in turn suggests differences in cuticle composition between cell types (Schreiber 2005).

Despite this indirect evidence suggesting lateral differences in wax composition, a direct analysis of cell-specific wax composition is lacking to date. This may partly be due to the difficulty in isolating cuticular lipids free of both intracellular contamination and lipids from other cell-types. In order to circumvent this problem, molecular genetic approaches combined with chemical analyses are required. Because of the size and conspicuous nature of trichomes, significant advances have been made into the regulation of trichome development. Genetic studies have identified several genes that, singularly and in combination, regulate trichome density and thus also the ratio of trichomes to pavement (List in Marks *et al.* 2009)). Mutations in *gl1* entirely prevent trichome formation (Herman *et al.* 1989). A previous study that analyzed the wax from this mutant concluded that it was similar to that of published wild-type wax of different accessions based only on TLC and GC-MS comparisons (Sieber *et al.* 2000). However, a simultaneous analysis of wild-type wax was not performed and quantitative data were not provided. Other combinations of mutants such as *cpc tcl1 etc1 etc3* cause a three-fold increase in trichome density as compared to wild type, thereby increasing the ratio of trichomes to pavement cells (Wang *et al.* 2008). Comparing the cuticular waxes of these lines and wax from isolated trichomes will enable direct evidence to be acquired on cell-type specific compositions. We confirmed the presence of wax on trichomes and answered the experimental questions: 1) What are the wax compositions on *Arabidopsis thaliana* trichomes and non-trichome epidermal cells and 2) how do these differ with respect to chain length

distribution (wax elongation) and compound class ratios (wax modification)? Ultimately, the answers to these questions will also help to establish trichomes as a model for furthering our understanding of the wax biosynthetic pathway, as the ability to isolate these epidermal cells facilitates combining wax analyses with metabolomics.

4.3 Methods

4.3.1 Plant material

Wild type (Columbia), trichomeless *gl1* (Herman *et al.* 1989; SALK_039478; Alonso *et al.* 2003; Seeds obtained from the Arabidopsis Biological Resource Centre, Columbus, USA), and trichome-abundant quadruple mutant *cpc tcl1 etc1 etc3* seeds (Gift from Dr. J.-G. Chen) were plated on Arabidopsis minimal media agar (Somerville *et al.* 1982), stratified for 2-3 days at 4°C, and then germinated under continuous light (~150 μmol $m^{-2}s^{-1}$ photosynthetically active radiation) for 7-10 days at 20°C. Seedlings were transplanted into soil (Sunshine mix 4), grown under the same light and temperature conditions as for germination, and watered twice weekly with MiracleGro. Homozygous lines were confirmed by visual inspection of an absence or excess of leaf and stem trichomes. Mature leaves and stems at least one month old were harvested for trichome isolation or wax analyses.

4.3.2 Trichome isolation

Trichome isolation largely followed Marks *et al.* (2008) with minor modifications: Leaves were submerged in a 0.5M EGTA solution in water and vortexed with silica beads (50 μm diameter). The resulting mixture was first strained though a wire mesh (1 mm pore size) to remove the plant organs before filtering through a 120 μm pore mesh to separate the trichomes from the filtrate and other epidermal cells. The isolated trichomes were washed three times with water. E andxternally-adhering water droplets were blown offsuperficia briefly dried under a gentle stream of N_2 gas for less than 30 minutes before immediately proceeding with the extraction of their waxes from the trichomes.

4.3.3 Wax extraction and derivatization

Leaves, stems, or isolated trichomes were consecutively submerged in two aliqouts of $CHCl_3$ for 30 sec per aliqout. The two solutions were pooled and a known amount of *n*-tetracosane was added as an internal standard. The $CHCl_3$ was then removed under vacuum before

derivatizing with bis-N,O-(trimethylsilyl)trifluoroacetamide (BSTFA) in pyridine for 30 min at 70°C. The solvents were then evaporated under a gentle stream of N_2 gas while heating at 50°C before $CHCl_3$ was again added to the wax.

4.3.4 Wax identification and quantification

Wax constituents were separated by capillary GC (6890N, Agilent, Avondale, PA, USA; column 30 m HP-1, 0.32 mm i.d., df=0.1 μm) using the following temperature regime: on-column injection at 50°C, oven held for 2 min at 50°C, raised by 40°C min^{-1} to 200°C, held for 2 min at 200°C, raised by 3°C min^{-1} to 320°C, and held for 30 min at 320°C. For compound identification, the GC was linked to a mass spectrometric detector (5973N, Agilent) and the inlet pressure programmed for a constant 1.4 ml min^{-1} flow of He carrier gas. For compound quantification, the GC with inlet pressure programmed for constant flow of 2.0 ml min^{-1} of H_2 carrier gas was connected to a flame ionization detector (FID). The quantity (μg) was established by comparison to a defined amount of n-tetracosane, the internal standard added into the total wax extracts. To determine the extracted surface area, apparent surface areas were calculated with ImageJ software (Abramoff *et al.* 2004) from digital photographs of the samples and multiplied by 2 or π for total leaf and stem surface areas, respectively. The additional surface area resulting from the three-dimensional, projecting structure of trichomes was not included in calculating the true surface area. Wax loads (μg cm^{-2}) were determined by dividing the compound quantity by the corresponding extracted surface area.

4.4 Results

Two complementary experiments were performed on stem and then leaf waxes to determine the cell-type specific wax compositions of trichomes versus other epidermal cells. First, wax from the trichome-absent mutant *gl1* provided a baseline composition of non-trichome epidermal cells and was examined before waxes from lines that had medium (WT) and high (*cpc tcl1 etc1 etc3*) densities of trichomes. Neither of these lines exhibited gross, morphometric changes such as differences in leaf or plant size as compared to WT. Differences between *cpc tcl1 etc1 etc3* and *gl1* and, less drastically, between wild type and *gl1* should reflect trichome wax composition. Second, trichomes were isolated from wild type and *cpc tcl1 etc1 etc3*. Waxes extracted from these detached trichomes were directly analyzed for trichome specific wax composition and again compared to the bulk wax from *gl1*.

4.4.1 Bulk stem wax

The bulk wax load extracted from the stems of *gl1* mutants totaled 30±4 μg/cm^2. This wax contained the same compound classes as have been reported previously for Arabidopsis stem wax (Figure 4.1). One third of this was straight-chain alkanes (11±2 μg/cm^2), the most abundant compound class. One quarter of the wax was a ketone, specifically nonacosan-15-one (8±1 μg/cm^2), while one tenth was the secondary alcohol nonacosan-15-ol (3.2±0.6 μg/cm^2). Lesser quantities of primary alcohols (3.1±0.4 μg/cm^2), free fatty acids (0.2±0.1 μg/cm^2), esters (1.6±0.7 μg/cm^2), aldehydes (0.2±0.1 μg/cm^2), and triterpenoids (0.2±0.2 μg/cm^2) were also found. One tenth of the wax (2.2±0.2 μg/cm^2) could not be identified.

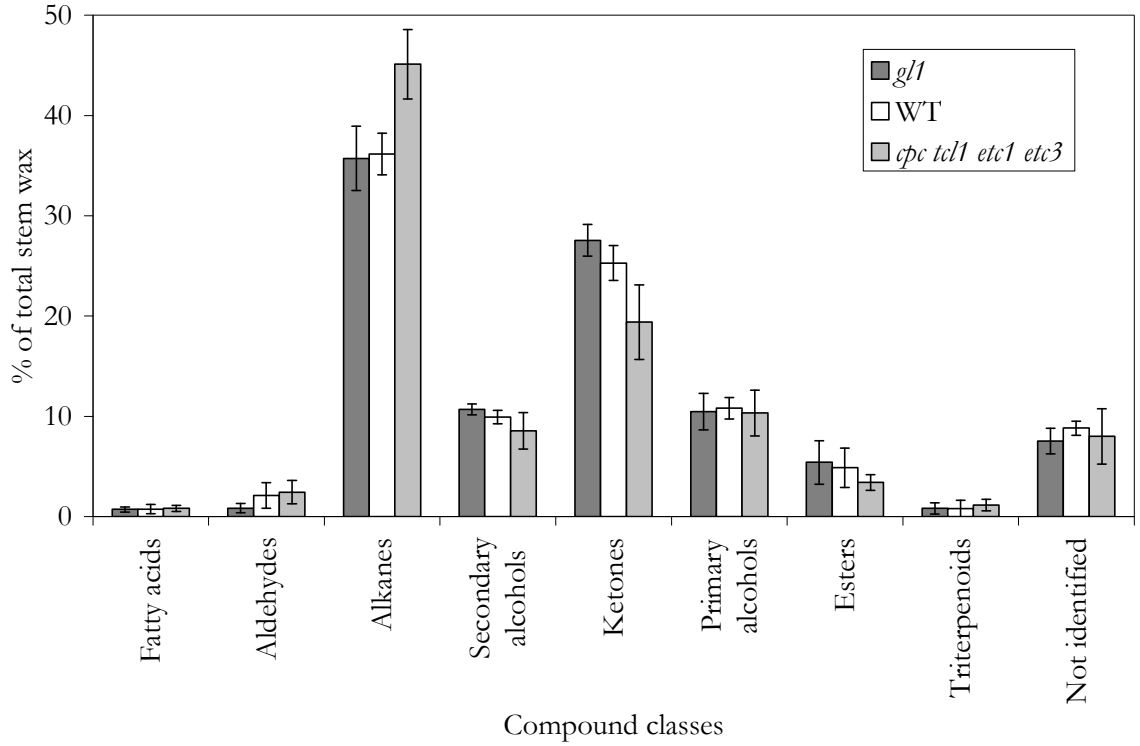

Figure 4.1 Relative quantities (% ± SD) of wax compound classes found in *Arabidopsis thaliana* stem wax of *gl1*, wild type, and *cpc tcl1 etc1 etc3* (n = 5).

The chain length distributions within each compound class in *gl1* wax were further examined (Figure 4.2). Within the alkane fraction, compounds ranged from 27 to 33 carbons in length

with nonacosane dominating (94±1%). Although odd numbered chain lengths were most abundant within the alkanes, trace quantities (<0.5%) of octacosane and triacontane were also observed. The other compound classes were dominated by even-numbered chain lengths. Primary alcohols ranged in length from 24 to 32 carbons, peaking at 28 carbons. For both the free fatty acids and aldehydes, equal ratios between 28 and 30 carbon compounds were found. The chain lengths of the esters ranged from 40 to 50 carbons and were composed of hexadecanoic or octadecanoic acid plus the complementary alcohol. The most abundant ester contained 44 carbons, the sum of the most abundant alcohol (28 carbons) plus a C16 acid. Two triterpenoids, namely β-amyrin and trinorlupeol, comprised approximately 1% each of the total wax.

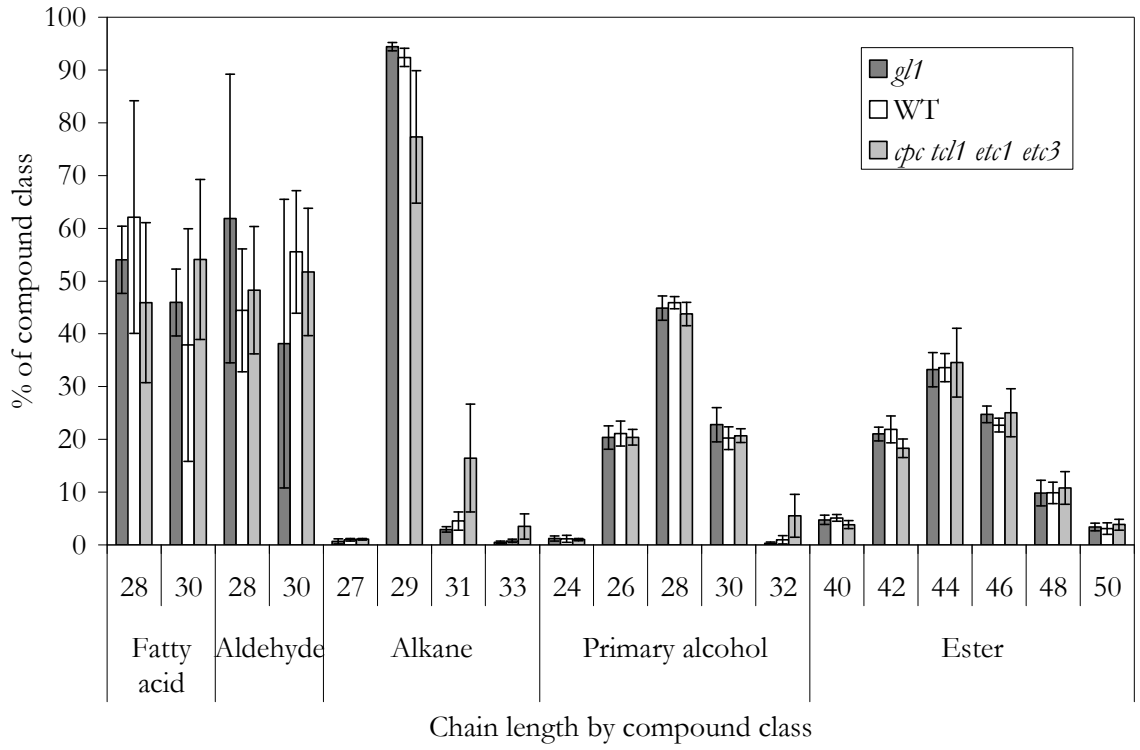

Figure 4.2 Relative distribution (% ± SD) of compound chain lengths within each compound class of *Arabidopsis thaliana* stem wax of *gl1*, wild type, and *cpc tcl1 etc1 etc3* (n = 5).

The total wax load from wild-type stems (29±8 μg/cm^2), even with the presence of trichomes, did not differ from that of *gl1*. The compound classes (both absolute and relative quantities) equaled those of *gl1* as well (Figure 4.1). Moreover, no differences were observed in the relative chain length distributions of compounds within their respective classes (Figure 4.2).

The dramatic increase in the number of trichomes found in the quadruple mutant *cpc tcl1 etc1 etc3* did not alter the total stem wax load (28±12 μg/cm^2). Differences occurred in relative percentages of compound classes between the three lines (Figure 4.1). The alkane percentage increased by nearly 10% in *cpc tcl1 etc1 etc3* (45±3%) as compared to both WT (36±2%) and *gl1* (36±3%). Correspondingly, ketones were down by approximately 7% in *cpc tcl1 etc1 etc3* (19±4%) in relation to WT (25±2%) and *gl1* (28±2%). Slight decreases in secondary alcohols and esters were also observed from *cpc tcl1 etc1 etc3* to WT to *gl1* while an inverse slight increase was seen for aldehydes.

Chain length ranges within stem wax compound classes were the same for *cpc tcl1 etc1 etc3* as compared to *gl1* and WT but the distribution within these ranges differed (Figure 4.2). Greater relative quantities of C31 and C33 alkanes and correspondingly less C29 alkane were found in *cpc tcl1 etc1 etc3* as compared to *gl1* and WT. Similarly, a higher percentage of C32 alcohol was found in the excess-trichome mutant in comparison with the other lines. For the remaining compound classes, no differences in chain-length distributions were found.

4.4.2 Bulk leaf wax

The total wax load extracted from the leaves of *gl1* equalled 0.9±0.1 μg/cm^2. Only four compound classes were identified within this mixture, less that that observed in stems (Figure 4-3). Alkanes formed the largest class with one-third of the wax (0.33±0.08 μg/cm^2) while primary alcohols (0.17±0.04 μg/cm^2) and free fatty acids (0.16±0.05 μg/cm^2) each contributed approximately one-fifth to the total wax load. Aldehydes contributed 0.06±0.02 μg/cm^2. The remaining wax (0.2±0.07 μg/cm^2) was not identifiable.

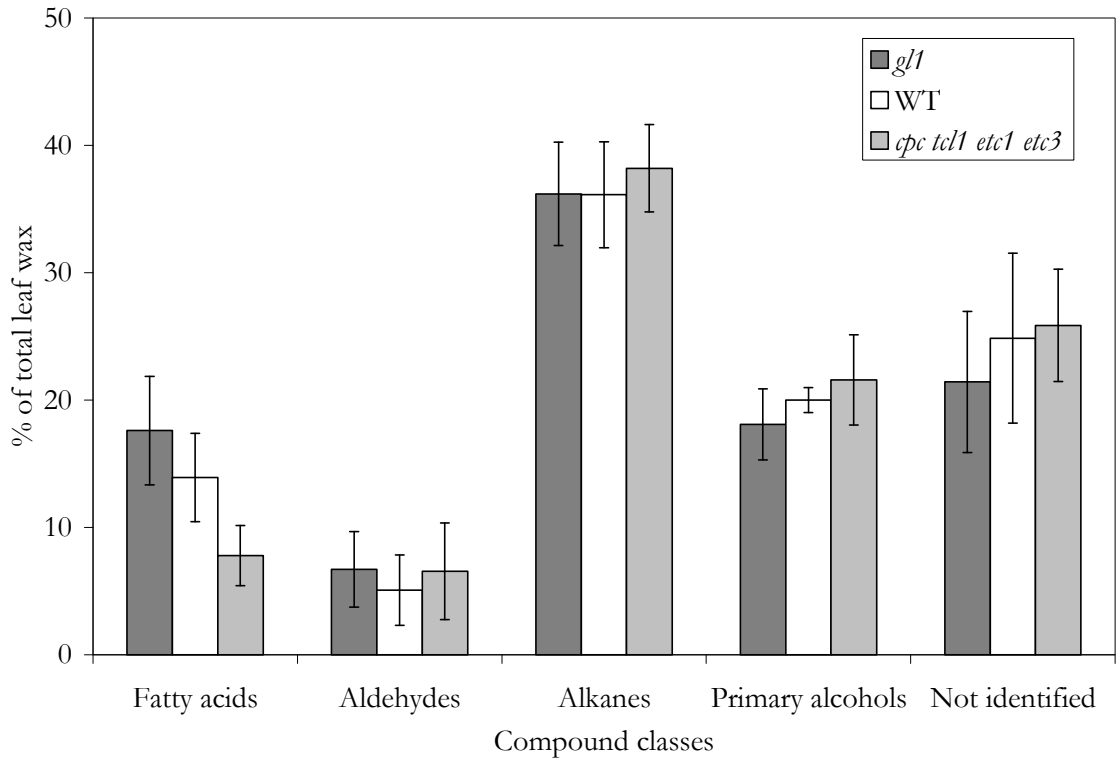

Figure 4-3 Relative quantities (% ± SD) of wax compound classes found in *Arabidopsis thaliana* leaf wax of *gl1*, wild type, and *cpc tcl1 etc1 etc3* (n = 5).

The distributions of compounds within each class in *gl1* leaves were further examined (Figure 4.4). Alkane chain lengths ranged from 27 to 37 carbons with C31 (45%) and C29 (35%) predominating. As in stems, odd-numbered carbon chains were most abundant but small quantities (2%) of C30 and C32 alkane were detected. The rest of the compound classes contained mainly even numbers of carbons with minor quantities of odd-number carbon compounds. The primary alcohols contained both branched (60%) and straight chain (40%) compounds. Branched alcohols ranged from 30 to 34 carbons total (including branched carbons) and peaked at 32 (33% of class). The *n*-alcohols exhibited a much broader chain length distribution, ranging from 26 to 34 carbons with a maximum at 30 (12% of class). Free fatty acids spanned a 10-carbon range, from C24 to C34. Although C26 acid predominated (40%), the remaining compounds did not form a normal distribution but instead fluctuated between 10 to 15% of the class. The aldehydes contained the narrowest range (28-34 carbons) with a maximum at C32.

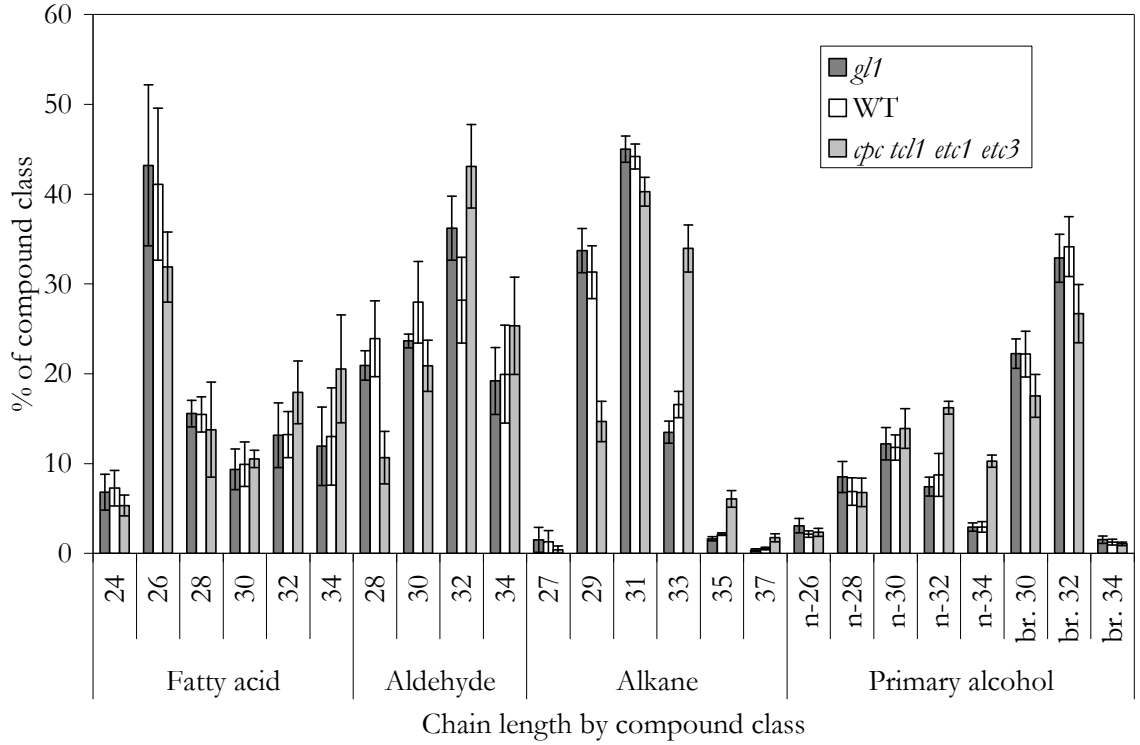

Figure 4.4 Relative distribution (% ± SD) of compound chain lengths within each compound class of *Arabidopsis thaliana* leaf wax of *gl1*, wild type, and *cpc tcl1 etc1 etc3* (n = 5).

Similar to the stems, the total wax load from wild-type leaves (1.1±0.2 μg/cm^2) equaled that of *gl1* despite the small increase in surface area caused by the presence of trichomes. Similarly, the absolute and relative quantities of compound classes did not differ from those of *gl1* (Figure 4-3). For individual compounds, almost all contained the same relative chain length distribution found in *gl1* leaf wax with two exceptions (Figure 4.4). Hentriacosane and tritriacosane were present at higher relative amounts.

The total wax load and the absolute quantities of compound classes were not affected by the large increase in the number of trichomes in *cpc tcl1 etc1 etc3*. In contrast, the relative quantity of fatty acids in the quadruple mutant as compared to the other two lines decreased with corresponding but negligible increases in the remaining compound classes (Figure 4-3).

Although the range of compound chain lengths within each compound class did not vary between the three lines, increases in absolute and relative quantities between individual

compounds were observed for longer chain length compounds in *cpc tcl1 etc1 etc3* leaf wax (Figure 4.4). Within the alkanes from *cpc tcl1 etc1 etc3*, the percentages of nonacosane decreased by half and hentriacosane slightly decreased slightly while the percentages of alkanes with chain lengths longer than this more than doubled. This effect was driven by higher absolute quantities of tritriacosane (0.18±0.06 versus 0.05±0.01 $\mu g/cm^2$ in *cpc tcl1 etc1 etc3* and *gl1*) and pentatriacosane (0.03±0.01 versus 0.005±0.001 $\mu g/cm^2$ in *cpc tcl1 etc1 etc3* and *gl1*). Similarly, large increases in the percentage of C32 and C34 *n*-alcohols. However, the equivalent chain lengths for the branched alcohols decreased. Within the aldehydes, the percentage of hexacosanal decreased with complementary increases spread between dotriacosanal and tetratriacosanal. A trend towards higher percentages of the longer chain lengths of fatty acids was also noted. These differences as described above were most obvious between *cpc tcl1 etc1 etc3* and *gl1* but the same patterns were observed between WT and *gl1*.

To further assess the differences observed in chain lengths, the relative percentages by compound class of each compound in *cpc tcl1 etc1 etc3* were subtracted from the respective percent from *gl1* (Figure 4.5 and Figure 4.6). Negative numbers indicate higher percentages in non-trichome epidermal cells while positive numbers reflect higher percentages in trichome wax. Within the stem waxes, compounds with shorter chain lengths were always negative while longer compounds were positive (Figure 4.5). The change-over between negative and positive occurred between compounds containing 28 and 30 carbons for free acids and aldehydes, 29 and 31 carbons for alkanes, 30 and 32 carbons for primary alcohols, and 42 and 44 carbons for esters. For the leaf waxes, a similar trend from negative to positive with increasing chain lengths occurred for all classes except for the branched alcohol sub-class (Figure 4.6). Specifically, the change from negative to positive appeared between compounds containing 28 and 30 carbons for free acids and straight-chain alcohols, 30 and 32 carbons for aldehydes and 31 and 33 carbons for alkanes.

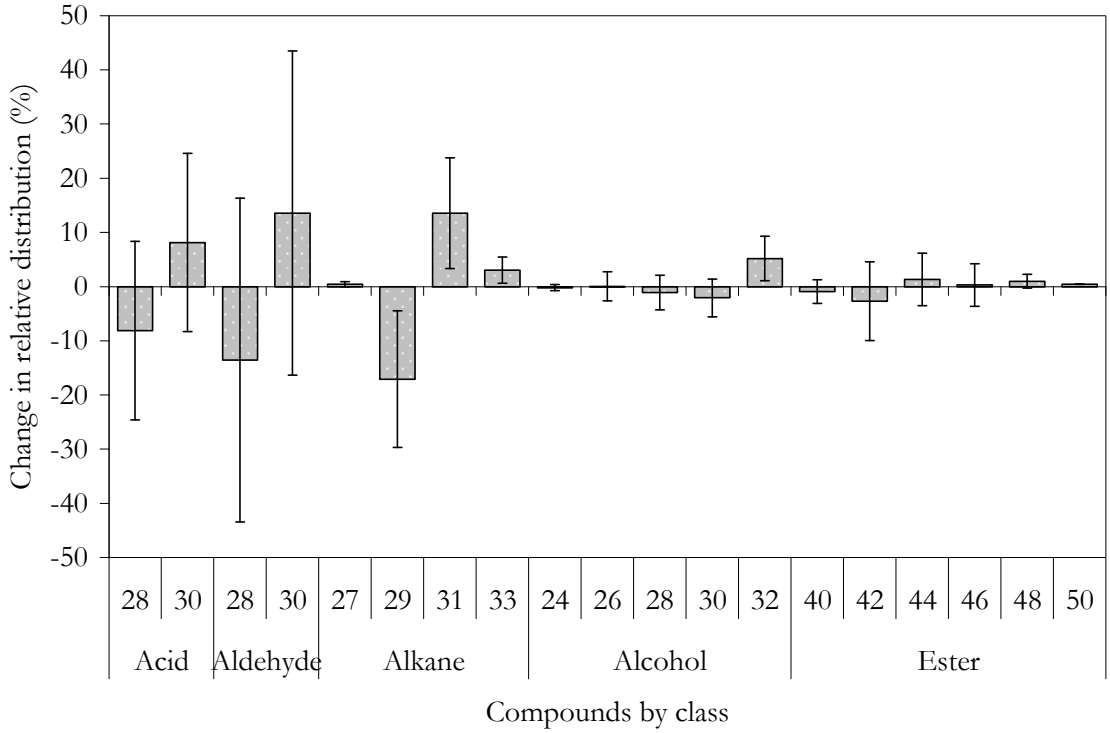

Figure 4.5 Difference in relative distribution of compounds obtained by subtracting the relative quantity of stem wax compounds within their respective compound class in *gl1*(n=5) from that in *cpc tcl1 etc1 etc3* (n=5; change in % ± SD)

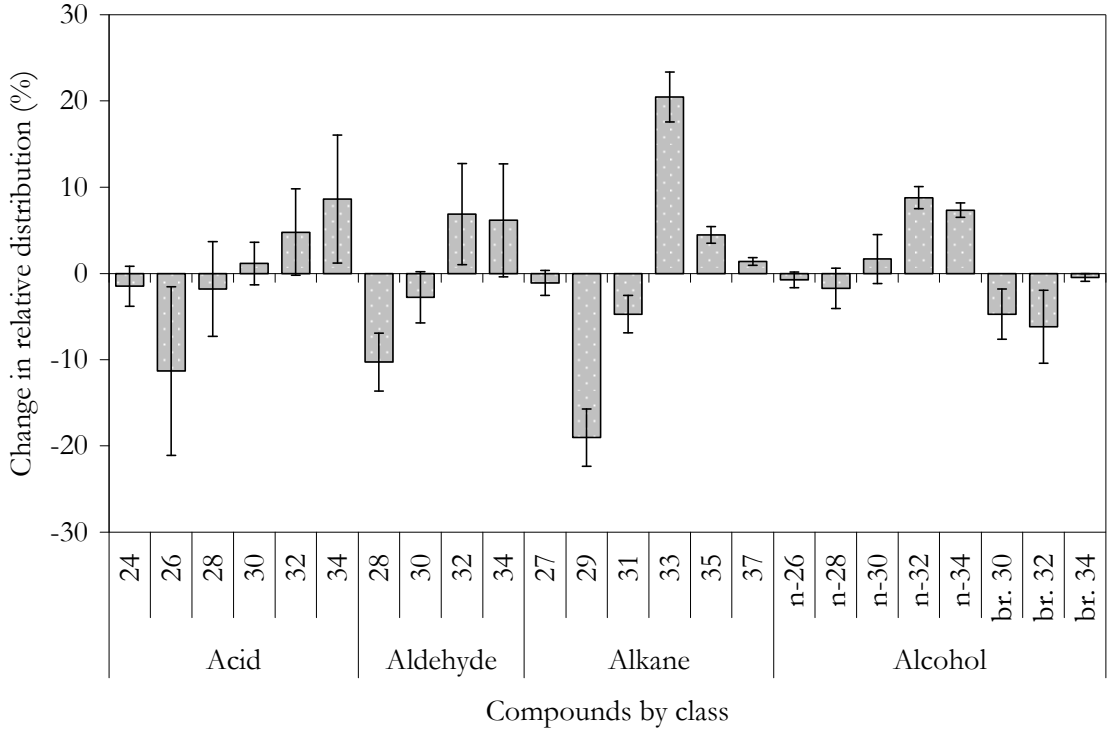

Figure 4.6 Difference in relative distribution of compounds obtained by subtracting the relative quantity of leaf wax compounds within their respective compound class in *gl1* (n=5) from that in *cpc tcl1 etc1 etc3* (n=5; change in % ± SD)

4.4.3 Leaf trichome wax

To probe the cell-type specificity of wax composition further, trichomes were separated from the other epidermal cells prior to wax extraction and in this way trichome wax was directly and specifically analyzed. Trichome isolation was first attempted on stem trichomes but the method also removed epicuticular wax crystals, preventing reliable extraction of solely trichome wax.

Extracted wax from WT leaf trichomes revealed only two compound classes (Figure 4.7). Alkanes (nearly 70%) dominated the wax while primary alcohols contributed only 10%. Slightly over 20% of the wax could not be identified, mirroring the percentage of unidentified compounds in the bulk leaf wax extraction. Within the alkanes, compounds ranged in chain length from 27 to 37 carbons (Figure 4.8). C31 (45%) and C33 (30%) alkanes accounted for most of the alkane wax. The primary alcohols contained both branched (10% of alcohols) and straight-chain (90% of alcohols) compounds. Only two branched alcohols, with total carbons

numbering 30 and 32, were found and both contributed approximately 5% to the alcohols. The straight-chain alcohols ranged from 26 to 34 carbons in length. C32 alcohol was the most abundant at 25% followed closely by C34 alcohol at 20%.

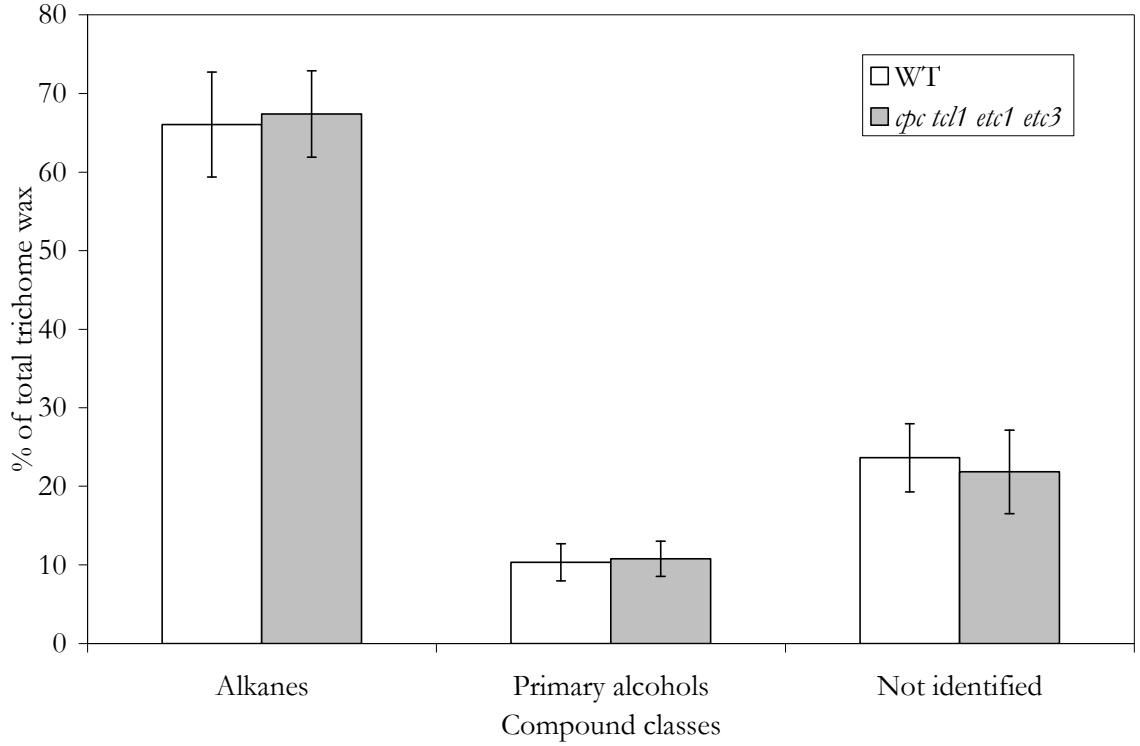

Figure 4.7 Relative quantities (% ± SD) of wax compound classes found in *Arabidopsis thaliana* leaf trichomes of wild type and *cpc tcl1 etc1 etc3* (n=5).

The wax compositions from WT and *cpc tcl1 etc1 etc3* trichomes were identical for the relative quantities of compound classes (Figure 4.7). Chain length distributions were also similar, with no differences observed for the alcohols but a slight increase in alkanes with longer chain lengths over short chain lengths (Figure 4.8). Of note, no glycerolipids and only minor quantities of hexadecanoic and octadecanoic acid were detected in any of the samples extracted from isolated trichomes. This confirmed that membrane lipids and general intracellular lipids were not extracted and that the method is specific to cuticular lipids.

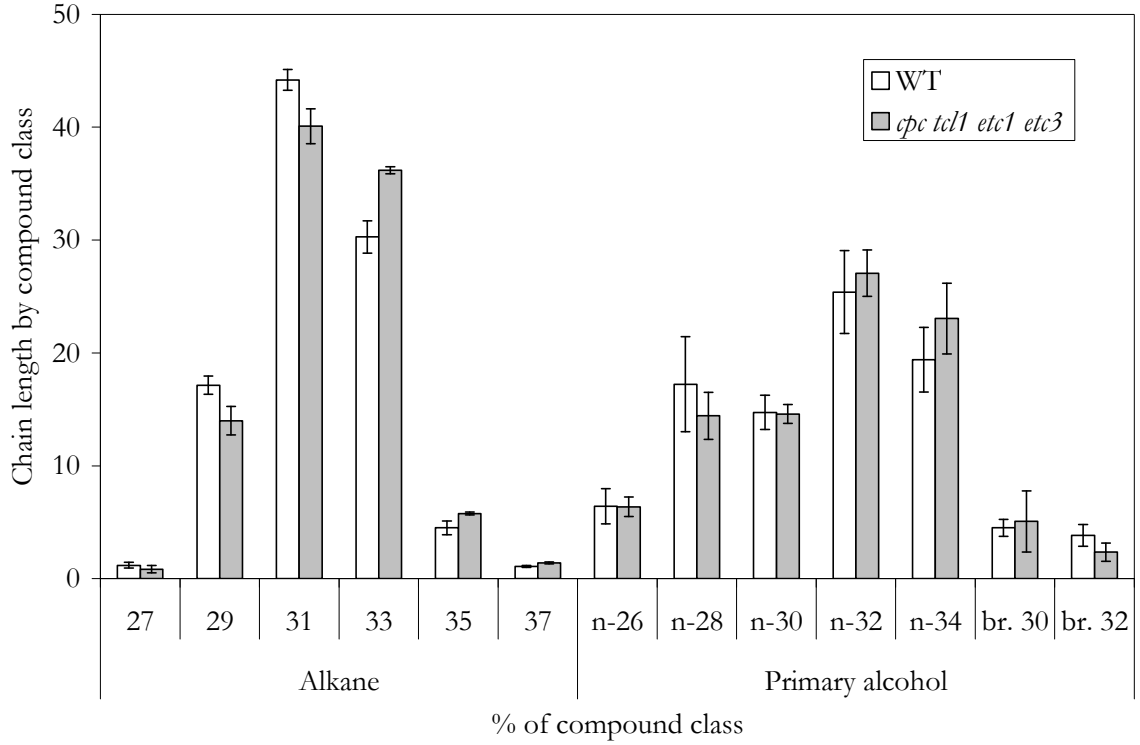

Figure 4.8 Relative distribution (% ± SD) of compound chain lengths within each compound class of *Arabidopsis thaliana* leaf trichome wax of wild type and *cpc tcl1 etc1 etc3* (n = 5).

4.5 Discussion

In order to probe the cell-type specificity of wax composition, waxes from trichome-absent mutants (*gl1*), wild type, and excess-trichome quadruple mutants (*cpc tcl1 etc1 etc3*) as well as isolated trichomes from WT and *cpc tcl1 etc1 etc3* were examined. The wax composition of *gl1* (no trichomes) compared to the differences between *cpc tcl1 etc1 etc3* and *gl1* (and to a lesser degree between WT and *gl1*) provide indications of wax specificity between cell types, although pleiotrophic effects resulting from the mutated genes could indirectly influence wax composition. Further corroborating indications of wax specificity were obtained by comparing isolated trichomes to the the bulk leaf wax. Cell-type specificity on stems and leaves occurred at two levels, namely compound classes and compound chain length distributions. This specificity and the ramifications for the respective biosynthetic machinery will be discussed at each level.

4.5.1 Compound class differences

Comparing the stem wax classes of *gl1* to the differences in classes between *cpc tcl1 etc1 etc3* and *gl1* revealed cell-type specific compositions. Wax from non-trichome epidermal cells was dividable into eight classes with no single class contributing more than 40% to the total. For trichomes, a major increase in the relative quantity of alkanes was observed in *cpc tcl1 etc1 etc3* as compared to *gl1*. As this was the largest change in compound classes, it appears likely that alkanes greatly dominate stem trichome wax. Moreover, small decreases in the percentages of secondary alcohols and ketones in *cpc tcl1 etc1 etc3* wax as compared to pavement cell wax suggest that these classes are either present at low percentages or perhaps even absent in stem trichome wax. In support of this, MAH1, the single enzyme responsible for catalyzing the formation of both these classes, was localized strictly to pavement cells and absent from trichomes (Greer *et al.* 2007). Similarly, a slight decrease in the percentage of esters suggest that this class may also be absent from trichomes. Overall, stem trichome wax appears to have a reduced number of compound classes and a higher proportion of alkanes as compared to pavement cells.

In leaves, the comparison of *gl1* wax to the difference between *cpc tcl1 etc1 etc3* and *gl1* waxes revealed few differences. Slight decreases in alkanes and alcohols and an increase in acids from *cpc tcl1 etc1 etc3* to *gl1* suggests that trichomes have more alkanes and alcohols but less acids than pavement cells. This comparison is partially confirmed by the wax from isolated trichome. As compared to *gl1* wax, wax from isolated trichomes contained twice the percentage of alkanes, similar percentages of primary *n*-alcohols, and negligible or no detectable percentages of branched primary alcohols, aldehydes, and free fatty acids. Leaf pavement cells, which have these latter three compound classes, show a much greater diversity in their wax compound classes than leaf trichomes and a corresponding decrease in alkane dominance.

The presence of primary alcohols in pavement cell wax of stems and leaves indicates the presence of a fatty-acyl reductase (FAR). However, FAR3/CER4, the only wax-specific FAR identified to date, was shown in leaves to be expressed in trichomes but not in pavement cells (Rowland *et al.* 2006). Thus, the cellular localization of CER4 could be misleading.

Alternatively, one or more of the remaining seven FARs might act on longer substrates than have so far been determined (Domergue *et al.* 2010).

4.5.2 Chain length distribution differences

A major difference in trichome wax as compared to other epidermal cell wax was the increase in chain length. For stems, compounds longer than 30 carbons were increased in *cpc tcl1 etc1 etc3* as compared to *gl1* (except within the esters). In leaves, compound longer than 32 carbons in length showed a clear increase in *cpc tcl1 etc1 etc3* over *gl1*. This is further supported by the isolated trichome wax that showed a two carbon increase in dominant chain lengths as compared to *gl1*. The ratios of alkanes between 29 and 35 carbons and of alcohols between 26 and 32 carbons determined here for isolated trichomes paralleled the ratios found by Ebert *et al.* (2010) in a trichome metabolomics study.

The increase in chain lengths between cell types is similar in magnitude to increase in chain length observed from stems to leaves. However, the factors controlling the length differences between organs have not been determined to date. As the leaf trichome wax contained compounds even longer than the leaf wax, several of the extra-very-long-chain compounds (longer than 34 carbons) were detectable. These have not been commonly described for Arabidopsis leaf wax. Specifically, C37 alkane is not known to have been reported before for Arabidopsis. Overall, a shift towards higher chain lengths is found in trichome wax compounds as compared to pavement wax in both leaves and stems.

Since trichome wax and non-trichome waxes were shown to have distinct compound distributions with classes, the elongation machinery for each cell type must also contain (at least some) unique enzymes and/or differential regulation. The extra elongation cycles observed in trichomes may result from additional proteins that direct substrate towards additional elongation rather than compound class formation. Alternatively, but much less likely, chain extension to these extra-very-long chain lengths may by catalyzed by alternative elongases such as the 4 ELO-like genes found in the Arabidopsis genome (Dunn *et al.* 2004).

Most likely, differences in chain lengths between trichomes and pavement cells are caused by the presence or absence of specific KCS(s). It is well accepted that the chain length is determined by the KCS but not the three final steps (reduction by KCR, dehydration by PAS2,

and reduction by CER10) in elongation (Millar *et al.* 1997). From the 21-gene family of KCSs in Arabidopsis, KCS2 (DAISY; Franke *et al.* 2009), KCS6 (CER6; Jenks *et al.* 1995), KCS18 (FAE1; Millar *et al.* 1997), and KCS20 (Lee *et al.* 2009) have been shown *in planta* to have product specificity while other KCSs have shown activity in yeast (Trenkamp *et al.* 2004; Paul *et al.* 2006; Blacklock *et al.* 2006). From these, the KCS performing the longest known extensions is KCS6, which elongates from 26 to 30 carbons (Weidenhamer *et al.* 1993; Millar *et al.* 1999; Fiebig *et al.* 2000). Thus, nothing is known about elongation to the longest chain lengths observed in leaf trichomes (31-35 carbons) but they likely result from one or more of the uncharacterized KCSs. Research is underway in our lab to characterize the gene(s) responsible for the longer chain lengths.

What possible advantages are caused by longer chain lengths in trichomes? Longer chain-lengths may more effectively prevent water loss, which is more important for trichomes with their higher cell-atmosphere surface area to volume ratio as compared to pavement cells. This is further supported by the increase in alkane chain lengths observed in drought stressed Arabidopsis leaves (Kosma *et al.* 2009). Further studies are needed to clarify whether longer chain lengths confer a functional advantage: Cloning and over-expression of the respective KCS(s) followed by cuticular permeability analyses (see Chapter 6 for an example) may reveal whether the barrier effectiveness substantially increases with the modest increases in wax chain lengths. It will also be interesting to determine the wax composition on guard cells as compared to that of both pavement cells and trichomes and how, if at all, this contributes to stomatal functioning.

The conclusion that both trichome and pavement cell types have independent wax biosynthesis machineries raises the question whether lateral diffusion can cause exchange of wax compounds between neighbouring cells, and whether the chemical differences in their surface composition might be even more pronounced without diffusion. Although diffusion would not affect the analysis of *gl1* wax since it lacks trichomes, the observed trichome wax may be contaminated by basal and/or pavement cell wax compounds diffusing into the trichome wax. The diffusion coefficients of 26 to 27 carbon wax compounds (regardless of class) in wax is approximately 10^{-21} m^2/sec as determined by Schreiber *et al.* (1993). After thirty days (approximate time from trichome formation to wax analysis) and no additional

biosynthesis of the compound, the compound would reach a concentration of 1/e (approx. 0.367) of the original concentration at a distance of only 0.1 μm. Increasing compound length by 10 carbons would decrease the distance to 0.01 μm. Considering that trichome stalks are around 100 μm in length, diffusion is not fast enough to significantly alter the wax composition. Moreover, if diffusion were to occur, it would only lessen the observed differences instead of causing or enhancing them. Consequently, the detected compositions reflect the minimum differences between epidermal cell types.

The original *cpc* mutant was generated in the Wassilewskija ecotype. Subsequent crossings with the other three mutants (Columbia-0 ecotypes) diminished but likely did not eliminate the genetic contributions of this parent towards wax biosynthesis. Moreover, mutations causing trichome density reductions frequently also affect root hair numbers; root hairs compose only 3% of epidermal cells in *cpc tcl1 etc1 etc3* as compared to 42% for wild type (Wang *et al.* 2008). A decrease in root hairs may generate drought stress which in turn may influence wax composition. For these two reasons, trichomes from wild-type leaves were isolated in sufficient quantity to analyze their wax. No differences in composition were observed between trichome waxes from these lines. This confirms that the observed trichome wax composition is cell-type specific and not influenced by other physiological factors.

Trichome lipid analyses may provide a method for clarifying the wax biosynthetic pathway. Because trichomes are the only epidermal cells that can be easily isolated, they provide a unique tool for analyzing cuticular lipids and potentially non-secreted intermediates devoid of mesophyll contamination. Combining this with developed microarrays, established metabolite profiling methods, and known cuticle mutants makes a powerful tool for cuticle research.

Chapter 5
Composition differences between cuticular wax substructures

5.1 Summary

The protective coating of the wax on plant surfaces has long been considered non-uniform in composition at a sub-cellular scale. In recent years, direct evidence has started to accumulate showing quantitative compositional differences between the epicuticular wax (i.e. wax exterior to cutin that can be mechanically peeled off) and intracuticular wax (i.e. wax residing within the mechanically resistant layer of cutin) layers in particular. This review provides a first synthesis of the results acquired for all the species investigated to date in order to directly assign chemical information to cuticle substructures, together with an overview of the methods used and a discussion of possible mechanisms and biological functions. The development of methods to probe the wax for z-direction heterogeneity began with differential solvent extractions. Further research employing mechanical wax removal by adhesives permitted the separation and analysis of the epicuticular and intracuticular wax. In wild-type plants, the intracuticular (1-30 μg cm^{-2}) plus the epicuticular wax (5-30 μg cm^{-2}) combined to a total of 8-40 μg cm^{-2}. Cyclic wax constituents, such as triterpenoids and alkylresorcinols, preferentially or entirely accumulate within the intracuticular layer. Within the very-long-chain aliphatic wax components, primary alcohols tend to accumulate to higher percentages in the intracuticular wax layer, while free fatty acids and alkanes in many cases accumulate in the epicuticular layer. Compounds with different chain lengths are typically distributed evenly between the layers. The mechanism causing the fractionation remains to be elucidated but it seems plausible that it involves, at least in part, spontaneous partitioning due to the physico-chemical properties of the wax compounds and interactions with the surrounding intracuticular polymers. The arrangement of compounds likely directly influences cuticular functions.

5.2 Introduction

Land plants must cope with adverse conditions including high doses of ultraviolet light, prolonged exposure to a dry atmosphere, leaching by heavy rains, harmful concentrations of air-borne pollutants, shading by contaminating surface particulate, and attack by pathogens and herbivores. These above-ground abiotic and biotic stresses initially affect the plant surface and

therefore may be countered effectively by protective mechanisms located in an outer skin. Over non-woody plant parts, these protective functions are performed by a lipid coating called the cuticle.

Plant cuticles are lipophilic structures deposited onto the outer side of epidermal cell walls. Two major components of plant cuticles are typically distinguished based on their solubility in organic solvents: the lipophilic compounds released by solvent extraction are collectively designated as "cuticular wax", whereas the second lipophilic component that cannot be extracted due to its polymer structure is called "cutin". Cutin is a polyester of C16 and C18 hydroxy-fatty acids and glycerol, although dicarboxylic acids may also be prominent compounds (Walton 1990; Nawrath 2006; Pollard *et al.* 2008). Cuticular wax, on the other hand, is typically a complex mixture of dozens of compounds with diverse hydrocarbon chain or ring structures (Walton 1990; Jetter *et al.* 2007). The most ubiquitous - and frequently most prominent - group of compounds are aliphatics with fully saturated (no C=C double bonds), unbranched hydrocarbon chains containing at least 20 carbons. These "very-long-chain" (VLC) compounds are biosynthesized by elongation of fatty acids beyond chain lengths of C18, and by further modification into corresponding alkanes, aldehydes and ketones, primary and secondary alcohols, as well as the esters formed by combining fatty acids and alcohols (Samuels *et al.* 2008). A second group of compounds accumulating in the cuticular wax of many plant species are the pentacyclic triterpenoids. These alicyclic constituents also have largely saturated aliphatic structures, but contain condensed hydrocarbon rings rather than chains (Jetter *et al.* 2007). Aromatic compounds can also be found in low quantities in cuticular wax mixtures from certain plant species (Jetter *et al.* 2007).

Based on microscopic evidence, it has long been recognized that the cuticular wax is dispersed across the entire depth of the cuticle, with some of the wax embedded within the cutin polymer matrix and some of it deposited on the outer surface of the polymer (Jeffree 1996). The former has been designated as "intracuticular wax" while the latter is the "epicuticular wax". The two layers of wax thus defined are the major sub-structures occurring within the cuticular wax of all vascular plants. It must be noted, however, that many reports erroneously use the term "epicuticular wax" to refer to the bulk soluble cuticular waxes, such as are extracted by organic solvents. Although various attempts have been made over the years,

reliable information on the composition of these two layers has been scarce until recently. It was not clear whether compositional differences, and thus gradients in one or more of the wax constituents, existed between the two wax compartments. It was, therefore, also not clear how much each of the wax compounds and layers contributes to the overall biological functions of the cuticular wax.

Beyond the distinction between epi- and intracuticular wax layers, two further small-scale features may be observed within cuticles in certain cases. The first of these are lamellae that may be seen within the intracuticular layer using TEM, but whose chemical composition and mode of formation remain elusive (Jeffree 2006). The second nano-scale structural element are wax crystals protruding from the epicuticular layer into the atmosphere, present in many plant species and varying dramatically between them as documented by SEM (Barthlott *et al.* 1998). Indirect evidence mainly acquired from comparisons across species or between mutant lines within species showed correlations between crystal shapes and corresponding bulk wax compositions (Baker 1982; Jeffree 2006). This led to the conclusion that certain crystal types are formed by specific compounds. However, since these conclusions were based on total cuticular wax composition, the contribution of specific compounds could only be inferred indirectly. In order to quantify the exact crystal composition, selective sampling and analysis of only the epicuticular wax crystals is required.

Over the past decade, new methods have been devised that allow the selective removal of epicuticular waxes, finally enabling the composition of the epicuticular layer to be quantified directly. Where it could be shown that the methods were able to remove the epicuticular material exhaustively, the remaining intracuticular wax could also be analyzed selectively. Even though a number of species have been investigated with these methods over the past decade, the accumulated evidence has not been been reviewed so far. Therefore, the current review will summarize our current knowledge on the composition of intra- and epicuticular wax layers, in an attempt to directly assign chemical information to cuticle substructures.

Previous reviews on cuticle structure rarely connected it to chemical composition of the waxes. Conversely, most reviews on the chemical composition of plant cuticular waxes did not correlate it with cuticle substructures. However, two noteworthy exceptions are a review on the chemical composition of epicuticular wax crystals (Baker 1982) and a recent, very

comprehensive book chapter on cuticle structures (Jeffree 2006) that also summarizes the mainly indirect, correlative evidence on the formation and composition of epicuticular crystals. To complement these reviews, the present paper will focus more on the composition of the intracuticular wax layer and summarize our knowledge on the epicuticular composition mainly to contrast it against the adjacent intracuticular wax.

Specifically, this review will evaluate the various methods that are now available for selective sampling of epi- and intracuticular waxes (see "Review of method developments" section), summarize our current knowledge on the compositions of both layers and on possible differences between them (see "Differences in wax composition between layers" section), and finally address the biological implications of these results (see sections on "Possible mechanisms causing compositional differences between intra- and epicuticular wax layers" and "Implications of wax depth partitioning on cuticle functions").

5.3 Review of method developments: selectivity of wax sampling procedures

It had long been surmised that the intracuticular and epicuticular wax layers might differ in composition for a given plant species and organ. Accordingly, over the past three to four decades methods have been devised that aimed to selectively sample both wax compartments. These methods will be briefly described here, approximately following the order of their first descriptions in the literature.

5.3.1 Brief versus extended extraction with organic solvents

Originally, all methods for sampling cuticular waxes involved dipping intact plant organs into organic solvents. It seemed possible to preferentially probe the epicuticular waxes by using extremely short dipping times. In contrast, exhaustive extraction using extended time, hot organic solvent, or even overnight Soxhlet reflux should yield all of the cuticular wax. The intracuticular wax composition was inferred either by applying both methods in parallel to two samples and then subtracting the compositions or, alternatively, by employing both methods consecutively on the same sample in order to first extract the epicuticular wax preferentially and then extract the remaining (mainly) intracuticular material.

The discriminating extraction protocols were employed in some studies conducted in the 1970's in the laboratory of E.A. Baker (Silva Fernandes *et al.* 1964; Baker *et al.* 1975; Baker *et al.*

1982). The authors found differences between the waxes obtained by short and long extractions, thereby indicating that different depths within the cuticle exhibited compositional gradients as previously hypothesized. They also showed that the extraction protocols were indeed able to enrich portions of cuticular wax in the different extracts. However, this approach had clear limitations: first, even though this method showed qualitative gradients within the cuticular wax, they could not be quantified. Second, while these methods tended to sample parts of the wax that were located more towards the exterior or more towards the interior parts of the cuticle, they could not precisely differentiate between distinct, pre-defined layers within the cuticle. Third, solvents may preferentially extract certain compound classes due to differing solubilities. Thus, the results could not be interpreted strictly in terms of cuticle substructures, such as the epi- and intracuticular wax layers.

5.3.2 Collodion silver

Haas and Rentschler (1984) noticed discrepancies between widely ranging thicknesses of intracuticular compartments as judged by microscopy on cross sections and the apparent intracuticular wax yields determined by differential extraction for various plant species (Haas *et al.* 1984). The authors argued that, at least for species with thin epicuticular and large intracuticular wax layers, superficial extraction was not sufficiently selective and another, non-extractive method was required. They adapted a protocol involving mechanical removal of surface material for microscopy samples to instead allow chemical analyses: Collodion, a nitrocellulose-based polymer, was applied to the plant surface in liquid solution and, after drying, was peeled off, concomitantly stripping the surface wax. Analysis of the wax attached to the collodion film yielded quantitative data on both the relative composition of the mixture and its coverage on the plant surface in $\mu g\ cm^{-2}$. The collodion samples, generated by mechanical wax removal rather than chemical extraction, were interpreted to reflect the entire epicuticular wax layer. Conversely, the intracuticular wax was assumed to remain intact, accessible by superficial extraction of the (previously collodion-treated) specimen.

The collodion method was an important step towards selective sampling of wax layers, since it introduced the two ideas of mechanical wax stripping and of studying wax layers by removing them consecutively. However, the method had limitations regarding the accurate determination of both epi- and intracuticular wax compositions. First, it was not tested

whether the epicuticular wax had been completely removed prior to the extraction of the remaining material. Thus, the latter samples might have contained intracuticular wax together with unknown quantities of epicuticular wax. Second, it must be noted that collodion is typically applied in the presence of an organic solvent. In the initial study the polymer was dissolved in amyl acetate (6% w/v; Haas *et al.* 1984)), and commercial sources offer solutions in ether:ethanol (3:1, Merck Darmstadt). Organic solvent molecules can enter deep into the cuticle where they mobilize and mix intra- and epicuticular wax molecules (Jetter *et al.* 2000). Consequently, the collodion samples will contain not only surface compounds but also some intracuticular material, and the following extraction step will yield intracuticular wax together with some epicuticular material. Thus, even though the collodion stripping can be assumed to remove mainly material located near the tissue surface, the overall method has limited selectivity for the wax layers.

5.3.3 Surface swiping with dry glass fabric

In one study focusing on plant epicuticular wax crystals and their ecological role in surface interactions with protective ants, dry glass fabric was employed to mechanically sample waxes from epidermal surfaces of plant stems (Markstädter *et al.* 2000). Glass fabric was repeatedly swiped over the plant surface and then exhaustively extracted. Relatively high wax quantities could be obtained after swiping small surface areas, showing that the dry swipes captured substantial amounts of material. However, the wax yield per surface area was not determined, presumably because of difficulties in uniformly swiping a set area. It also remains unknown whether the swiping removed only a part of the epicuticular crystals, the entire crystal layer, crystals and the epicuticular wax film, or even parts of the intracuticular wax. While the selectivity of the method can thus not be assessed quantitatively, it seems very likely that it did achieve a strong enrichment of epicuticular crystals in the samples, allowing their relative composition to be determined fairly accurately. The dry swiping method should therefore be noted as a method with (likely) relatively high selectivity for analyzing epicuticular crystals, but not the overall epicuticular layer and/or the intracuticular wax.

5.3.4 Peeling with cryo-adhesives

The idea of mechanical wax sampling was further developed by Jeffree (1996) who introduced a method using frozen glycerol to transfer surface wax onto artificial substrates for electron

microscopy. Experimental details were not described at the time, and it took several years before the method was further developed by (Ensikat *et al.* (2000). The authors showed by SEM, TEM, and AFM that the epicuticular crystals could be pulled off with the help of frozen droplets of polar solvents. The crystal shapes and arrangements were perfectly preserved in the process, indicating that the ice coating acted as a glue that exerted enough force to break the crystals off the plant surface, but not enough to alter them. Presumably, the liquid wetted the surface crystals just enough to embed their tips, but did not act as a solvent that would cause (partial) disassembly into molecular components.

Schäffer *et al.* (2000) adapted this method for chemical analysis of epicuticular material. The authors first tested it on a plant surface covered by a smooth epicuticular wax film devoid of micro-crystal protrusions (Jetter *et al.* 2000). They showed that both glycerol and water could be used as cryo-adhesives. Consecutive adhesive applications yielded wax amounts rapidly declining to zero, whereas much greater quantities of wax could be released by consecutive solvent extraction of the same surface. This revealed a sharp boundary between two wax layers defined by the mechanical accessibility of the outer compartment. It was concluded that, since the polymer cutin is the only cuticle component resistant to mechanical stress, it was responsible for blocking mechanical wax removal beyond a certain point. Hence, the waxes sampled by cryo-stripping came from the exterior layer deposited outside the cutin matrix, i.e. the epicuticular wax. By repeating the mechanical removal of epicuticular wax, it was made exhaustive and the following solvent extraction consequently released exclusively intracuticular wax. The two sampling methods together for the first time allowed the quantitative analysis of both layers with high selectivity.

5.3.5 Peeling with carbohydrate polymer films

After the first method for the consecutive mechanical epicuticular and extractive intracuticular sampling had been established, it could serve as a point of reference to judge the layer-selectivity for other methods. Jetter and Schäffer (2001) demonstrated that aqueous solutions of gum arabic, an adhesive prepared from *Acacia senegal* or *Acacia seyal* trees, could be painted onto leaf surfaces and, after drying, form a glue that could lift off epicuticular wax as effectively as the cryo-adhesives. SEM observations provided additional visual support for the effectiveness of this method. Coward (2007) then showed that other carbohydrates can also

be used to remove and transfer epicuticular wax crystals. However, in this study the effectiveness of the sampling method was confirmed only by SEM and not also by chemical analysis.

In a series of studies it was shown that the gum arabic method is fairly versatile, successfully removing the epicuticular wax layer (both smooth films and films with crystals) from leaves and fruit of diverse plant species (see below). However, cellular protrusions limit the effectiveness. For example, trichomes contaminate the stripped epicuticular wax while papillose cells prevent exhaustive extraction of the epicuticular wax along the cell margins. On the other hand it should be noted that, unlike all previous methods, this method can be performed *in vivo* and thus is useful for epicuticular wax regeneration studies.

5.4 Differences in wax composition between layers

The different methods described above have been used to study various plant species over the past three decades. Specifically, the gum arabic and cryo-adhesive methods have been applied to over 20 plant surfaces, including the adaxial and abaxial leaf surfaces of *Kalanchoe daigremontiana* (Hamet et Perr. de la Bathie; van Maarseveen *et al.* 2009), *Macaranga tanarius* (Guhling *et al.* 2005), *Pisum sativum* cv Avanta (Gniwotta *et al.* 2005), and *Taxus baccata* L. (Wen *et al.* 2006); the adaxial leaf surfaces of *Ligustrum vulgare* L. (Buschhaus *et al.* 2007b), *Prunus laurcerasus* L. (Jetter *et al.* 2001), and *Rosa canina* L. (Buschhaus *et al.* 2007a); the abaxial leaf surface of *Secale cereale* L. (Ji *et al.* 2008); the inner, slippery surfaces of pitchers from *Nepenthes alata* Blanco (Riedel *et al.* 2003), *N. albomarginata* Lobb ex Lindl. (Riedel *et al.* 2007), *N. khasiana* (Riedel *et al.* 2007), *N. x henriana* (Riedel *et al.* 2007), *N. x intermedia* (Riedel *et al.* 2007), and *N. x superba* (Riedel *et al.* 2007); and the fruit of both wild-type *Solanum esculentum* and the *lecer6* mutant (Vogg *et al.* 2004). The results from these studies will be summarized below, first addressing the overall coverages and thicknesses of epicuticular and intracuticular wax layers, and then the distribution of individual compound classes.

Table 5.1: Samples where the intra- and epicuticular waxes have been selectively and quantitatively measured along with various parameters.

Species	**Organ**	**Surface**	**Method (times applied; replicates)**	**Crystals**	**SEM Confirmation**	**Reference**
Kalanchoe daigremontiana	Leaf	Adaxial Abaxial	Gum arabic (4x; n=5)	Twisted ribbons (AD, AB)	Before	Van Maarseveen and Jetter, (2009)
Ligustrum vulgare	Leaf	Adaxial	Gum arabic (3x; n=5)	Film	Before; After 1x (line); After 3x	Buschhaus *et al*., (2007)
Macaranga tanarius	Leaf	Adaxial Abaxial	Gum arabic (2x; n=n.r.)	Film with granules (AD); Platelets (AB)	Before; After 1x (line); G.A.	Guhling *et al*., (2005)
Pisum sativum cv Avanta	Leaf	Adaxial Abaxial	Gum arabic (4x; n=5)	Platelets (AD); Ribbons (AB)	Before	Gniwotta *et al*., (2005)
Prunus laurocerasus	Leaf	Adaxial	Gum arabic (3x; n=6)/Cryo	Film with granules	Before; After 1x (line); G.A.	Jetter and Schäffer, (2001)
Rosa canina	Leaf	Adaxial	Gum arabic (3x; n=4)	Film	Before; After 1x (line)	Buschhaus *et al*., (2007)
Secale cereale	Leaf	Abaxial	Gum arabic (4x; n=6)	n.r.	n.r.	Ji and Jetter, (2008)
Taxus baccata	Needle	Adaxial Abaxial	Gum arabic (3x; n=5)	Tubules (AD, AB)	Before; After 1x (line); After3x (AB); After $CHCl_3$ (AB); G.A..	Wen *et al*., (2006)
Nepenthes alata	Pitcher	Slippery zone	Cryo (4x; n=5); Gum arabic	Platelets	Before; After 1x (line); G.A.	Riedel *et al*., (2003)
Nepenthes albomarginata	Pitcher	Slippery zone	Cryo (5x; n=4)	Platelets	Before; After 1x (line); After $CHCl_3$	Riedel *et al*., (2007)
Nepenthes x henriana	Pitcher	Slippery zone	Cryo (3x; n=3)	Platelets	Before; After 1x (line); After $CHCl_3$	Riedel *et al*., (2007)

Species	Organ	Surface	Method (times applied; replicates)	Crystals	SEM Confirmation	Reference
Nepenthes x intermedia	Pitcher	Slippery zone	Cryo (5x; n=4)	Platelets	Before; After 1x (line); After $CHCl_3$	Riedel *et al*., (2007)
Nepenthes khasiana	Pitcher	Slippery zone	Cryo (5x; n=3)	Platelets	Before	Riedel *et al*., (2007)
Nepenthes x superba	Pitcher	Slippery zone	Cryo (4x; n=2)	Platelets	Before; After 1x (line); After $CHCl_3$	Riedel *et al*., (2007)
Solanum lycopersicum	Fruit	WT *lecer6*	Gum arabic (2x; n=5)	Film	n.r.	Vogg *et al*., (2004)
n.r. = not reported; g.a. = gum arabic; 1x = 1 treatment application; 3x = 3 treatment applications; line = dividing line between treated and untreated surface						

5.4.1 Wax quantities in epi- and intracuticular layers

As the gum arabic and cryo-adhesive methods have been used most frequently and provide reliable data, the results from all studies using them and reporting quantitative data have been compiled and, as necessary, standardized to $\mu g/cm^2 \pm$ SD (Figure 5.1; see Table 5.1 for a complete list of references). The reporting of wax quantities as mass per area permitted this meta-analysis; wax mass per fresh weight would not have allowed such comparisons. Absolute quantities of waxes in both intracuticular and epicuticular layers showed a wide range, similar to the great variability of total extractable wax reported across analyzed species. Total wax loads ranged from 8 $\mu g\ cm^{-2}$ to over 40 $\mu g\ cm^{-2}$. Within these overall wax coverages, intracuticular wax amounts ranged from 1 $\mu g\ cm^{-2}$ to 30 $\mu g\ cm^{-2}$ (10-80% of the total wax) with a median of 7 $\mu g\ cm^{-2}$. For the epicuticular wax layer, quantities varied from 5 $\mu g\ cm^{-2}$ to nearly 30 $\mu g\ cm^{-2}$ (20-90% of the total wax). Assuming a density of 0.8-1.0 x 10^6 g m^{-3} (Le Roux 1969), this equates to thicknesses of 10-375 nm for the intracuticular layer (excluding cutin) and 50-375 nm for the epicuticular wax. This in turn corresponds to an approximate range of 14-100 molecules stacked head to tail for the epicuticular layer, assuming an all-*trans*-conformation for the compounds. Since the presence of great quantities of epicuticular wax did not in all cases coincide with the occurrence of epicuticular wax crystals on the surface, other factors likely also contribute to the formation of crystals such as the relative concentration of individual compounds or the chemical structure of surrounding non-wax compounds (e.g. cutin). The ratios of intracuticular wax to epicuticular wax also showed great

variability, ranging from as little as 1:9 for *P. sativum* (Gniwotta *et al.* 2005) to as high as 4:1 for *L. vulgare* (Buschhaus *et al.* 2007b). The ratios do not correlate with the absolute quantities of extractable wax.

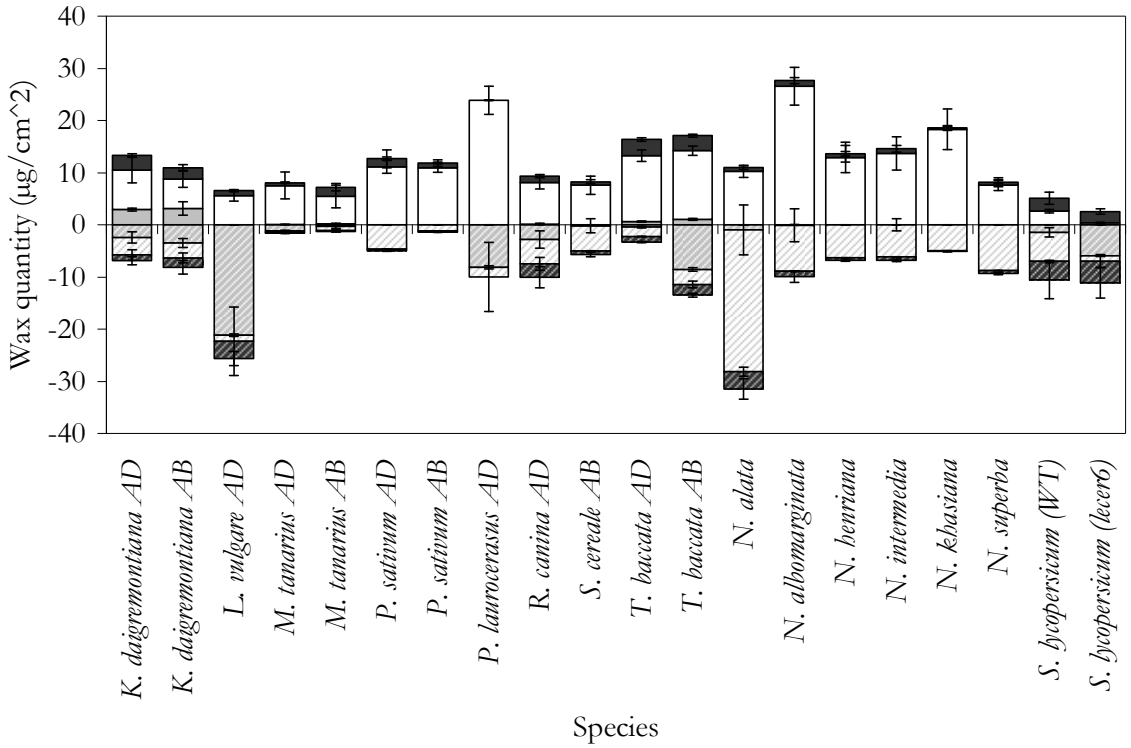

Figure 5.1 Absolute quantities (µg/cm^2 ± SD) of straight-chain (white), cyclic (gray), and non-identified (black) compounds in epicuticular (solid) and intracuticular (hashed) wax. The total epicuticular and intracuticular wax is represented by the bar height above and below zero, respectively. Together these sum to the total extractable wax. Samples were from adaxial (AD) or abaxial (AB) leaf surfaces, the slippery zones of pitchers, or fruit.

The extracted wax can be further divided into three large categories of constituents, namely cyclic, straight-chain, and not-identifiable compounds (Figure 5.1). Excluding the fruit of the *S. lycopersicon* mutant *lecer6*, cyclic compounds constituted 0-75% of the total, identifiable wax while conversely straight-chain compounds formed 25-100%. These numbers changed within the individual wax layers. In the intracuticular layer, cyclic compounds accounted for as low as 0% and as high as 95% of the identified wax while straight-chain compounds formed the balance. Smaller percentages of cyclic compounds (0-35%) and correspondingly greater percentages of straight-chain compounds (65-100%) were found for the identifiable wax in the

epicuticular layer. The ratios between cyclic and straight-chain compounds did not correlate with the total quantity of wax within the respective layer. For example, *M. tanarius* leaves were found to contain 1.5 μg cm^{-2} and 1.3 μg cm^{-2} of intracuticular wax on their adaxial and abaxial surfaces, respectively (Guhling *et al.* 2005). However, on the top surface, the ratio of straight-chain:cyclic compounds was approximately 4:1 while on the lower surface it was 1:3. On the other hand, although the *L. vulgare* leaf and *N. alata* pitcher both had over 25 μg cm^{-2} of intracuticular wax, cyclic compounds greatly dominated in *L. vulgare* (Buschhaus *et al.* 2007b) while straight-chain compounds were greatly in excess for the pitcher surface (Riedel *et al.* 2003).

In most cases differences in the relative compositions of the epi- and intracuticular wax layers were found. In some instances, these dissimilarities between the exterior and interior wax compartments were rather subtle, manifested only as small percentage variations that affected only minor compounds or only chain length distributions within compound classes. In many other cases, however, drastic differences were reported, including cases where a compound was absent from one layer and enriched at high concentration in the other. General trends suggesting which compounds tend to accumulate in which layer are slowly emerging and these trends will be summarized in the following sections.

5.4.2 Cyclic wax constituents

In the original studies establishing both the cryo-adhesive and the gum arabic methods on *P. laurocerasus* leaf waxes, it was shown that triterpenoid acids were entirely restricted to the intracuticular wax layer in this species, while various VLCFA derivatives were found distributed between both wax compartments (Jetter *et al.* 2000; Jetter *et al.* 2001). Subsequent examinations on several species showed a similar trend with the vast majority (or frequently all) of the triterpenoids located within the intracuticular layer (Figure 5.1). This pattern does not appear to depend on absolute (from 0.3 μg cm^{-2} in *M. tanarius* [Guhling *et al.* 2005] to over 20 μg cm^{-2} in *L. vulgare* intracuticular wax [Buschhaus *et al.* 2007b]) or relative (from 20% in *M. tanarius* to over 80% in *L. vulgare* intracuticular wax) wax quantities, nor does it matter which triterpenoid derivatives are involved (e.g. triterpenoid alcohols *versus* triterpenoid acids).

Kalanchoe daigremontiana leaf wax follows the same trend, albeit only weakly, with nearly equal absolute amounts of triterpenoids in the epi- and intracuticular layers but higher relative

proportions in the inner layer (van Maarseveen *et al.* 2009). It was speculated that, in this case, surface crystals might be formed out of the triterpenoids. It must yet be determined whether or not the epicuticular film beneath these crystals is composed of a triterpenoid-containing wax mixture. It is possible that the film may entirely lack triterpenoids (except for those being transported towards the crystals) although being surrounded by triterpenoid-containing intracuticular wax and epicuticular crystals. Why the triterpenoids also partition into the epicuticular wax (and crystals) in this species remains unknown, as other species (*L. vulgare* [Buschhaus *et al.* 2007b] and *P. laurocerasus* [Jetter *et al.* 2001]) contain both higher relative and absolute quantities of triterpenoids yet do not have triterpenoids in the epicuticular wax.

Like for most pentacyclic triterpenoids, steroids in *S. cereale* leaves were also restricted to the intracuticular wax layer (Ji *et al.* 2008). Other terpenoids seem to follow the same trend, as tocopherols have been found in minor quantities exclusively in the intracuticular layer on yew needles (Wen *et al.* 2006). Overall, terpenoids displace the aliphatic constituents in intracuticular wax to varying degrees. The evidence collected to date, covering a wide range of terpenoid structures and concentrations, suggests that mere chemical partitioning within the wax itself is insufficient to explain the triterpenoid gradients but instead that they occur because of either the chemical/physical nature of a second player – perhaps cutin – or a yet unknown transport mechanism (see section 5.5).

Aromatic compounds have sporadically been described in plant waxes and, similar to other cyclic compounds, they have been found to mainly accumulate within intracuticular wax. For example, the phenylethyl esters were located exclusively in the intracuticular wax of *L. vulgare* (0.6 μg cm-2; 2%; Buschhaus *et al.* 2007b). In *T. baccata*, the absolute quantities of phenylpropanoid and phenylbutanoid esters were similar to aromatic esters in *L. vulgare*, ranging from 0.7 to 1.6 μg cm-2 (Wen *et al.* 2006). However, as a percentage of the total wax within the layer, the intracuticular wax layer as compared to the epicuticular layers contained nearly 8-fold and 2-fold higher levels on the adaxial and abaxial surfaces, respectively. Leaves of *R. canina* contained minor quantities of phenylethyl esters (0.1 μg cm-2) in each layer; they contributed 1.1% to the intracuticular wax versus 0.9% to the epicuticular wax layer (Buschhaus *et al.* 2007a). The single study reporting the localization of benzyl esters indicated that they occur in the intracuticular wax layer (0.3 μg cm-2; 3%) of the leaves of *R. canina* at

nearly ten times the absolute and relative quantity found in the epicuticular wax layer (0.04 μg cm-2; 0.4%; (Buschhaus *et al.* 2007a).

A single report to date describes the localization of cuticular alkylresorcinols (Ji *et al.* 2008). In leaves of *S. cereale*, alkylresorcinols occur exclusively in the intracuticular layer (0.2 μg cm-2; 2%). Although the universality of this finding remains to be confirmed, it does follow the trend set by other cyclic wax compounds. Moreover, the intracuticular localization of alkylresorcinols suggests that the presence of the aromatic group outweighs the presence of an alkyl group in determining the partitioning of these compounds. It must yet be determined whether the addition of high concentrations of cyclic compounds would partially shift alkylresorcinols to the epicuticular wax and, if so, whether these would amalgamate into the film or form crystals.

5.4.3 Very-long-chain fatty acid derivative classes

Very-long-straight-chain classes are ubiquitous in plant waxes; frequently, they contribute the majority or sometimes the totality of the wax. The absolute quantities of any given VLC compound or compound class can vary dramatically between the intra- and epicuticular wax layers. Moreover, plants contain various combinations of VLC compound classes and unique distributions of homologous series of chain lengths within each class. Considering such variability, do gradients exist within this category of straight, very-long-chain compounds?

Partitioning occurs in various VLC compound classes (Figure 5.2). By comparing the percentage (within the total VLC compounds) of a specific compound class in the epicuticular layer to the percentage in the intracuticular layer, partitioning can be assessed. If the percentages are equal between the two layers for every compound class, then the wax can be assumed to be homogenous between the two layers. Conversely, differences in percentages imply preferential partitioning of a compound class into a respective layer.

Primary alcohols occurred at higher percentages within the intracuticular wax layer in one third of the species where leaf waxes were analyzed, namely the adaxial surfaces of *L. vulgare*, *P. laurocerasus*, *R. canina*, and the abaxial surface of *P. sativum* (Jetter *et al.* 2000; Gniwotta *et al.* 2005; Buschhaus *et al.* 2007a; Buschhaus *et al.* 2007b). Higher percentages of primary alcohols were also observed in the intracuticular layer of pitchers of all six *Nepenthes* species tested

(Riedel *et al.* 2003; Riedel *et al.* 2007). For the remaining species investigated, the percentages of primary alcohols were approximately equal between the intra- and epicuticular layers; in no cases have the percentages of this constituent class been shown to be higher in the epicuticular wax.

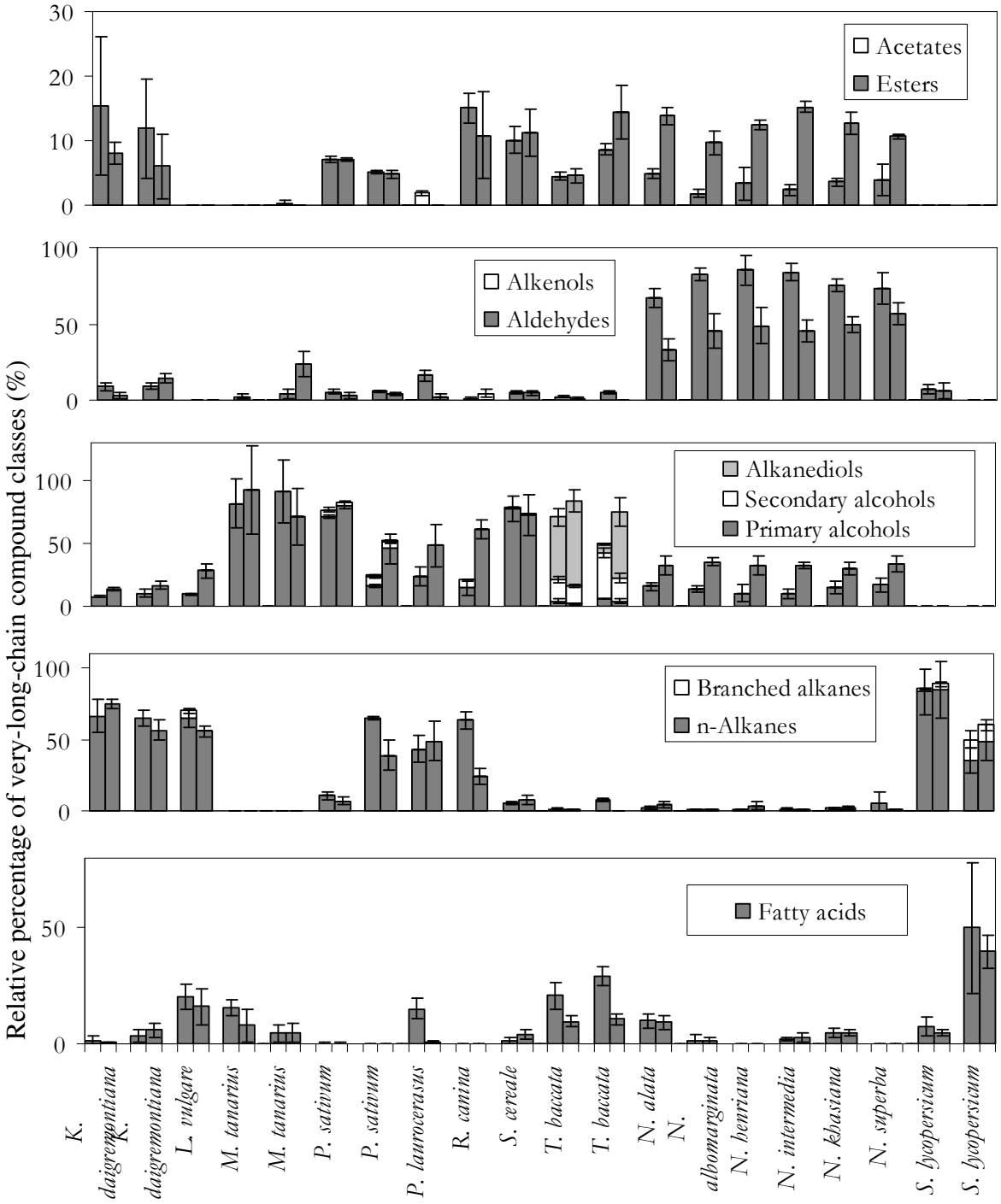

Figure 5.2 Relative quantities (% ± SD) of very-long-chain compound classes. Relative quantities were determined as the quantity per total straight chain compounds with the respective layer. The left and right bars for each species are the epicuticular and intracuticular layers, respectively.

Diols appear to also parallel the same trend as primary alcohols with a two-fold higher percentage in the intracuticular layer on the adaxial surface of *T. baccata* than in the epicuticular wax (Wen *et al.* 2006). Approximately equal percentages of diols were found between the two layers for *P. sativum* (Gniwotta *et al.* 2005) and for the abaxial surface of *T. baccata* (Wen *et al.* 2006). Analyses of more species containing cuticular diols are needed to see how far this trend can be generalized.

In contrast to the primary alcohols and diols, secondary alcohols tend to accumulate to higher percentages in the epicuticular layer then in the intracuticular, as was observed in the adaxial leaves of *R. canina* and *T. baccata* (Wen *et al.* 2006; Buschhaus *et al.* 2007a). The other four leaf surfaces that contain secondary alcohols (*P. sativum* – adaxial and abaxial, *S. cereale* – adaxial, and *T. baccata* – abaxial) contained similar percentages between the two layers (Gniwotta *et al.* 2005; Wen *et al.* 2006; Ji *et al.* 2008).

Alkanes and free fatty acids also existed at equal or higher percentages in epicuticular wax as compared to intracuticular wax; the adaxial surface of *R. canina* (Buschhaus *et al.* 2007a), the abaxial surface of *P. sativum* (Gniwotta *et al.* 2005), and both upper and lower surfaces of *T. baccata* (de Bary 1871) had higher percentages of alkanes in their epicuticular layers than in the intracuticular. The same pattern was observed for free fatty acids on the adaxial surfaces of *P. laurocerasus* and *T. baccata* (Jetter *et al.* 2000; Wen *et al.* 2006). For all of the other surfaces tested, not a single one had significantly higher percentages of alkanes or free fatty acids in the intracuticular layer.

Aldehydes and alkyl esters did not display consistent trends. Aldehydes were present at higher percentages in the intracuticular wax as compared to the epicuticular wax on the abaxial surface of *M. tanarius* leaves (Markstädter *et al.* 2000) but, conversely, at lower percentages on the adaxial surfaces of *M. tanarius*, *P. laurocerasus*, and *T. baccata* leaves (Markstädter *et al.* 2000; Jetter *et al.* 2000; Wen *et al.* 2006). For the leaves of other species, no differences in percentages were found. Moreover, aldehydes also formed a higher percentage of the epicuticular wax layer in all of the pitchers of the *Nepenthes* species as compared to the intracuticular wax layer (Riedel *et al.* 2003; Riedel *et al.* 2007). Esters constituted a greater portion of the very-long-chain compounds in epicuticular wax than in the intracuticular layer on the abaxial side of *M. tanarius* (Markstädter *et al.* 2000) and the adaxial side of *P. laurocerasus*

leaves (Jetter *et al.* 2000). The opposite trend was observed for the pitchers of all of the analyzed *Nepenthes* species (Riedel *et al.* 2003; Riedel *et al.* 2007).

More definitive trends are likely obscured by the combination of dramatic inter-species wax variability coupled with class partitioning possibly depending in part on the presence and abundance of other classes. Overall, however, primary alcohols and diols tended to accumulate to higher concentrations in the intracuticular wax layer while alkanes, free fatty acids, and secondary alcohols tended towards the epicuticular layer. No consistent trends were observed for aldehydes and esters.

5.4.4 Chain lengths of very-long-chain fatty acid derivatives

No trends in chain length partitioning consistently occurred across the tested species (see species list in Table 1). Most species showed no differences in the relative chain length distribution for any compound class with exceptions in the fatty acids and alcohols in *L. vulgare* and *T. baccata* (Wen *et al.* 2006; Buschhaus *et al.* 2007b), and fatty acids in *S. cereale* (Ji *et al.* 2008). In those three cases where chain length differences were observed, the intracuticular wax layer contained a higher percentage of the shorter compounds within the homologous series. No examples are known where the longer chain lengths of a homologous series dominate the intracuticular wax layer.

5.5 Possible mechanisms causing compositional differences between intra- and epicuticular wax layers

With the evidence accumulating that compositional gradients exist between the intra- and epicuticular wax layers on organs of many plant species, the question arises: what causes the observed gradients between the intracuticular and epicuticular wax layers?

In general terms, the spatial segregation of different wax compounds into the two sub-compartments within the cuticle can be explained as a phase separation of constituents. Numerous experiments using mostly artificial binary mixtures have shown that (very-) long-chain aliphatic lipids may, to varying degrees, spontaneously separate into two solid and/or liquid phases, depending on the physical conditions and the differences in molecular geometry between compounds (Small 1984). For example, pairwise combinations of n-alkanes in the chain length are immiscible at room temperature if their chain lengths differ by more than six

methylene units. Similarly, it can be expected that more complex natural mixtures of wax aliphatics would also undergo phase separation, albeit only partially due to the presence of many different homologues with a contiguous chain length distribution. Further segregation is known to occur between compound classes where differences between the shape and polarities of molecules are too big to allow mixed packing in a condensed phase.

In the plant cuticular wax mixtures, such differences in molecule geometry are most pronounced between the VLCFA derivatives and cyclic compounds such as aromatics and triterpenoids. While the former are thought to exhibit largely one-dimensional molecule geometries, due to the long and narrow all-*trans* conformation of the hydrocarbon chains (Kreger 1948; Small 1984), the pentacyclic triterpenoids are relatively compact molecules extending in two dimensions. Both types of molecules cannot be packed effectively together in the condensed state and, therefore, must be expected to form separate phases. It has been hypothesized that the VLCFA derivatives form crystalline domains within the wax, while triterpenoids together with other constituents segregate into amorphous regions surrounding the crystals (Riederer *et al.* 1995).

However, while the phase separation model described above seems to be in accordance with the (at least partial) segregation of triterpenoids and VLCFA derivatives into intra- and epicuticular wax layers, it must be interpreted with caution. On the one hand, the length scales differ widely between the predicted crystalline/amorphous domains (Riederer *et al.* 1995) and the observed intra- and epicuticular layers (Jeffree 2006). On the other hand, even though the model may explain segregation of VLCFA derivatives and triterpenoids, it does not predict a preference for either of the compounds and phases to be associated with the intracuticular wax. Nevertheless, the triterpenoids were found to accumulate primarily in the intracuticular layer (see above), an effect that must be explained by mechanisms beyond simple phase separation. Three such mechanisms seem feasible and will be outlined below.

First, proteins or other molecules could chaperone the wax compounds to their respective locations. Since this mechanism would be essentially reversible, it could also explain the decline in specific wax compounds observed over time in *P. laurcerasus* (Jetter *et al.* 2001). However, the paucity of detected proteins within the cuticle argues against this option (Martin *et al.* 1970; Pyee *et al.* 1994; Yeats *et al.* 2010), along with the fact that the diffusive movement

of bulky protein molecules, or of smaller chaperones with cargo, through a semi-crystalline lipid layer would likely be very slow.

Second, layered partitioning could result from the differential biosynthesis of compound classes. If wax is simply extruded, with newer compounds being accrued to the inner parts of the growing cuticle and displacing older wax layers towards the atmosphere, then gradients could be achieved by simply regulating wax biosynthesis to stagger the production of specific compound classes. While developmental changes in compound class quantity do occur, such as have been seen in time-course experiments of *Prunus laurocerasus* and other species (Hauke *et al.* 1998; Jetter *et al.* 2001; Bringe *et al.* 2006), these changes do not follow a sequential epicuticular to intracuticular order where those layers have been investigated. Thus, partitioning due to ontogenetically regulated waves of wax biosynthesis appears unlikely. Further, the high reproducibility of the gradients within a species across sample batches, whether they are harvested over the course of a growing season or across years, counters this suggestion.

Third, the differences in composition between the intra- and epicuticular wax layers may be due to differential interaction of the wax constituents with the polymers present only in the intracuticular space. The cutin matrix and/or the adjacent cell wall fibrils (both polymers are characteristic of the intracuticular compartment) contain more oxygen functionalities and, hence, are more polar than the wax compounds. Consequently, the more polar of the wax constituents will interact more strongly with the matrix, and accumulate preferentially in the intracuticular compartment. This effect may enhance the phase separation between wax compound classes, further separating the phases of VLC aliphatics and of cyclic compounds, expanding them to larger scales and orienting them to the epi- and intracuticular layers, respectively.

Furthermore, fractionation based on polarity differences within the waxes may also account for the gradients observed between various classes of VLC aliphatics, as alkanes (least polar) tend to accumulate in the epicuticular wax layer while alcohols (mid-polarity) have been found to remain in the intracuticular layer. Long-chain aliphatic acids are known to form hydrogen-bonded dimers in the condensed state, rendering them relatively unpolar (Huey *et al.* 1995; Takahashi 1995). If such dimer structures exist between free fatty acids within waxes as well,

then they could be expected to partition into the epicuticular layer due to their low polarity. Finally, it also seems plausible that functional groups of the cutin polymer may interact specifically with some of the functional groups on wax compounds, for example in hydrogen bonds between cutin hydroxyacids and wax alcohols or triterpenoids, thereby preferentially retaining certain compound classes.

5.6 Implications of wax depth partitioning on cuticle functions

Finally, we can consider the implications which the distinct layer compositions within the cuticle may have for its biological functions. Plant cuticular waxes perform a variety of functions, the most important of them being the protection of the tissue against non-stomatal water loss (Riederer *et al.* 1995). For the tomato fruit wax, it has been shown that the water barrier is formed mainly by the VLCFA derivatives in the wax mixture, and that the cuticular triterpenoids make little direct contribution to the physiological function (Vogg *et al.* 2004). While barrier function necessitates a continuous, hydrophobic zone coating the apoplast, it could be equally effective if present in either the intra- or epicuticular (or both) layers. To date, the location of the water barrier has been determined only for one case, the tomato fruit, where Vogg *et al.* (2004) found that approximately equal parts of the transpiration resistance were located in the intracuticular and the epicuticular wax layers. However, it is possible that the barrier location within the two wax layers may vary between species and/or organs, and more species have to be studied before general conclusions can be drawn. With the methods summarized here for the stepwise removal of epi- and intracuticular waxes, it is possible in principle to generate samples that will allow the permeances (and transpiration resistances) of both layers to be determined independently.

Because the water barrier function is crucial for plant survival, it cannot be compromised and will take priority over other, secondary functions. Consequently, these functions must be either performed by the same compounds and are then likely centred in the same layer as the transpiration barrier, or else the additional functions must be performed in a separate layer so as not to hamper the physiological function. The additional cuticle functions can be divided into two broad categories based on the location of the required compounds – those functions that must be exerted at the very surface of the plant and those independent of the surface.

First, several cuticle functions are achieved by compounds that must be located external to the epidermal cells to be effective, but not at the plant-atmosphere interface. A prominent example for one such function is the protection of underlying tissues against UV damage. Aromatic compounds are known to absorb UV-B and UV-C, and the cuticular concentrations of these wax constituents were shown to be high enough to provide moderate UV protection at least in some of the plant species investigated (Krauss *et al.* 1997). It should be noted that the aromatics and triterpenoids may also function as anti-feedants to smaller organisms or as chemical signalling compounds for those herbivores that probe into the plant surface (Eigenbrode *et al.* 1995). All these functions depend on the molecular properties of the compounds, and not on their physical organization within the cuticle. For these compounds, therefore, the exact location within the cuticle is not essential, and they can be located in either the intracuticular or the epicuticular wax, or in both. However, taken together with the general finding that the same compound classes tend to accumulate preferentially in the intracuticular compartment, the major part of the cuticular UV screening and the anti-feeding function may be assigned to this inner layer of the waxes. These functions, then, reside in the same layer as the transpiration barrier or underneath it.

On the other hand, some functions can only be performed at the plant-atmosphere interface and must therefore be performed by the epicuticular wax layer. For example, the self-cleaning surface properties (i.e. the Lotus effect) for the removal of dust, spores, and other foreign matter require a hydrophobic micro-relief on the surface (Barthlott *et al.* 1997). Certain cell-cell interactions between plant tissues and the signalling between plants and small herbivores likely also occur on the outer surface of the cuticle, even though the mechanisms and thus compounds involved remain unknown (Müller 2006).

Finally, plant organs may also be protected against walking insect herbivores, or serve to catch insect prey in some carnivorous plants, through the action of epicuticular wax (Müller 2006). It has been shown that the presence of epicuticular wax crystals renders the cuticle surface slippery for insect feet, and the resulting non-adhesive surfaces of vertical plant parts can be insurmountable mechanical barriers for walking insect herbivores (Knoll 1914; Harley 1991; Federle *et al.* 1997). In many plant species, the slippery epicuticular wax crystals are formed by VLCFA derivatives, for example aldehydes and their polymer derivatives on the inner surfaces

of *Nepenthes* pitchers (Riedel *et al.* 2003; Riedel *et al.* 2007). Because, in these cases, the plant-insect interaction is mediated through crystals composed of similar compound types to those of the transpiration barrier, both functions may (or may not) coincide in the epicuticular layer. In contrast, the slippery stem surfaces of *Macaranga* species mediating interactions with various ant species rely on the presence of triterpenoid crystals on the plant surface (Markstädter *et al.* 2000). In these cases, the water barrier must be located in a layer below the surface where VLCFA derivatives are sufficiently concentrated and triterpenoid concentrations are low.

In order to understand the various functions performed by cuticular waxes, the distinct compositions of the intra- and epicuticular wax layers must be considered in the context of the possible mechanisms causing the partitioning into wax layers. If plants could precisely position each compound type irrespective of physico-chemical properties, through chaperone guidance or differential regulation of biosynthesis generating ontogenetic waves of compounds, then multiple, optimized functions could be achieved in each of the discrete layers.

However, it appears likely that the depth partitioning of the intra- and epicuticular layers is largely driven by the physico-chemical properties of waxes in combination with the cutin/polysaccharide matrices (see above). Thus, the scope of molecular properties given by the available VLCFA structures and cyclic wax components will define the possibilities for partitioning, and it probably sets strict limits to the layered structures that can be realized. Plant cuticles might be fundamentally restricted to developing only two layers, with gradients in only some wax constituents, with sometimes only shallow concentration differences and only one possible direction of the gradient. It might also be difficult to maintain a contiguous layer close to the apoplast, and/or to minimize the thickness of the functional layer. In this case, the barrier function would dictate a certain chemical composition and this, in turn, would restrict the realization of layered arrangements. Only those secondary functions that are compatible with the barrier composition and structure could be exerted, and a balance between fulfilling the primary physiological function and certain secondary ecological functions would be imposed. Although such trade-offs between one major and multiple minor functions may be hard to quantify, more detailed investigations into the layered structure of the cuticle and the biological functions associated with the layers will certainly shed some light on these questions.

5.7 Future perspectives

Great gains in our knowledge of cuticle composition have been made over the last decade: two discrete, compositionally distinct layers of wax can now be quantified. It would now be of particular interest to advance to mutant and transgenic plant lines, exploiting the many recently identified genes involved in cuticle formation to further elucidate the observed partitioning patterns and/or the mechanisms controlling partitioning. However, to this end it will be essential to adapt the methods described here to plant species for which the necessary genetic tools are available. It will be especially important to investigate the intracuticular and epicuticular wax layers of *Arabidopsis thaliana* leaves, a very important species for which the composition of both wax layers has not been reported to date. If the methods for probing both wax layers can be used on this model system, then it will become possible to address the following questions: if cyclic compounds are synthesized in plants/organs where they do not naturally occur, do they still preferentially accumulate in the intracuticular layer? Which compounds (or compound classes) constitute the intracuticular wax, if alcohols are omitted? Do the same partitioning patterns occur if the cutin composition and/or structure is modified? Does a set intracuticular (cutin) layer have a maximum wax capacity?

The progress made on defining the intracuticular and epicuticular wax layers also opens up larger issues that will require additional tool development: It remains possible that additional, chemically distinct sub-layers exist within these two larger layers. Moreover, the lateral distribution of wax components will have to be taken into consideration, together with the properties of these compounds. The precise (absolute and relative) wax composition at a particular location on different epidermal cell types and on different parts of each cell will need to be examined to develop a clear understanding how cuticles perform their many functions.

Chapter 6
Leaves of *Arabidopsis thaliana* expressing the triterpenoid synthase *AtLUP4* accumulate β-amyrin in the intracuticular wax layer to the detriment of their water barrier

6.1 Introduction

Plants prevent desiccation by producing a cuticle, a lipophilic layer coating all aerial, primary tissues. As the cuticle also forms the plant-environment interface, this primary function of blocking non-stomatal water loss (Riederer *et al.* 1995) must be balanced against other functions including deterring insects and pathogens, obstructing UV penetration, and maintaining surface cleanliness from spores and other particulate (Eigenbrode *et al.* 1995; Barthlott *et al.* 1997; Krauss *et al.* 1997; Müller 2006). The balance of all these functions is a direct result of the composition of the cuticle. Although many of these functions may be achieved by the same composition, other functions may require unique compounds that hinder other functions.

Cuticles are composed of two components, the insoluble and mechanically robust polymer cutin and organic-soluble compounds termed wax (Walton 1990; Nawrath 2006; Pollard *et al.* 2008). Wax ubiquitously comprises linear very-long-chain compounds, including varying ratios of acids, primary and secondary alcohols, esters, aldehydes, alkanes, and ketones (Jetter *et al.* 2007; Samuels *et al.* 2008). In addition, cyclic compounds such as pentacyclic triterpenoids frequently occur in wax (Jetter *et al.* 2007).

Wax composition varies between species but also between different locations within one species down to the sub-cuticular level. At the smallest level, two layers of wax within the cuticle may be distinguished (reviewed in Chapter 5). The outer layer termed epicuticular wax could be physically stripped from the surfaces of many robust leaves and fruit using aqueous glue (Jetter *et al.* 2001). Consecutive applications reached a physical limit (presumably cutin) at which no additional wax could be removed. Subsequent solvent extraction released additional wax that presumably resided within the cutin and is called intracuticular wax. Several studies have revealed that wax composition typically is not uniform between the two wax layers. (see Chapter 5) Most notably, cyclic compounds regularly accumulate almost exclusively into the

intracuticular wax layer (see Chapter 5). However, the mechanism governing such fractionation is not known.

To move beyond merely descriptive comparisons of water barrier properties and sub-cuticular wax partitioning, confounding factors such as differences in cutin quantity and composition must be eliminated. This requires analyses of single species prior to and after modification of the wax composition. This was attempted in a single study to date using a tomato fruit mutant with reduced VLC aliphatics (Vogg *et al.* 2004). In this species, the water barrier resulting mainly from VLC compounds was found to be split evenly between the epicuticular and intracuticular layers. The lack of easily available genetic tools has hampered further studies on other species.

Although tomato has the advantage of producing robust, astomatous fruit cuticles, *Arabidopsis thaliana* already has a suite of characterized cuticular wax mutants (Reviewed in Samuels *et al.* 2008). Moreover, unlike tomato fruit and Arabidopsis stems, Arabidopsis leaves do not naturally produce detectable quantities of cuticular pentacyclic triterpenoids and thus serve as a clean background for studying the effect of these compounds. Despite this, detailed analyses of wax composition on the two different sides of the leaf and at the sub-cuticular level are lacking for Arabidopsis, in part due to the inability to remove the aqueous glue without severing trichomes and thereby damaging the cuticle. Through the use of the *glabrous1* mutant devoid of trichomes (Herman *et al.* 1989), Arabidopsis may now be exploited to answer the following questions: 1) As compared to the total leaf wax, how distinct is the wax composition on the adaxial and abaxial surfaces of the leaf? 2) Within the adaxial leaf wax, what are the absolute and relative contributions of the epicuticular and intracuticular wax layers? 3) Where do non-naturally occurring triterpenoids (specifically β-amyrin) partition if they are produced in a clean leaf background? 4) How much does each wax layer block water movement? And 5) how does the presence of cyclic triterpenoids affect cuticular water barrier properties?

6.2 Methods

6.2.1 Plant material

Seeds from the trichomeless mutant *gl1* (SALK_039478 Col-0 background; Herman *et al.* 1989; Alonso *et al.* 2003) from *Arabidopsis thaliana* and the *AtLUP4* over-expressor in a *gl1* background were plated on Arabidopsis media agar (Somerville *et al.* 1982), stratified for 2-3 days at 4°C, and then germinated under continuous light (~150 μmol $m^{-2}s^{-1}$ photosynthetically active radiation) for 7-10 days at 20°C. Seedlings were transplanted into soil (Sunshine mix 4), grown under 12 hour days/nights at the same temperature conditions as for germination, and watered twice weekly with MiracleGro.

6.2.2 Construction of the AtLUP4 over-expressor

AtLUP4 (At1g78950) was PCR amplified from cDNA obtained from the stems of wild-type *Arabidopsis thaliana* (Columbia) using gene specific forward 5'- and reverse 5'- primers. The PCR product was transferred into pDONR-221 using Gateway cloning kits (Invitrogen) and then sequenced. Subsequently the gene-of-interest was transferred into pMDC32 (Curtis *et al.* 2003) behind double constitutive cauliflower mosaic virus 35S promoters using Gateway cloning kits (Invitrogen), creating pMDC32-LUP4. The Arabidopsis mutant *gl1* (SALK_039478) was transformed with the construct using the *Agrobacterium tumefaciens*-mediated floral-dip plant transformation method (Clough *et al.* 1998).

6.2.3 Wax extraction and derivatization

For bulk wax extraction, leaves were submerged for 30 sec in $CHCl_3$ containing a defined quantity of *n*-tetracosane as an internal standard. Samples were re-submerged for 30 sec in fresh $CHCl_3$ and the two solutions were pooled. For side-specific wax extraction, a glass cylinder was pressed on to the leaf surface (Jetter *et al.* 2000). $CHCl_3$ with a defined quantity of *n*-tetracosane was added for 30 sec with gentle agitation and then removed. A second wash with $CHCl_3$ for 30 sec was added and the two solutions pooled. If leakage ocurred, samples were discarded. Layer-specific extraction was performed according to (Jetter *et al.* 2001): An aqueous solution of gum arabic (1 mg/ml) was applied to the leaf surface, allowed to dry, and then peeled off. The gum arabic was then extracted with chloroform to obtain epicuticular wax. Subsequent to gum arabic treatment, the cylinder method (above) was applied to the leaf surface to extract the intracuticular wax. For each of the samples collected by the various,

above methods, the solvent was evaporated under a gentle stream of N_2 gas while heating at 50°C before derivatizing with excess of bis-N,O-(trimethylsilyl)trifluoroacetamide (BSTFA) in pyridine for 30 min at 70°C. The solvents were then dried before $CHCl_3$ was again added to the wax.

6.2.4 Wax identification and quantification

Wax constituents were separated by capillary GC (6890N, Agilent, Avondale, PA, USA; column 30 m HP-1, 0.32 mm i.d., df=0.1 μm) using the following temperature regime: on-column injection at 50°C, oven held for 2 min at 50°C, raised by 40°C min^{-1} to 200°C, held for 2 min at 200°C, raised by 3°C min^{-1} to 320°C, and held for 30 min at 320°C. For compound identification, the GC was linked to a mass spectrometric detector (5973N, Agilent) and the inlet pressure programmed for a constant 1.4 ml min^{-1} flow of He carrier gas. For compound quantification, the GC with inlet pressure programmed for constant flow of 2.0 ml min^{-1} of H_2 carrier gas was connected to a flame ionization detector (FID). The quantity (μg) was established by comparison to a defined amount of n-tetracosane, the internal standard added into the total wax extracts. The extracted surface areas were measured with ImageJ software (Abramoff *et al.* 2004) from digital photographs of the samples (and multiplied by 2 for the total leaf). Alternately, for the cylinder method, the dimensions of the cylinders were measured as used as the surface area.

6.2.5 Minimum water conductance analyses

Water loss was measured following Knoche *et al.* (2001). Briefly, leaves were sealed across the opening of a cylindrical water-filled chamber with silicon grease applied along the ring of leaf-chamber contact. The surfaces facing the water were scratched to ensure continuous access of water into the leaves. Chambers were placed over silica desiccant in order to create gradients approaching 100% internal water to 0% external water. Samples were allowed to equilibrate overnight at 25°C before gravimetrically measuring water loss. Dividing the water flux by the change in concentration (equal to the density of water at 25°C) yielded the minimum water conductance (MWC). MWC are reported as geometric means in accordance with Baur (1997). Statistical differences were tested using Welch's T-tests on log-normal-transformed values. Controls were created by puncturing sub-millimetre holes through the cuticle using a fine needle attached to a micromanipulator.

6.3 Results

In order to produce a pentacyclic triterpenoids in Arabidopsis leaf wax, the triterpenoid synthase *AtLUP4* wax over-expressed in leaves, as previous studies in yeast (gene characterization; Shibuya *et al.* 2009) and Arabidopsis (mutant wax analyses; Buschhaus, unpublished data) demonstrated that this gene product produces the single product β -amyrin. Leaves of eleven Arabidopsis lines over-expressing *AtLUP4* were screened for the presence of β-amyrin; all lines produced low quantities (approx. 1-2%) within the leaf wax. The line with the highest quantity was compared against *gl1*, the control, to assess 1) the cuticular wax composition and 2) the corresponding water barrier properties. Specifically, waxes from the entire leaf, abaxial and adaxial surfaces, and the adaxial epicuticular and intracuticular layers were examined with respect to the quantity of wax, the relative quantities of compound classes, and chain length distribution within each class. Further, the minimum water conductance was determined for the adaxial surface before removing any wax, after removing the epicuticular wax layer, and after removing all wax.

6.3.1 Total leaf wax

The extractable wax from the leaves of the *gl1* mutant totalled 0.9±0.1 μg/cm^2. The largest portion of the identified wax was alkanes (0.32±0.05 μg/cm^2; Figure 6.1). Lesser quantities of free acids (0.22±0.04 μg/cm^2) and primary alcohols (0.19±0.01 μg/cm^2) and very minor amounts of aldehydes (0.016±0.002 μg/cm^2) were also present. The remainder of the wax (0.13±0.04 μg/cm^2) could not be identified. No pentacyclic triterpenoids were detected.

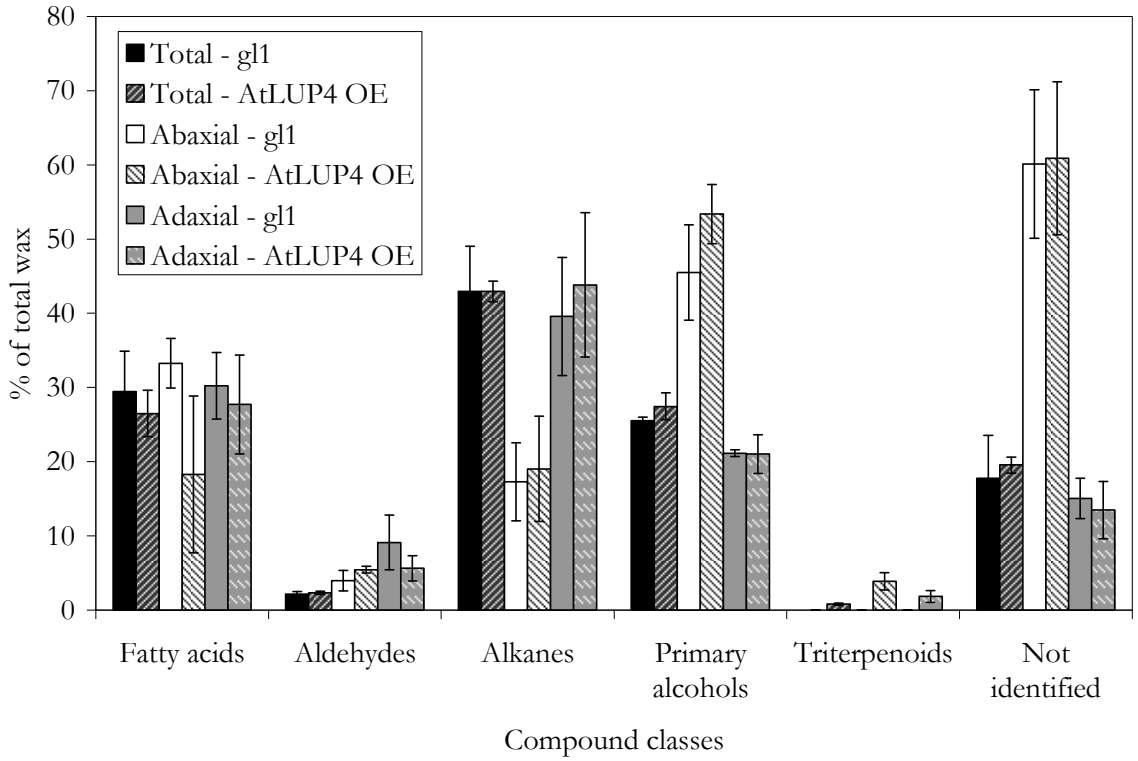

Figure 6.1 Relative quantities of compound classes in *Arabidopsis thaliana* leaf waxes. The percentages of all compound classes in the total, adaxial, and abaxial leaf waxes from *gl1* and the *AtLUP4* over-expressor are shown (% ± SD)

The distribution of compound chain lengths in each class paralleled previous findings (Figure 6.2). Alkanes ranged from 27 to 35 carbons in length and peaked at 31 carbons (49±1% of the alkane fraction). Alkanes with odd carbon numbers predominated although minor quantities with even numbers of carbons were also detected. The free fatty acids contained 24 to 34 carbons, with C_{34} acid being the most abundant. Primary alcohols were present both as straight chain (40%) and branched (60%) compounds. The *n*-alcohol chain length range was nearly as broad as that of the acids, with compounds ranging from 26 to 34 carbons in length. The branched-chain primary alcohols displayed a more restricted range from 30 to 32 carbons (including carbons in branches) with branched C_{32} alcohol constituting 40% of the total alcohols. The chain length distribution of aldehydes paralleled that of branched alcohols; C_{30} and C_{32} aldehyde were present in almost equal relative quantities. These final three classes of compounds were all dominated by homologs with even numbers of carbons.

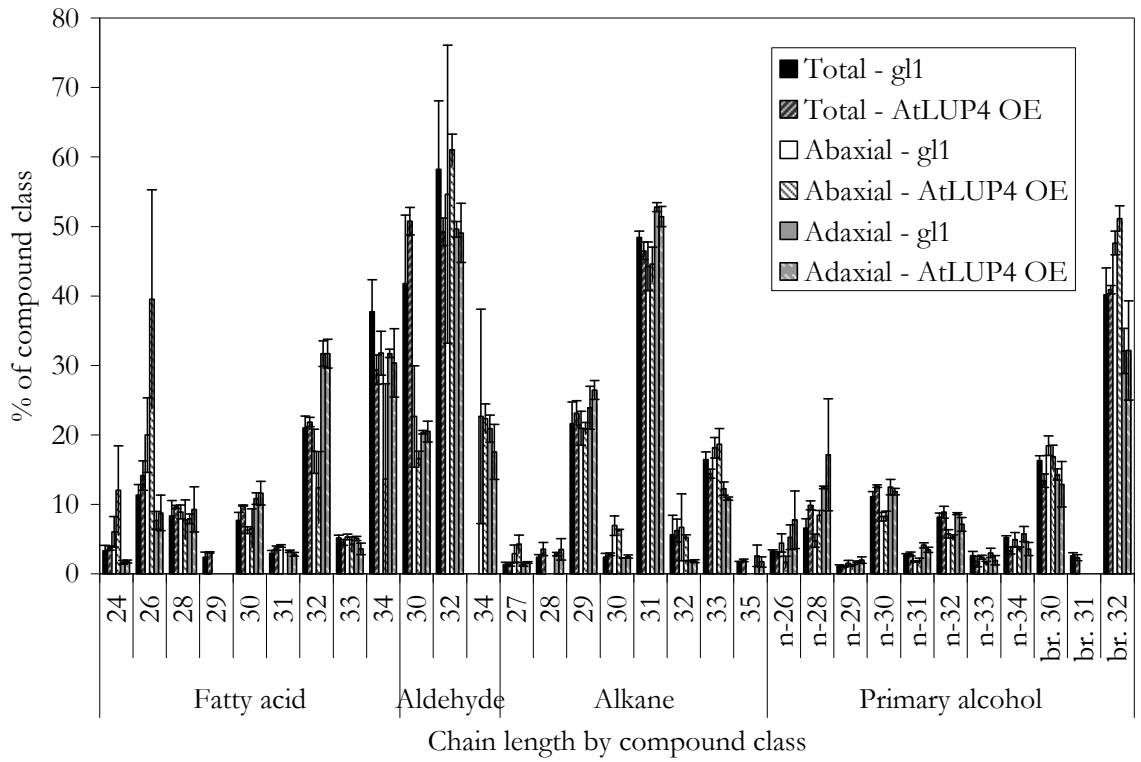

Figure 6.2 Relative quantities of individual compounds in *Arabidopsis thaliana* leaf waxes. The percentages of each chain length within the respective compound class in total, adaxial, and abaxial leaf waxes of *gl1* and the *AtLUP4* over-expressor are shown (% ± SD)

The total wax load found for *AtLUP4* over-expressor (0.8±0.1 μg/cm^2) was equivalent to that of *gl1*. Similarly, the absolute and relative quantities of compound classes were identical for both lines with one exception (Figure 6.1). Leaves over-expressing *AtLUP4* leaves contained 0.005±0.001 μg/cm^2 of the triterpenoid β-amyrin corresponding to 0.8±0.2% of the identified wax. Chain length distributions within classes did not vary between the two lines (Figure 6.2).

6.3.2 Adaxial versus abaxial leaf wax

To further resolve the wax compositions on different parts of the Arabidopsis leaf, wax was analyzed separately from the top and bottom leaf surfaces of the *gl1* mutant. The wax load on the adaxial surface totalled 0.8±0.1 μg/cm^2. The same four compound classes were detected on the adaxial surface as for the total leaf wax samples (Figure 6.1). Alkanes (0.29±0.4 μg/cm^2) contributed the largest portion (40% of identified wax) to the adaxial wax. Free acids (0.22±0.05 μg/cm^2) and primary alcohols (0.12±0.02 μg/cm^2) formed 30% and 20% of the

wax, respectively. Aldehydes were present at very low levels (0.07±0.03 μg/cm^2). A total of 0.11±0.03 μg/cm^2 could not be identified and pentacyclic triterpenoids were not detected.

The adaxial leaf surface of the *AtLUP4* over-expressor contained identical compound classes in the same abundance as found for *gl1* (Figure 6.1). In addition, 0.015±0.0064 μg/cm^2 of β-amyrin (2±1%) was also present. The distribution of chain lengths within the classes for the adaxial sides of both *gl1* and the *AtLUP4* over-expressor matched those found in the total leaf wax except for the aldehydes, where the chain length range extended up to 34 carbons and C_{32} aldehyde was the dominant aldehyde (Figure 6.2).

The abaxial surface of *gl1* was covered in much less wax (0.4±0.1 μg/cm^2) than the adaxial side of the leaf. Moreover, the relative and absolute abundance of classes differed from the adaxial surface (Figure 6.1). The proportions between alcohols and alkanes were reversed from the adaxial layer. Primary alcohols formed the most abundant class (0.10±0.01 μg/cm^2) while alkanes were present at half the quantity (0.04±0.02 μg/cm^2). Similar to the adaxial surface, one-third of the identified wax was free acids (0.08±0.02 μg/cm^2) while aldehydes constituted only 0.01±0.005 μg/cm^2. No pentacyclic triterpenoids were detected and 0.13±0.02 μg/cm^2 remained unidentified. Although the quantities of the compound classes differed from both the adaxial surface and the total leaf wax, the distribution of chain lengths within each class did not differ from that of the adaxial surface.

The abaxial leaf surface of the *AtLUP4* over-expressor contained less wax (0.2±0.1 μg/cm^2) than the same surface of the *gl1* mutant. Similar percentages were found for all compound classes except acids, where the absolute (and relative) quantity decreased to 0.03±0.02 μg/cm^2 (Figure 6.1). In addition, 4% (0.005±0.001 μg/cm^2) of the wax from the abaxial leaf surface of the AtLUP4 over-expresser was β-amyrin. No differences were found in the relative distribution of individual compounds within their respective classes as compared to the abaxial surface of *gl1* and the adaxial surfaces of *gl1* and the *AtLUP4* over-expressor (Figure 6.2).

6.3.3 Intracuticular versus epicuticular leaf wax

After determining the specific wax composition of the upper leaf surface in comparison to the lower surface, the adaxial surface was selected to further examine possible partitioning of classes between the epicuticular and intracuticular wax layers (Figure 6.3). A single application

of gum arabic removed 0.8±0.1 μg/cm^2 of wax from *gl1*. The majority of wax identified in this layer (60%) consisted of alkanes (0.4±0.1 μg/cm^2). Primary alcohols (0.09±0.01 μg/cm^2) and free acids (0.11±0.4 μg/cm^2) contributed equal amounts (approximately 15% each). Aldehydes were the least abundant at 0.05±0.01 μg/cm^2. Only 15% of the wax sampled by gum arabic (0.12±0.2 μg/cm^2) was not identified. The epicuticular wax layer was found to have the same chain length distribution within classes as the overall adaxial wax (see above).

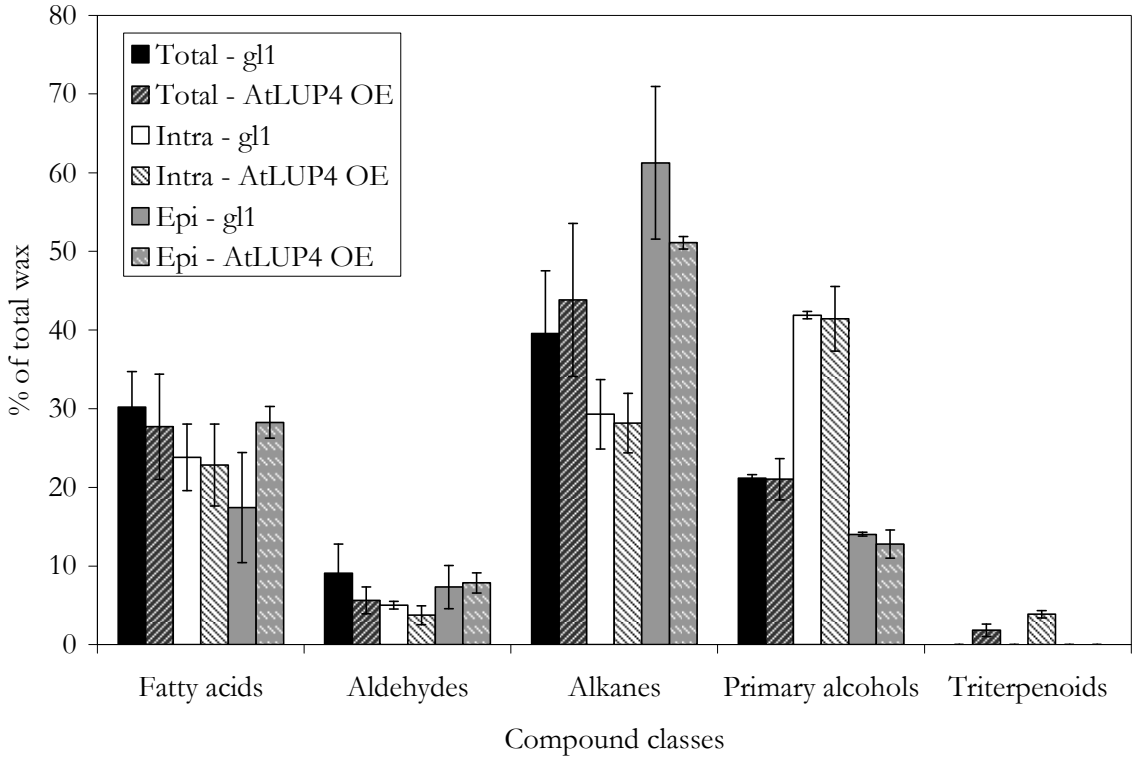

Figure 6.3 Relative quantities of compound classes in *Arabidopsis thaliana* leaf waxes. The percentages of all compound classes in the total adaxial leaf wax (Total) as well as the epicuticular (Epi)and intracuticular (Intra) wax layers from the adaxial surface of leaves of *gl1* and the *AtLUP4* over-expressor are shown (% ± SD)

The total quantities as well as the absolute and relative amounts of the various classes were nearly identically between wax samples prepared by gum arabic from the adaxial surfaces of *gl1* and the AtLUP4 over-expressor (Figure 6.3). The only difference between both samples was an increase in free acids from 17±7% in *gl1* to 28±2% in the over-expressor. This difference

was also reflected in the absolute quantities of the free acids. Notably absent from the epicuticular wax of the *AtLUP4* over-expressor was β-amyrin. Relative percentages of compounds within classes were identical to those in the *gl1* mutant.

Subsequent treatments of Arabidopsis leaves with gum arabic caused significant damage and prevented further testing. In three cases (once for *gl1* and twice for the AtLUP4 over-expressor) gum arabic application was applied successfully a second time to release 0.12±0.01 $\mu g/cm^2$ of wax of which only 33% could be identified. With respect to absolute quantities of identifiable wax, the second application of gum arabic released less than 6% of the first. Since single applications of gum arabic removed most of the wax accessible to adhesive treatment, it was decided to perform the extraction of the intracuticular wax in the following experiment immediately after the first gum arabic application.

The intracuticular wax totalled a mere 0.16±0.03 $\mu g/cm^2$, slightly more than the quantity removed by the second application of gum arabic. This low quantity of total wax was reflected in the absolute quantity of each compound class. In addition to this, the relative distribution of compound classes shifted between the epicuticular and intracuticular wax layers (Figure 6.3). Out of the identifiable wax, only one third was alkanes (0.025±0.02 $\mu g/cm^2$) as compared to two-thirds in the epicuticular wax layer. Conversely, primary alcohols increased from 14% in the epicuticular wax layer to 40% in the intracuticular wax layer (0.035±0.003 $\mu g/cm^2$). Equal percentages of free acids (0.020±0.005 $\mu g/cm^2$) and aldehydes (0.004±0.001 $\mu g/cm^2$) were found in the two layers. Half of the intracuticular wax sample (0.08±0.2 $\mu g/cm^2$) could not be identified.

Small differences in chain length distributions were observed between the intracuticular and epicuticular layers (Figure 6.4). Within the alkanes, C_{29} alkane accounted for approximately 10% more of the alkane fraction in the inner layer than the outer layer while the inverse occurred for C_{31} alkane. The intracuticular layer also contained higher relative amounts of branched C_{32} alcohol and C_{32} aldehyde while the epicuticular layer had slightly higher percentages of C_{32} and C_{34} *n*-alcohol.

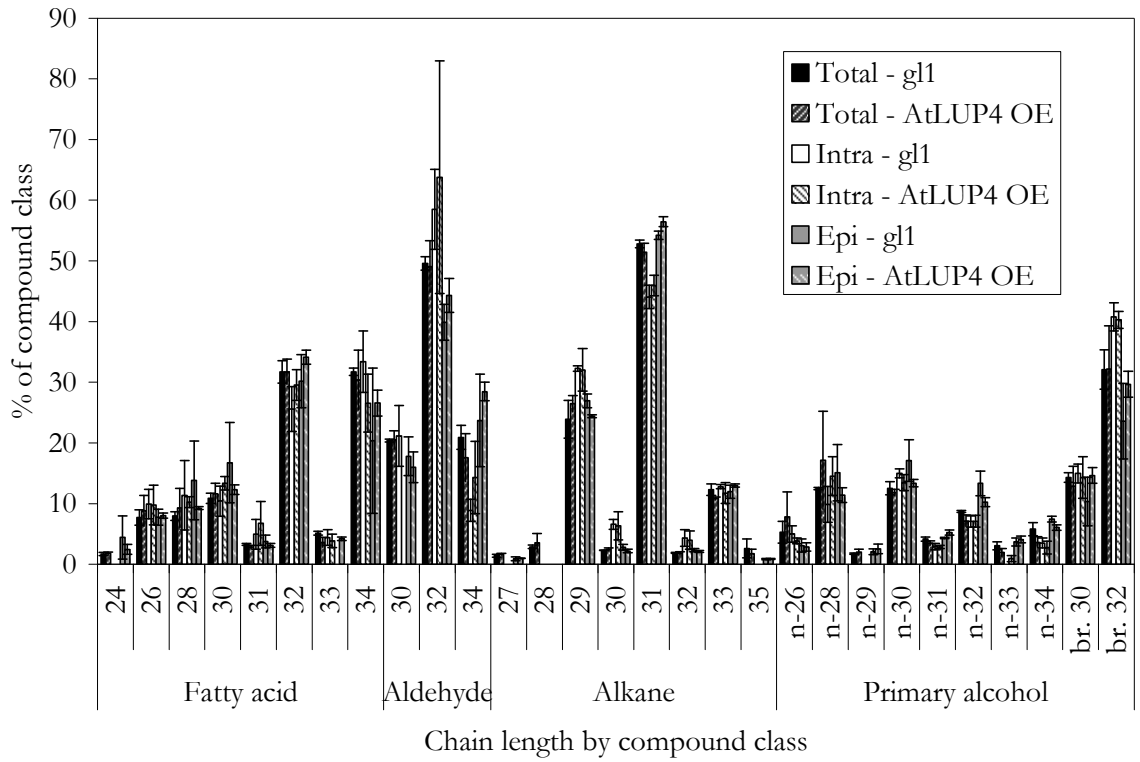

Figure 6.4 Relative quantities of individual compounds in *Arabidopsis thaliana* leaf waxes. The percentages of each chain length within the respective compound class from the total adaxial leaf wax as well as the epicuticular and intracuticular wax layers from the adaxial surface of leaves of *gl1* and the *AtLUP4* over-expressor are shown (% ± SD)

The intracuticular wax layer of the *AtLUP4* over-expressor had a composition matching that of *gl1* in quantity, relative class composition, and relative chain length distributions (Figure 6.3 and Figure 6.4). The single exception was the presence of β-amyrin (0.004±0.001 μg/cm^2), present at 4% of the identifiable wax and equal in absolute quantity (that is, in μg/cm^2) to that found in the total adaxial wax.

6.3.4 Water barrier properties

After determining the specific wax composition of the adaxial cuticle and further refining the differences in composition between the epicuticular and intracuticular wax layers, the role of waxes on the primary function of cuticles, namely blocking uncontrolled water loss (Riederer *et al.* 1995), was examined. Water barrier properties were determined for the adaxial surface of leaf discs with intact wax, with the epicuticular layer removed, and the entire wax mixture

removed. To calculate the minimum water conductance, water loss per time was first measured. If the R^2 value of the slope (equalling the water flux) of the best fit line of water loss per time was less than 0.99, the sample was discarded. Similarly, samples with intact wax or epicuticular wax removed samples were also discarded if the measured fluxes were greater than the geometric means of fluxes from corresponding leaf discs punctured with a single micro-hole were also discarded.

Water resistances decreased as wax layers were removed (Figure 6.5). For the *gl1* mutant, the resistance for leaves with intact wax equalled 1.1±0.1 x 10^4 s/m. Removal of the epicuticular wax layer reduced the resistance by 60% to 4.0±0.5 x 10^3 s/m. Solvent extraction of all wax decreased the water barrier to 6.0±0.3 x 10^2 s/m, approximately 5% of the original value.

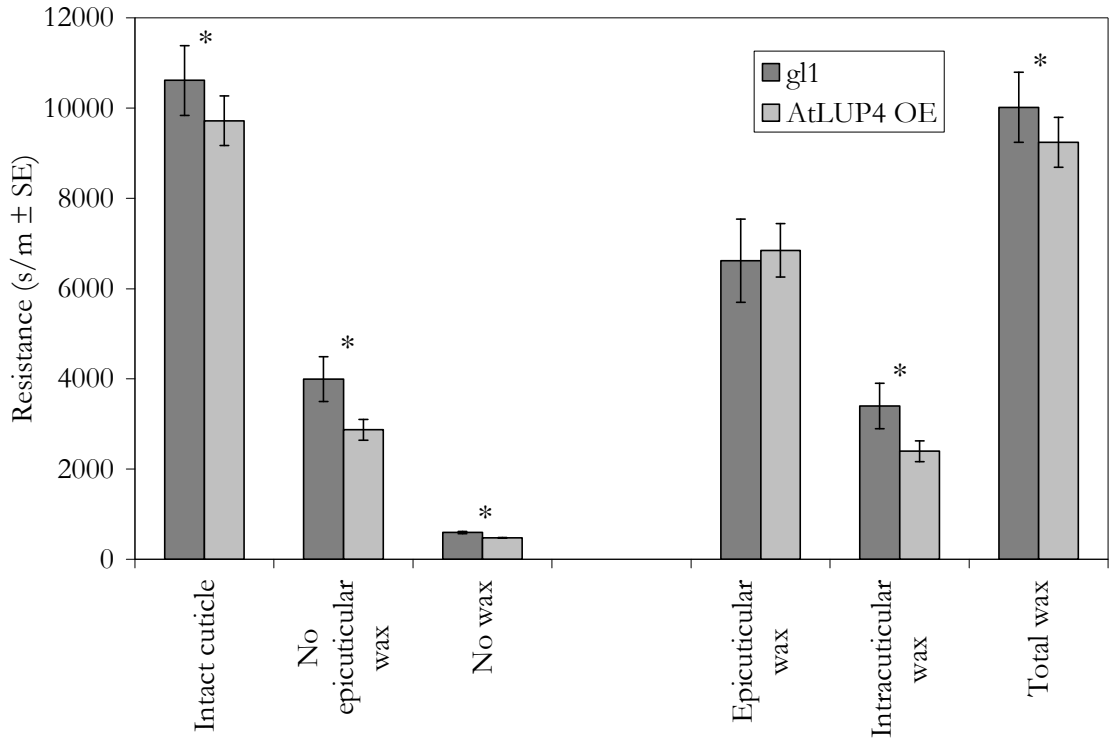

Figure 6.5 Transpiration barrier analysis of *Arabidopsis thaliana* leaf surfaces. Water resistances of the intact adaxial leaf cuticle, of the adaxial cuticle without epicuticular wax, and of the adaxial cuticle without wax are shown along with the calculated resistance values for wax and the intra- and epicuticular layers of wax from *gl1* and the *AtLUP4* over-expresser (s/m ± SE). Pairs marked with a * indicate significant differences (p = 0.05)

Resistances for the *AtLUP4* over-expresser followed a similar pattern as found for *gl1* leaves (Figure 6.5). The resistance for leaf discs with intact wax ($1.0\pm0.1 \times 10^4$ s/m) did not differ from that of *gl1*. However, removal of the epicuticular wax layer lowered the resistance ($2.9\pm0.2 \times 10^3$ s/m) by 70%, more than the decrease observed for the same treatment in *gl1*. Removal of all wax decreased the water resistance ($4.76\pm0.03 \times 10^3$ s/m) to 5% of the original, a percentage identical to that found for *gl1*.

The water barrier properties of cuticles after puncturing with a fine needle were also determined (Figure 6.6). The minimum water conductance increased linearly with increasing numbers of holes by approximately 6×10^{-5} m/s per hole for the intact leaf disc. A similar linear increase was observed for holes in leaf discs with the epicuticular layer removed (data not shown).

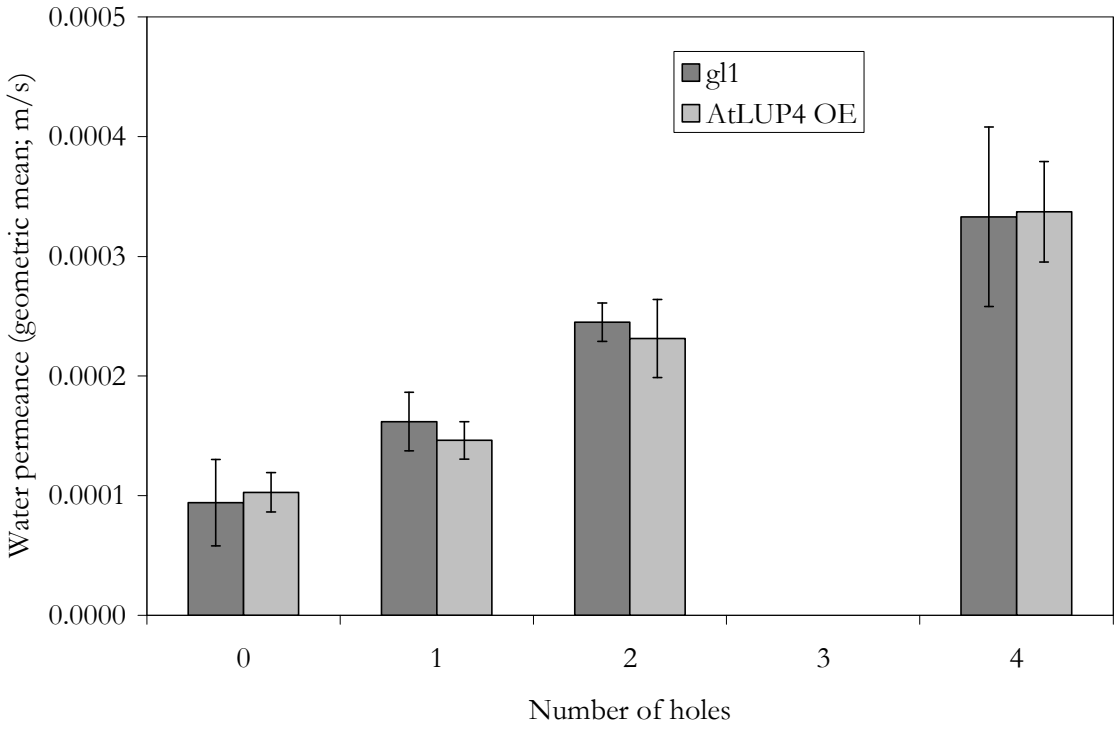

Figure 6.6 Transpiration analysis of punctured *Arabidopsis thaliana* leaf surfaces. Minimum water conductance through the adaxial leaf surfaces (wax intact) from *gl1* and the *AtLUP4* over-expressor after puncturing with one, two, or four holes (m/s ± SD)

6.4 Discussion

Although wax biosynthesis in the model plant *Arabidopsis thaliana* has been extensively studied, little is known about the distribution of wax compounds on scales smaller than the organ level. This in turn has hampered studies seeking to correlate wax composition with function. To remedy this, the wax compositions on the adaxial and abaxial surfaces were individually assessed here in the trichomeless *gl1* mutant. Not only does use of this mutant avoid confounding the composition of pavement cells with the unique wax found on trichomes, it also permits analyses of distinct wax layers within the cuticle.

6.4.1 Distinct wax compositions

Waxes from the adaxial and abaxial leaf surfaces showed distinct total loads and compositions. Relative distributions of compound classes differed between the surfaces although the chain length distributions did not. This suggests that the enzymes responsible for chain length elongation and/or the substrate-specificity of the modifying enzymes do not differ between the upper and lower epidermis layers. However, the regulation, biosynthetic enzymes, and/or export machinery for the various classes appears to differ between the epidermal layers on both sides of the leaf. As only the single enzyme CER4 (Rowland *et al.* 2006) is required for forming alcohols, higher expression of the corresponding gene on the lower surface could account for the observed effect. Alternatively, a lower expression level of the gene coding for the enzyme that catalyzes the first committed step in alkane formation would also produce similar effects.

The upper surface contained twice the wax quantity as the lower surface. However, the absolute quantities of both surfaces do not average to the quantity extracted from the total leaf. Because the average is lower for each compound class, it remains possible that the discrepancy results either from differing methods for determining extracted surface areas between the analyses (digital photos versus area of pressed-on cylinders; see 'Methods') or from difficulties in removing all the chloroform from the cylinders without puncturing the leaf and thus causing a loss in extracted product. However, since the same method was applied to the upper and lower surfaces, the values determined for the ratio of total wax as well as the relative abundance of individual compounds remain valid.

The amounts and composition of the adaxial wax determined by total wax extraction from this leaf side was then used as a reference value for the following investigations. The amounts of epicuticular and intracuticular waxes found after separate sampling added up to the total adaxial wax quantity. The epicuticular wax layer accounted for the majority of the wax, with six times the quantity as found in the intracuticular layer. It has been reported that other species have similarly higher proportions of wax in the epicuticular layer (Gniwotta *et al.* 2005; Guhling *et al.* 2005; Ji *et al.* 2008). Although the quantity of wax removed by a second gum arabic application was 15 to 20% of the quantity extracted from the first application, only one-quarter of it was identified as VLC aliphatics that are typical wax components. Thus, a second application of gum arabic likely released only an additional 5-10% of the first adhesive treatment.

Differences in the compound class distributions were observed between the epicuticular and intracuticular wax layers. The outer layer contained mainly non-polar alkanes, following a trend observed across several species tested to date where in all cases the outer wax layer had equal or higher percentages of alkanes as compared to the inner layer. Conversely, the intracuticular wax layer on the adaxial side of Arabidopsis leaves contained a higher proportion of alcohols (see Chapter 5 Section 5). A similar partitioning has also been observed in several species, and it has been speculated that hydrogen bonding between alcohols and cutin restricts diffusion of wax alcohols into the epicuticular wax layer (see Chapter 5 Section 4.3).

In addition to differences in compound classes, small differences in chain lengths were found between the epicuticular and intracuticular layers for individual compounds. However, as no general trends were observed, this chain length partitioning cannot be interpreted at this point. It is unlikely that the differences in chain lengths between both wax layers resulted from differing diffusion rates.

6.4.2 β-amyrin in cuticular wax

Previous studies had shown a tendency for cyclic compounds to accumulate within the intracuticular wax layer (Reviewed in Chapter 5). To test this, *AtLUP4* was over-expressed *in planta* resulting in the presence of cuticular β-amyrin, confirming previous yeast expression studies (Shibuya *et al.* 2009). Specifically, β-amyrin accumulated solely in the intracuticular wax layer; the very low levels of detected typical cell membrane lipids lends support the extraction

of β-amyrin from the cuticle as opposed to accidental extraction of the cell membrane (data not shown). As leaf wax is normally devoid of cuticular pentacyclic triterpenoids, the localization of the newly accumulating β-amyrin shows that a general mechanism likely directs their distribution. It seems plausible that triterpenoid partitioning is based on the physico-chemical properties of common cuticular components.

How does β-amyrin travel from the site of synthesis inside epidermal cells to the cuticle? Since it is unlikely that triterpenoids diffuse from the cell membrane and into the aqueous cell wall (*en route* to the cuticle), export likely is facilitated by proteins. Because pentacyclic triterpenoids are naturally absent from the leaf cuticle of Arabidopsis, leaf epidermal cells likely do not express transporters specific to these compounds. Instead, it is possible that steroid or lipid transporters may be present that have a relatively broad substrate capacity capable of handling pentacyclic triterpenoids. Sterols have been shown to be transported by some ABCG transporters (Reviewed in Tarr *et al.* 2009), which have homology to the cutin and wax exporters ABCG11 and ABCG12/CER5 in Arabidopsis (Kunst *et al.* 2009). As well, a lipid transfer protein has been shown to bind steroids (Cheng *et al.* 2004). This in turn suggests that transfer proteins capable of transporting diverse triterpenoids out of the cell normally exist in leaves. If such a transporter with broad substrate capacity exists, then other triterpenoids including brassicasterol, campesterol, and sitosterol found in wax samples (and notably mainly leaf wax but not stem wax, which contains pentacyclic triterpenoids) may not simply be contamination from damaged epidermal cells but instead might be *bona fide* wax constituents.

6.4.3 Water barrier properties

Methods capable of providing reproducible, quantitative values of water barrier effectiveness for layers of the cuticle and modified plants versus controls have been applied to many species. However, studies examing the cuticular water barrier properties in Arabidopsis have relied upon comparative and inexact methods assessing, for example, differential rates of staining by dyes (i.e.: toluidine blue; Tanaka *et al.* 2004), rates of desiccation (Goodwin *et al.* 2005), or rates of surrogate compound uptake (i.e.: benzoic acid; Kerstiens *et al.* 2006). Here I have achieved for the first time the combination, applying the quantitative methods to Arabidopsis. The minimum water conductance for an intact *gl1* leaf disc (1.0×10^{-4} m/s) fell between the 25th

and 50th percentiles (median: 1.5 x 10^{-4} m/s) of 80 stomatous species examined using similar methods (Kerstiens 1996a).

The location and structural basis of the water barrier were further probed by examining the contribution of both total wax and individual layers of wax. For barriers in series such as the epicuticular wax layer versus the rest of the cuticle, individual resistances (inverse of MWC) may be summed or subtracted (Riederer *et al.* 1995). For example, by subtracting the resistance of the cuticle without epicuticular wax from the resistance of the intact leaf, the resistance of the epicuticular wax may be determined. The epicuticular wax resistance (6.6±0.9 x 10^3 s/m) was twice as large as the intracuticular wax resistance (3.4±0.5 x 10^3 s/m) and thus the epicuticular wax layer was twice as effective at blocking water loss. In comparison, the epicuticular wax layer had five times more wax than the intracuticular layer, suggesting that the relative composition and/or alignment of compounds contributes significantly to the barrier properties. Further studies modifying VLC aliphatic classes followed by water resistance analyses using the methods established here may answer the question which compounds specifically aid the barrier. Together, the epicuticular and intracuticular wax resistances of Arabidopsis leaves were found here to sum to 10.0±0.8 x 10^3 s/m for the total water resistance caused by wax. Thus, wax provided nearly 95% of the water barrier effectiveness.

The water barrier effectiveness was also analyzed for the *AtLUP4* over-expressor. The water resistance caused by the epicuticular wax layer (6.8±0.6 x 10^3 s/m) equaled the corresponding value in the control (*gl1*). Since the epicuticular wax compositions were identical in absolute and relative quantities between the two lines, this finding is expected and further supports the unbiased reproducibility of the method. The intracuticular wax resistance (2.4±0.2 x 10^3 s/m), however, was only one-third as large as the epicuticular wax, and less than the corresponding resistance in *gl1*, despite the equal absolute and relative quantities of VLC constituents. Instead, the decrease in water resistance in the intracuticular wax layer corresponds with the presence of β-amyrin in the AtLUP4 over-expressor.

The decrease in water resistance co-occurring with the presence of β-amyrin supports the proposed mechanism of the cuticular wax water barrier (Riederer *et al.* 1995). Crystalline domains formed from the parallel alignment of VLC aliphatic compounds in all-trans conformations occlude water. Instead, water is thought to follow a tortuous path around the

crystalline domains through amorphous regions of functional groups and non-linear molecules surrounding the crystals. Accordingly, additional triterpenoids such as β-amyrin would likely increase the volume of the amorphous domain, either by decreasing the size of crystals by blocking aggregation or increasing the distance between the crystals. This in turn would provide a shorter route and/or more routes through which water might diffuse, thereby increasing the permeability or decreasing the resistance of the cuticle overall.

Since triterpenoids appear to hinder cuticular water barriers, why do some (organs of) plants produce them and export them to the cuticle? Triterpenoids likely participate in secondary functions, such as protection from UV-C or plant defense. Alternatively, the plant may produce triterpenoids to help maintain flexibility in the cuticle, sacrificing additional water loss for the sake of avoiding cuticular cracks.

6.4.4 Conclusion

Arabidopsis leaves contain unique wax compositions on their upper and lower surfaces. Moreover, within the adaxial wax, the epicuticular layer contains more wax and a higher relative quantity of alkanes while the intracuticular wax has a higher percentage of alcohols. The wax forms a barrier for transpirational water loss with the outer layer contributing to the barrier twice as effectively as the inner layer. The over-production of β-amyrin leads to accumulation of the triterpenoid solely in the intracuticular wax layer and causes a reduction in the water barrier effectiveness of the this layer.

Chapter 7
Limitations and suggested expansion of the presented research

The collective surface area of cuticles, the outer surface of land plants, has been estimated at over one billion square kilometers (Riederer *et al.* 1995). This forms an immense interface for diverse plant-environment interactions. Because cuticles potentially contain great ecological importance, many plant cuticle researchers have sought to address three fundamental questions raised at the beginning of this dissertation: (1) Why do cuticles exist? What are their functions? (2) How do they perform these functions? What are their compositions and how are the components physically arranged? (3) How effectively do they perform these functions? Through the research presented in the preceding chapters, I have furthered the scientific responses to the second two questions. Specifically, I have identified new cuticle constituents, refined the spatial distribution of wax components, and provided quantitative values for cuticle effectiveness in its primary function of preventing uncontrolled water loss. Each of these three points will be dealt with in turn, first by briefly discussing and critiquing my new contributions and second by suggesting further avenues of research based on my results.

7.1 Identification of novel compounds

Hundreds of very-long-chain compounds have been described in cuticular wax obtained from diverse species. Typically, these compounds range from 20 to 40 carbons with one or more functional groups containing oxygen (except for alkanes). In Chapter 3, I report the identification of 20 novel compounds belonging to the diol and ketol classes. Previous compounds identified within these classes contained secondary functional groups around the centre of the chain, predominantly on odd-numbered carbons. In contrast, the secondary functional group in the newly identified compounds is predominantly on the even-numbered carbon C-2, although present also in minor quantities on C-3.

The identification of the α- and β-ketols relied on polarity data obtained from TLC migration in conjunction with mass spectrometry (MS) fragments of multiple derivatives of the respective compounds. Although the major ions were assigned a probable fragment structure, this does not constitute definitive proof of the compound identities. The potentially easiest

method to confirm the structure entails synthesizing the corresponding standards and then comparing the retention times and MS fragmentation between the standard and respective wax compound.

Further exploration of the petal wax from *C. bipinnatus* is predicted to lead to the discovery of (at least) one additional compound class, depending on the biosynthetic sequence as outlined in Chapter 3. If oxidation of C-2 (or C-3) occurs before the reduction of C-1 in the formation of 1,2(3)-diols, then the intermediate 2(3)-hydroxy acyl-CoA is formed. While the majority of this appeared to be reduced to the corresponding diol, it is likely that a minor portion would not be reduced but instead be exported as 2(3)-hydroxy-alkanoic acid. This would parallel the presence of the minor quantities of free fatty acids found in most cuticular waxes. Identifying α-hydroxlyated fatty acids would thus also provide an indication of the order of steps in the biosynthetic pathway.

In addition, yet another compound class is expected under the assumption that the same enzyme performs all the reported α- and β-oxidations as hypothesized in Chapter 3. *Cosmos bipinnatus* petal wax contained the following relative quantities of these novel compounds from most to least abundant: 1,2-diol>>1,2-ketol>1,3-diol>>1,3-ketol. This suggests that the oxidizing enzyme has preference for the α-position. However, it can also catalyze the formation of the less favourable β-ketols. It seems likely, then, that this enzyme should also be able to produce detectable quantities of 1,2,3-triol and 1,3-hydroxy-alkan-2-one. However, it is unclear how these compounds would react under the current derivatization procedures required for GC analysis. The 1,2,3-triol could dehydrate, leaving a carbonyl and a hydroxyl group, while the 1,3-hydroxy-alkan-2-one probably results in several enetriol derivatization artifacts. Thus, examination of TLC bands more polar than 1,2-diols by high performance liquid chromatography (HPLC) is recommended in the search for these novel compound classes.

7.2 Spatial heterogeneity of wax constituents

7.2.1 Cell-type specific wax composition

Waxes coating plant surfaces have been shown to vary quantitatively and qualitatively at the macroscopic level, such as between species, organs, and regions of an organ (see Chapter 2 for

an example). Differences have also been observed at the subcellular level. For example, wax compositions are frequently distinct between intracuticular and epicuticular wax layers (Reviewed in Chapter 5) and the ratio of triterpenoids to alkanes has been found to be larger over anticlinal as compared to periclinal cell surfaces in *Prunus laurocerasus* (Yu *et al.* 2007). Despite this wealth of information on wax composition at these extreme scales, quantitative analyses were absent at the of cell-type level. In Chapter 4, the wax coating trichomes was shown to be distinct from the wax covering the surrounding epidermal cells for both stems and leaves of *Arabidopsis thaliana*. This raises possibilities for future research as will be outlined in the following paragraphs.

The selective removal of trichomes allowed their relative wax composition to be quantified. This removal, however, frequently resulted in trichome branches shearing from their stalk. These different shaped pieces of trichomes with their complex three-dimensional shape prevented calculation of the surface area. Moreover, the method did not exhaustively isolate every trichome from the leaves, thereby preventing back-calculation of trichome area from the leaf surface area. Consequently, the total quantity of wax per surface area of trichome remains to be established.

Differences between trichome wax and other epidermal cell wax raises the possibility that lateral variation in wax composition may occur between other cell types. Specifically, do guard cells produce a different wax from either pavement or trichome cells? Difficulties arise in answering this question as guard cells cannot currently be isolated; while trichomes protrude and can thus be mechanically dislodged, guard cells are flush with epidermal cells. Consequently, pure guard cell wax cannot be sampled. In order to avoid this problem, two complementary methods could be applied. First, several mutants exist that contain varying densities of guard cells. Using a subtractive approach similar to the comparison of *cpc tcl1 etc1 etc3* to *gl1* in Chapter 4 would provide an initial indication of wax specific composition. However, as stomata are essential for plant life, at best a mutant with reduced numbers of guard cells could be used against a mutant with many guard cells. Second, wax analyses using time of flight single ion mass spectrometry (TOF-SIMS) would permit sampling of individual cell types *in situ*. Drawbacks include restricted sampling to only the outer layer of wax,

difficulties in accurately quantifying compounds, and potential difficulties in identifying all the constituents since the mass spectrum combines all compounds present at the plant surface.

The determination of the wax composition on trichomes enables many future studies. In Chapter 4 I argue that the observed wax must be synthesized specifically within trichome cells because it is compositionally different from epidermal cell wax. It follows that trichomes contain the necessary biosynthetic machinery for producing wax. Previously, researchers attempting to elucidate the complete wax pathway relied on a microarray of stem epidermal cells as compared to all cells in the stem (Suh *et al.* 2005). By showing that trichomes also have this machinery, researchers can use already existent microarray data comparing trichome gene expression to either epidermal or mesophyll cell gene expressions. This increases the power for selecting candidate genes as the genes responsible for wax biosynthesis should be expressed more highly in both sets of comparisons.

In addition to selecting candidate genes, knowledge that trichomes synthesize wax permits a novel approach to elucidating the wax biosynthetic pathway. To date, the composition of wax mutants has been restricted to analyzing the respective surface wax, mainly to avoid the overwhelming contamination of cell membranes from internal tissue. This method is blind to intermediates that are not exported. Since trichomes can be isolated, the analyses of internal (not exported) lipophilic compounds in the trichomes of various wax mutants can now be cleanly investigated.

7.2.2 Cuticular layer specific wax composition

Several studies have reported intracuticular and epicuticular wax compositions across several species. These singular studies demonstrated individual cases of differences between cuticle layers. By performing a meta-analysis on these studies, common trends were identified (Chapter 5). Further studies are required to determine whether these partitioning trends are co-incidental or result from the physico-chemical properties of the cuticle.

In Chapter 6 I established a system to begin to address the questions raised by the meta-analysis. Briefly, by using an *Arabidopsis thaliana* mutant devoid of trichomes, a baseline composition for epicuticular and intracuticular wax was established. After manipulating the wax (e.g.: over-expressing AtLUP4 in order to produce β-amyrin), the compositions of these

layers could once again be assessed. It was shown that β-amyrin accumulated exclusively in the intracuticular wax layer as opposed to the outer wax layer. Further experiments on *A. thaliana* lines producing even more β-amyrin would demonstrate the maximum capacity for pentacyclic triterpenoids in the intracuticular wax layer and the quantity at which triterpenoids (may) partition into the epicuticular wax film and/or crystals as well. Creating such a line would likely necessitate first increasing the triterpenoid precursor 2,3-oxidosqualene levels by reducing flux towards the alternative path for steroid formation (through a *cas1* knock-down) and second, increasing the quantity of presumed triterpenoid transporters such that the synthesized pentacyclic triterpenoids actually reach the cuticle.

Similar wax composition analyses assessing partitioning could also be performed for other cyclic compounds (e.g.: alkylresorcinols) after the genes responsible for their biosynthesis are determined. In parallel to cyclic compounds, partitioning of straight very-long-chain compounds may also be examined using combinations of the many mutants and over-expressing lines available that affect specific compound classes and/or chain lengths.

7.3 Contribution of wax components to cuticle functions

Nearly thirteen billion tonnes of water escape daily into the atmosphere through imperfectly sealed plant cuticles, based on a median permeability of astomatous cuticles of 1.7×10^{-5} m/s and near-plant humidity of 50% (Riederer *et al.* 1995; Kerstiens 1996a). Considering this loss, the question arises: Why are cuticles such permeable barriers? It is widely believed that cuticles balance the function of preventing water loss with other secondary functions. Petals specifically were expected to have significant secondary functions that would compete with water barrier effectiveness because of their need to attract and interact with pollinators. However, no studies had quantified the effectiveness of the water barrier in petal cuticles. In Chapter 2, I show that for *Cosmos bipinnatus*, the petals block water poorly as compared to literature values of leaves from other species. This conclusion, however, is based on a petal permeance value from only a single species. More studies on diverse species are required to test the universality of this finding. In addition, the highly reticulate nature of the leaves of *C. bipinnatus* prevented quantification of the corresponding leaf permeability. Thus, further studies are also needed on species that contain both broad petals and broad leaves in order to

compare cuticle effectiveness between organs of the same species, thereby ascertaining whether cuticle effectiveness is species or organ dependant.

Although analyzing petal permeability provides information at the organ level of how plants restrict uncontrolled water loss, it fails to adequately address the question of how specific compounds contribute to this and other functions. To begin to address this more complex yet fundamental question, a system is needed whereby individual compounds can be manipulated without affecting the remaining cuticle constituents. Currently, no such system exists. Ultimately a completely *in vitro* model is necessary whereby predefined combinations of waxes can be placed on a defined matrix. However, new methods would first need to be developed to evenly coat the underlying matrix with predetermined wax gradients and/or percentages and dimensions of crystalline domains.

Until further research overcomes the major methodological challenges of an *in vitro* system, an alternative *in planta* system must be used where the wax can be intentionally manipulated. All such systems ultimately will be limited because the biosynthesis of various very-long-chain compounds is inseparably linked. For example, mutations that eliminate aldehydes also abolish alkanes as the former appear to be precursors of the latter. Similarly, all longer chain compounds are produced from shorter compounds and as such a completely clean system of only longer compounds is impossible. Despite these challenges, an *in planta* system does avoid the current problems encountered in an *in vitro* system.

Arabidopsis thaliana provides a logical choice for the *in planta* model as more is known about wax biosynthesis in this species than any other. Thus, in Chapter 6, the minimum water conductance was determined for the adaxial surface of Arabidopsis leaves with first an intact cuticle, second a cuticle with the epicuticular wax removed, and third a cuticle with all of the wax removed. The usefulness of this model was then demonstrated by increasing the triterpenoid concentration in cuticular wax and subsequently analyzing the minimum conductance. This experiment focused on alicyclic wax molecules in contrast to straight-chain compounds. However, the contributions of specific compounds within the non-cyclic compounds may also be ascertained in future studies using parallel methods. Several of these compound classes are predicted to increase crystallinity and thus increase water resistance. Included are alkanes and primary alcohols, since neither contain secondary functional groups

or bulky primary functional groups that might prevent close packing. Using the *cer1* and *cer4* Arabidopsis mutants and a similar procedure to the one outlined above, the roles of alkanes and primary alcohols respectively in blocking water movement may also be determined.

Not all wax compounds, however, are predicted to increase crystallinity or the barrier effectiveness. In addition to cyclic compounds, plant wax contains several other compounds that might disrupt the crystalline domain. For example, the novel compounds identified in Chapter 3, and methyl-branched compounds such as found in the petal wax of *Antirrhinum majus* (Goodwin *et al.* 2002) or leaf pavement cell wax in *A. thaliana* (Chapter 4) would likely disrupt the crystalline domains. The negative contribution of these compound classes to the water barrier may also be examined using the developed system.

Until this point, only direct correlations between composition and function have been discussed. One final aspect remains to be elucidated: the structural arrangement of compounds at the molecular level within the intra- and epicuticular wax. This must be determined in order to understand the mechanism behind the barrier functions. After successfully establishing correlations between cuticle composition (alicyclic versus aliphatic compounds) and water resistance, the crystallinity must also be measured. Although no method currently exists to quantify the geometries or dimensions of the crystalline or amorphous domains, the ratio of crystalline to amorphous regions may be determined using horizontal attenuated total reflection Fourier transform infrared (h-ATR-FTIR) spectroscopy (Merk *et al.* 1998). Corroboration between this data and the composition-water resistance correlations would support the current models for cuticular wax arrangement and water pathways/barriers and thus provide support for the mechanism of water resistance.

After determining which compounds such as β-amyrin have been shown to hinder the water barrier, the question then arises: Why are the disruptive compounds present? The most plausible answer is that they participate in secondary functions and that the plant has reached a compromise in composition to permit both functions. After developing lines of Arabidopsis with different wax concentrations of the compound of interest, the lines may further be used to address questions on secondary functions. For example, do some cuticular compounds act as anti-fungal, anti-microbial, or anti-feedant compounds? Do compounds act as signaling molecules to other plants or animals? Do specific compounds block the entry of xenobiotics,

such as herbicides, pesticides, or pollutants? Does the cuticle restrict the movement of other permeants, such as scent molecules or other plant volatiles? Overall, as many other secondary functions have been ascribed to the cuticle, the larger goal must be to associate individual compounds with all of their various corresponding functions.

REFERENCES

Abramoff M, Magelhaes P, Ram S (2004) Image processing with ImageJ. Biophot Int 11: 36-42

Akihisa T, Inoue Y, Yasukawa K, Kasahara Y, Yamanouchi S, Kumaki K, Tamura T (1998) Widespread occurrence of syn-alkane-6,8-diols in the flowers of the compositae. Phytochem 49: 1637-1640

Akihisa T, Nozaki A, Inoue Y, Yasukawa K, Kasahara Y, Motohashi S, Kumaki K, Tokutake N, Takido M, Tamura T (1997) Alkane diols from flower petals of *Carthamus tinctorius*. Phytochem 45: 725-728

Alonso J, Stepanova A, Leisse T, Kim C, Chen H, Shinn P, Stevenson D, et al. (2003) Genome-wide insertional mutagenesis of *Arabidopsis thaliana*. Science 301: 653-657

Bach L, Michaelson LV, Haslam R, Bellec Y, Gissot L, Marion J, Da Costa M, Boutin J-P, Miquel M, Tellier F, Domergue F, Markham J, Beaudoin F, Napier J, Faure J-D (2008) The very-long-chain hydroxy fatty acyl-CoA dehydratase PASTICCINO2 is essential and limiting for plant development. Proc Natl Acad Sci USA 105: 14727-14731

Baker EA (1982) Chemistry and morphology of plant epicuticular waxes. In D Cutler, K Alvin, C Price, eds, The plant cuticle, Linnean Society Symposium Series Vol. 10, Academic Press, London, pp 139-165

Baker E, Bukovac M, Hunt G (1982) Composition of tomato fruit cuticle as related to fruit growth and development. In D Cutler, K Alvin, C Price, eds, The plant cuticle, Linnean Society Symposium Series, vol. 10, Academic Press, London, pp 33-44

Baker E, Procopiou J (1975) The cuticles of *Citrus* species. Composition of the intracuticular lipids of leaves and fruits. J Food Sci Agric 26: 1347-1352

Barthlott W, Neinhuis C (1997) Purity of the sacred lotus, or escape from contamination in biological surfaces. Planta 202: 1-8

Barthlott W, Neinhuis C, Cutler D, Ditsch F, Meusel I, Theisen I, Wilhelmi H (1998) Classification and terminology of plant epicuticular waxes. Botan J Lin 126: 237-260

Baudino S, Caissard J-G, Bergougnoux V, Jullien F, Magnard J-L, Scalliet G, Cock J, Hugueney P (2007) Production and emission of volatile compounds by petal cells. Plant Signal Behav 2: 525-526

Baur P (1997) Lognormal distribution of water permeability and organic solute mobility in plant cuticles. Plant, Cell Environ 20: 167-177

Baur P, Marzouk H, Schönherr J (1999) Estimation of path lengths for diffusion of organic compounds through leaf cuticles. Plant, Cell Environ 22: 291-299

Beaudoin F, Wu X, Li F, Haslam R, Markham J, Zheng H, Napier J, Kunst L (2009) Functional characterization of the *Arabidopsis thaliana* β-keto-acyl-CoA reductase candidates of the fatty acid elongase. Plant Physiol 150: 1174-1191

Blacklock B, Jaworski J (2006) Substrate specificity of Arabidopsis 3-ketoacyl-CoA synthases. Biochem Biophys Res Commun 346: 583-590

Bringe K, Schumacher CFA, Schmitz-Eiberger MA, Steiner U, Oerke E-C (2006) Ontogenetic variation in chemical and physical characteristics of adaxial apple leaf surfaces. Phytochem 67: 161-170

Burghardt M, Riederer M (2003) Ecophysiological relevance of cuticular transpiration of deciduous and evergreen plants in relation to stomatal closure and leaf water potential. J Exp Bot 54: 1941-1949

Buschhaus C, Herz H, Jetter R (2007a) Chemical composition of the epicuticular and intracuticular wax layers on adaxial sides of *Rosa canina* leaves. Ann Bot 100: 1557-1564

Buschhaus C, Herz H, Jetter R (2007b) Chemical composition of the epicuticular and intracuticular wax layers on the adaxial side of *Ligustrum vulgare* L. leaves. New Phytol 176: 311-316

Cheng C, Samuel D, Liu Y, Shyu J, Lai S, Lin K, Lyu P (2004) Binding mechanism of nonspecific lipid transfer proteins and their role in plant defense. Biochem 43: 13628-13636

Clough S, Bent A (1998) Floral dip: a simplified method for *Agrobacterium*-mediated transformation of *Arabidopsis thaliana*. Plant J 16: 735-743

Coward J (2007) A method for selective isolation and aggregation of epicuticular wax nanotubes in *Picea pungens*. Flora 462-470

Curtis M, Grossniklaus U (2003) A gateway cloning vector set for high-throughput functional analysis of genes *in planta*. Plant Physiol 133: 462-469

de Bary A (1871) Über die Wachsüberzüge der Epidermis. II. Bot Ztg 29: 145-154

Domergue F, Vishwanath S, Joubes J, Ono J, Lee J, Bourdon M, Alhattab R, Lowe C, Pascal S, Lessire R, Rowland O (2010) Three Arabidopsis fatty acyl-CoA reductases, FAR1, FAR4, and FAR5, generate primary fatty alcohols associated with suberin deposition. Plant Physiol 153: 1539-1554

Dunn T, Lynch D, Michaelson L, Napier J (2004) A post-genomic approach to understanding sphingolipid metabolism in *Arabidopsis thaliana*. Ann Bot 93: 483-497

Ebert B, Zöller D, Erban A, Fehrle I, Hartmann J, Niehl A, Kopka J, Fisahn J (2010) Metabolic profiling of *Arabidopsis thaliana* epidermal cells. J Exp Bot 61: 1321-1335

Ebizuka Y, Katsube Y, Tsutsumi T, Kushiro T, Shibuya M (2003) Functional genomics approach to the study of triterpene biosynthesis. Pure Appl Chem 75: 369-374

Eigenbrode S, Espelie K (1995) Effects of plant epicuticular lipids on insect herbivores. Annu Rev Entomol 40: 171-194

Ensikat H, Neinhuis C, Barthlott W (2000) Direct access to plant epicuticular wax crystals by a new mechanical isolation method. Int J Plant Sci 161: 143-148

Fazio G, Xu R, Matsuda S (2004) Genome mining to identify new plant triterpenoids. J Am Chem Soc 126: 5678-5679

Federle W, Maschwitz U, Fiala B, Riederer M, Hölldobler B (1997) Slippery ant-plants and skilful climbers: selection and protection of specific ant partners by epicuticular wax blooms in *Macaranga* (Euphorbiaceae). Oecologia 112: 217-224

Fiebig A, Mayfield J, Miley N, Chau S, Fischer R, Preuss D (2000) Alterations in *CER6*, a gene identical to *CUT1*, differentially affect long-chain lipid content on the surface of pollen and stems. Plant Cell 12: 2001-2008

Franke R, Höfer R, Briesen I, Emsermann M, Efremova N, Yephremov A, Schreiber L (2009) The *DAISY* gene from Arabidopsis encodes a fatty acid elongase condensing enzyme involved in the biosynthesis of aliphatic suberin in roots and the chalaza-micropyle region of seeds. Plant J 57: 80-95

Gniwotta F, Vogg G, Gartmann V, Carver T, Riederer M, Jetter R (2005) What do microbes encounter at the plant surface? Chemical composition of pea leaf cuticular waxes. Plant Physiol 139: 519-530

Goodwin S, Jenks M (2005) Plant cuticle function as a barrier to water loss. In M Jenks, P Hasagawa, eds, Plant Abiotic Stress, Ed 1 Blackwell Publishing Inc., Oxford, UK, pp 14-36

Goodwin S, Kolosova N, Kish C, Wood K, Dudareva N, Jenks MA (2002) Cuticle characteristics and volatile emissions of petals in *Antirrhinum majus* L. Physiol Plant 117: 435-443

Greer S, Wen M, Bird D, Wu X, Samuels L, Kunst L, Jetter R (2007) The cytochrome P450 enzyme CYP96A15 is the mid-chain alkane hydroxylase responsible for formation of secondary alcohols and ketones in stem cuticular wax of *Arabidopsis thaliana*. Plant Physiol 145: 653-667

Griffiths D, Robertson G, Shepherd T, Birch A, Gordon S, Woodford T (2000) A comparison of the composition of epicuticular wax from red raspberry (*Rubus idaeus* L.) and hawthorn (*Crataegus monogyna* Jacq.) flowers. Phytochem 55: 111-116

Guhling O, Hobl B, Yeats T, Jetter R (2006) Cloning and characterization of a lupeol synthase involved in the synthesis of epicuticular wax crystals on stem and hypocotyl surfaces of *Ricinus communis*. Arch Biochem Biophys 448: 60-72

Guhling O, Kinzler C, Dreyer M, Bringmann G, Jetter R (2005) Surface composition of myrmecophytic plants: cuticular wax and glandular trichomes on leaves of *Macaranga tanarius*. J Chem Ecol 31: 2325-2343

Haas K, Rentschler I (1984) Discrimination between epicuticular and intracuticular wax in blackberry leaves: ultrastructural and chemical evidence. Plant Sci L 36: 143-147

Harley R (1991) The greasy pole syndrome. In CR Huxley, DF Cutler, eds, Ant-plant interactions, Oxford University Press, Oxford, pp 430-433

Hauke V, Schreiber L (1998) Ontogenetic and seasonal development of wax composition and cuticular transpiration of ivy (*Hedera helix* L.) sun and shade leaves. Planta 207: 67-75

Heredia A (2003) Biophysical and biochemical characteristics of cutin, a plant barrier biopolymer. Biochim Biophys Acta 1620: 1-7

Herman P, Marks M (1989) Trichome Development in Arabidopsis thaliana. II. Isolation and Complementation of the GLABROUS1 Gene. Plant Cell 1: 1051-1055

Herrera J, Bartel B, Wilson W, Matsuda S (1998) Cloning and characterization of the *Arabidopsis thaliana* lupeol synthase gene. Phytochem 49: 1905-1911

Huey L, Hanson D, and Howard C (1995) Reactions of SF_6^- and I^- with atmospheric trace gases. J Phys Chem 99: 5001-5008

Husselstein-Muller T, Schaller H, Benveniste P (2001) Molecular cloning and expression in yeast of 2,3-oxidosqualene-triterpenoid cyclases from *Arabidopsis thaliana*. Plant Mol Biol 45: 75-92

Jeffree C (1996) Structure and ontogeny of plant cuticles. In G Kerstiens, ed, Plant Cuticles. An Integrated Approach, Ed 1 BIOS Scientific, Oxford, pp 33-82

Jeffree C (2006) The fine structure of the plant cuticle. In M Riederer, C Müller, eds, Biology of the Plant Cuticle, Ed 1 Vol 23. Blackwell, Oxford, pp 11-144

Jenks M, Tuttle H, Eigenbrode S, Feldmann K (1995) Leaf epicuticular waxes of the *eceriferum* mutants in *Arabidopsis*. Plant Physiol 108: 369-377

Jetter R, Kunst L, Samuels L (2007) Composition of plant cuticular waxes. In M Riederer, C Müller, eds, Biology of the Plant Cuticle, Ed 1 Vol 23. Blackwell, Oxford, pp 145-181

Jetter R, Schäffer S (2001) Chemical composition of the *Prunus laurocerasus* leaf surface. Dynamic changes of the epicuticular wax film during leaf development. Plant Physiol 126: 1725-1737

Jetter R, Schäffer S, Riederer M (2000) Leaf cuticular waxes are arranged in chemically and mechanically distinct layers: evidence from *Prunus laurocerasus* L. Plant, Cell Environ 23: 619-628

Ji X, Jetter R (2008) Very long chain alkylresorcinols accumulate in the intracuticular wax of rye (*Secale cereale* L.) leaves near the tissue surface. Phytochem 69: 1197-1207

Joubes J, Raffaele S, Bourdenx B, Garcia C, Laroche-Traineau J, Moreau P, Domergue F, Lessire R (2008) The VLCFA elongase gene family in *Arabidopsis thaliana*: phylogenetic analysis, 3D modelling and expression profiling. Plant Mol Biol 67: 547-566

Kerstiens G (1996a) Cuticular water permeability and its physiological significance. J Exp Bot 47: 1813-1832

Kerstiens G (1996b) Signalling across the divide: a wider perspective of cuticular structure-function relations. Trends Plant Sci 1: 125-129

Kerstiens G, Schreiber L, Lendzian K (2006) Quantification of cuticular permeability in genetically modified plants. J Exp Bot 57: 2547-2552

Knoche M, Peschel S, Hinz M, Bukovac M (2001) Studies on water transport through sweet cherry fruit surfaces: 2. Conductance of the cuticle in relation to fruit development. Planta 213: 927-936

Knoll F (1914) Über die Ursache des Ausgleitens der Insektenbeine an wachsbedeckten Pflanzenteilen. Jb wiss Bot 54: 448-459

Kolattukudy P (1972) Structure and cell-free synthesis of alkane-1,2-diols of the uropygial gland of white crowned sparrow (*Zonotrichia leucophrys*). Biochem Biophys Res Commun 49: 1376-1383

Kolattukudy P, Croteau R, Brown L (1974) Structure and biosynthesis of cuticular lipids. Hydroxylation of palmitic acid and decarboxylation of C28 C30 and C32 acids in *Vicia faba* flowers. Plant Physiol 54: 670-677

Kolesnikova M, Xiong Q, Lodeiro S, Hua L, Matsuda S (2006) Lanosterol biosynthesis in plants. Arch Biochem Biophys 447: 87-95

Kolesnikova M, Wilson W, Lynch D, Obermeyer A, Matsuda S (2007) Arabidopsis camelliol C synthase evolved from enzymes that make pentacycles. Org Lett 9: 5223-5226

Kosma D, Bourdenx B, Bernard A, Parsons E, Lu S, Joubes J, Jenks M (2009) The impact of water deficiency on leaf cuticle lipids of Arabidopsis. Plant Physiol 151: 1918-1929.

Krauss P, Markstädter C, Riederer M (1997) Attenuation of UV radiation by plant cuticles from woody species. Plant, Cell Environ 20: 1079-1085

Kreger D (1948) An x-ray study of waxy coatings from plants. Rec Trav Bot Neerl 41: 606-736

Kunst L, Jetter R, Samuels L (2007) Biosynthesis and transport of plant cuticular waxes. In M Riederer, C Müller, eds, Biology of the Plant Cuticle, Ed 1 Vol 23. Blackwell, Oxford, pp 182-215

Kunst L, Samuels L (2009) Plant cuticles shine: advances in wax biosynthesis and export. Curr Op in Plant Biol 12: 1-7

Kushiro T, Shibuya M, Masuda K, Ebizuka Y (2000) A novel multifunctional triterpene synthase from *Arabidopsis thaliana*. Tetrahedr L 41: 7705-7710

Le Roux J (1969) Fischer-Tropsch waxes. II. Crystallinity and physical properties. J appl Chem 19: 86-88

Lee S-B, Jung S-J, Go Y-S, Kim H-U, Kim J-K, Cho H-J, Park O, Suh M (2009) Two Arabidopsis 3-ketoacyl CoA synthase genes, *KCS20* and *KCS2/DAISY*, are functionally redundant in cuticular wax and root suberin biosynthesis, but differentially controlled by osmotic stress. Plant J 60: 462-475

Li F, Wu X, Lam P, Bird D, Zheng H, Samuels L, Jetter R, Kunst L (2008) Identification of the wax ester synthase/acyl-Coenzyme A:diacylglycerol acyltransferase WSD1 required for stem wax ester biosynthesis in Araibidopsis. Plant Physiol 148: 97-107

Lodeiro S, Xiong Q, Wilson W, Kolesnikova M, Onak C, Matsuda S (2007) An oxidosqualene cyclase makes numerous products by diverse mechanisms: a challenge to prevailing concepts of triterpene biosynthesis. J Am Chem Soc 129: 11213-11222

Marks M, Betancur L, Gilding E, Chen F, Bauer S, Wenger J, Dixon R, Haigler C (2008) A new method for isolating large quantities of Arabidopsis trichomes for transcriptome, cell wall and other types of analyses. Plant J 56: 483-492

Marks M, Wenger J, Gilding E, Jilk R, Dixon R (2009) Transcriptome analysis of *Arabidopsis* wild-type and *gl3-sst sim* trichomes identifies four additional genes required for trichome development. Mol Plant 2: 803-822

Markstädter C, Federle W, Jetter R, Riederer M, Hölldobler B (2000) Chemical composition of the slippery epicuticular wax blooms on *Macaranga* (Euphorbiaceae) ant-plants. Chemoecology 10: 33-40

Martin J, Juniper B (1970) The cuticles of plants. Edward Arnold, London

Merk S, Blume A, Riederer M (1998) Phase behaviour and crystallinity of plant cuticular waxes studied by Fourier transform infrared spectroscopy. Planta 204: 44-53

Millar A, Clemens S, Zachgo S, Giblin E, Taylor D, Kunst L (1999) *CUT1*, an *Arabidopsis* gene required for cuticular wax biosynthesis and pollen fertility, encodes a very-long-chain fatty acid condensing enzyme. Plant Cell 11: 825-838

Millar A, Kunst L (1997) Very-long-chain fatty acid biosynthesis is controlled through the expression and specificity of the condensing enzyme. Plant J 12: 121-131

Morlacchi P, Wilson W, Xiong Q, Bhaduri A, Sttivend D, Kolesnikova M, Matsuda S (2009) Product profile of PEN3: The last unexamined oxidosqualene cyclase in *Arabidopsis thaliana.* Org Lett 11: 2627–2630

Müller C (2006) Plant-insect interactions on cuticular surfaces. In M Riederer, C Müller, eds, Biology of the Plant Cuticle, Ed 1 Vol 23. Blackwell, Oxford, pp 398-422

Nawrath C (2006) Unraveling the complex network of cuticular structure and function. Current Opinion in Plant Biology 9: 281-287

Neinhuis C, Barthlott W (1997) Characterization and distribution of water-repellent, self-cleaning plant surfaces. Ann Bot 79: 667-677

Paul S, Gable K, Beaudoin F, Cahoon E, Jaworski J, Napier J, Dunn T (2006) Members of the Arabidopsis FAE1-like 3-ketoacyl-CoA synthase gene family substitute for the Elop proteins of *Saccharomyces cerevisiae*. J Biol Chem 281: 9018-9029

Pollard M, Beisson F, Li Y, Ohlrogge J (2008) Building lipid barriers: biosynthesis of cutin and suberin. Trends Plant Sci 13: 236-246

Pyee J, Yu H, Kolattukudy P (1994) Identification of a lipid transfer protein as the major protein in the surface wax of broccoli (*Brassica oleracea*) leaves. Arch Biochem Biophys 311: 460-468

Reynhardt E (1997) The role of hydrogen bonding in the cuticular wax of *Hordeum vulgare* L. Eur Biophys J 26: 195-201

Riedel M, Eichner A, Jetter R (2003) Slippery surfaces of carnivorous plants: composition of epicuticular wax crystals in *Nepenthes alata* Blanco pitchers. Planta 218: 87-97

Riedel M, Eichner A, Meimberg H, Jetter R (2007) Chemical composition of epicuticular wax crystals on the slippery zone in pitchers of five Nepenthes species and hybrids. Planta 225: 1517-1534

Riederer M, Schreiber L (1995) Waxes - The transport barriers of plant cuticles. In RJ Hamilton, ed, Waxes: Chemistry, molecular biology and functions, Ed 1 The Oily Press, West Ferry, pp 131-156

Riederer M, Schreiber L (2001) Protecting against water loss: analysis of the barrier properties of plant cuticles. J Exp Bot 52: 2023-2032

Rowland O, Zheng H, Hepworth S, Lam P, Jetter R, Kunst L (2006) *CER4* encodes an alcohol-forming fatty acyl-coA reductase involved in cuticular wax production in *Arabidopsis*. Plant Physiol 142: 866-877

Samuels L, Kunst L, Jetter R (2008) Sealing plant surfaces: cuticular wax formation by epidermal cells. Annu Rev Plant Biol 59: 683-707

Šantrůček J, Šimáňová E, Karbulková J, Šimková M, Schreiber L (2004) A new technique for measurement of water permeability of stomatous cuticular membranes isolated from *Hedera helix* leaves. J Exp Bot 55: 1411-1422

Schmitz B, Heinz E, Murawski U (1975) Keto-enediol-tautomerism of esters of 2,3-dihydroxy fatty acids. Chem Phys Lip 15: 248-251

Schreiber L (2005) Polar paths of diffusion across plant cuticles: new evidence for an old hypothesis. Ann Bot 95: 1069-1073

Schreiber L, Schönherr J (1993) Mobilities of organic compounds in reconstituted cuticular wax of barley leaves: determination of diffusion coefficients. Pestic Sci 38: 353-361

Schreiber L, Schorn K, Heimburg T (1997) ^{2}H NMR study of cuticular wax isolated from *Hordeum vulgare* L. leaves: identification of amorphous and crystalline wax phases. Eur Biophys J 26: 371-380

Segura M, Meyer M, Matsuda S (2000) *Arabidopsis thaliana* LUP1 converts oxidosqualene to multiple triterpene alcohols and a triterpene diol. Org Lett 2: 2257-2259

Shan H, Wilson W, Phillips D, Bartel B, Matsuda S (2008) Trinorlupeol: a mjaor nonsterol triterpenoid in *Arabidopsis*. Org Lett 10: 1897-1900

Shibuya M, Xiang T, Katsube Y, Otsuka M, Zhang H, Ebizuka Y (2007) Origin of structural diversity in natural triterpenes: direct synthesis of *seco*-triterpene skeletons by oxidosqualene cyclase. J Am Chem Soc 129: 1450-1455

Shibuya M, Katsube Y, Otsuka M, Zhang H, Tansakul P, Xiang T, Ebizuka Y (2009) Identification of a product specific [beta]-amyrin synthase from Arabidopsis thaliana. Plant Physiol Biochem 47: 26-30

Sieber P, Schorderet M, Ryser U, Buchala A, Kolattukudy P, Metraux J-P, Nawrath C (2000) Transgenic *Arabidopsis* plants expressing a fungal cutinase show alterations in the structure and properties of the cuticle and postgenital organ fusions. Plant Cell 12: 721-737

Silva Fernandes A, Baker E, Martin J (1964) Studies on the plant cuticle. VI. The isolation and fractionation of cuticular waxes. Ann Appl Biol 53: 43-58

Small D (1984) Lateral chain packing in lipids and membranes. J Lipid Res 25: 1490-1500

Somerville C, Ogren W (1982) Isolation of photorespiratory mutants of Arabidopsis. In R Hallick, N Chua, eds, Methods in Chloroplast Molecular Biology, Elsevier, New York, pp 129-139

Suh M, Samuels L, Jetter R, Kunst L, Pollard M, Ohlrogge J, Beisson F (2005) Cuticular lipid composition, surface structure, and gene expression in Arabidopsis stem epidermis. Plant Physiol 139: 1649–1665

Suzuki M, Xiang T, Ohyama K, Seki H, Saito K, Muranaka T, Hayashi H, Katsube Y, Kushiro T, Shibuya M, Ebizuka Y (2006) Lanosterol synthase in dicotyledonous plants. Plant Cell Physiol 47: 565-571

Takahashi S, Kumagai A (1995) Viscosity and density of liquid mixtures of n-alkanes with squalane. Int J Thermophys 16: 773-779

Tanaka T, Tanaka H, Machida C, Watanabe M, Machida Y (2004) A new method for rapid visualization of defects in leaf cuticle reveals five intrinsic patterns of surface defects in *Arabidopsis*. Plant J 37: 139-146

Tantisewie B, Ruijgriok H, Hegnauer R (1969) Die verbreitung der blausäure bei den kormophyten. Pharm Weekbl 104: 1341-1355

Tarr P, Tarling E, Bojanic D, Edwards P, Baldan A (2009) Emerging new paradigms for ABCG transporters. Biochim Biophys Acta 1791: 584-593

Trenkamp S, Martin W, Tietjen K (2004) Specific and differential inhibition of very-long-chain fatty acid elongases from *Arabidopsis thaliana* by different herbicides. Proc Natl Acad Sci USA 101: 11903-11908

van Maarseveen C, Jetter R (2009) Composition of the epicuticular and intracuticular wax layers on *Kalanchoe daigremontiana* (Hamet et Perr. de la Bathie) leaves. Phytochem 70: 899-906

Vogg G, Fischer S, Leide J, Emmanuel E, Jetter R, Levy A, Riederer M (2004) Tomato fruit cuticular waxes and their effects on transpiration barrier properties: functional characterization of a mutant deficient in a very-long-chain fatty acid β-ketoacyl-CoA synthase. J Exp Bot 55: 1401-1410

Wagner G, Wang E, Shepherd R (2004) New approaches for studying and exploiting an old protuberance, the plant trichome. Ann Bot 93: 3-11

Walton T (1990) Waxes, cutin and suberin. In JL Harwood, J Boyer, eds, Methods Plant Biochem, Vol. 4, pp 106-158

Wang S, Hubbard L, Chang Y, Guo J, Schiefelbein J, Chen J-G (2008) Comprehensive analysis of single-repeat R3 MYB proteins in epidermal cell patterning and their transcriptional regulation in Arabidopsis. BMC Plant Biology 8: 81

Wang Z, Yeats T, Han H, Jetter R (2010a) Cloning and characterization of oxidosqualene cyclases from *Kalanchoe daigremontiana*: Enzymes catalyzing up to ten rearrangement steps yielding friedelin and other triterpenoids. J Biol Chem (in press)

Wang Z, Guhling O, Yao R, Li F, Yeats T, Rose J, Jetter R (2010b) Two oxidosqualene cyclases responsible for the biosynthesis of tomato (Solanum lycopersicum) fruit cuticular triterpenoids. Plant Phys

Weidenhamer J, Macias F, Fischer N, Williamson G (1993) Just how insoluble are monoterpenes. J Chem Ecol 19: 1799-1807

Wen M, Buschhaus C, Jetter R (2006) Nanotubules on plant surfaces: Chemical composition of epicuticular wax crystals on needles of *Taxus baccata* L. Phytochem 67: 1808-1817

Xiang T, Shibuya M, Katsube Y, Tsutsumi T, Otsuka M, Zhang H, Masuda K, Ebizuka Y (2006) A new triterpene synthase from *Arabidopsis thaliana* produces a tricyclic triterpene with two hydroxyl groups. Org Lett 8: 2835-2838

Xiong Q, Wilson WK, Matsuda S (2006) An Arabidopsis oxidosqualene cyclase catalyzes iridal skeleton formation by grob fragmentation. Angew Chem Int Ed 45: 1285-1288

Yeats T, Howe K, Matas A, Buda G, Thannhauser T, Rose J (2010) Mining the surface proteome of tomato (*Solanum lycopersicum*) fruit for proteins associated with cuticle biogenesis. J Exp Bot 61: 3759-3771

Yu M, Konorov S, Schulze H, Blades M, Turner R, Jetter R (2007) In situ analysis by microspectroscopy reveals triterpenoid compositional patterns within leaf cuticles of *Prunus laurocerasus*. Planta 227: 823-834

Zheng H, Rowland O, Kunst L (2005) Disruptions of the Arabidopsis enoyl-CoA reductase gene reveal an essential role for very-long-chain fatty acid synthesis in cell expansion during plant morphogenesis. Plant Cell 17: 1467-1481